

2000

A Niche for Adult Neurogenesis: Analysis of BMP Signaling and Transcriptional Profiles of Adult Subventricular Zone Cells

Daniel A. Lim

Follow this and additional works at: http://digitalcommons.rockefeller.edu/student_theses_and_dissertations



Part of the [Life Sciences Commons](#)

Recommended Citation

Lim, Daniel A., "A Niche for Adult Neurogenesis: Analysis of BMP Signaling and Transcriptional Profiles of Adult Subventricular Zone Cells" (2000). *Student Theses and Dissertations*. 361.
http://digitalcommons.rockefeller.edu/student_theses_and_dissertations/361

This Thesis is brought to you for free and open access by Digital Commons @ RU. It has been accepted for inclusion in Student Theses and Dissertations by an authorized administrator of Digital Commons @ RU. For more information, please contact mcsweej@mail.rockefeller.edu.



**A Niche for Adult Neurogenesis:
Analysis of BMP Signaling and Transcriptional Profiles
of Adult Subventricular Zone Cells**

Daniel A. Lim

A thesis submitted to the faculty of
The Rockefeller University
in partial fulfillment
of the requirements for the degree of
Doctor of Philosophy

New York, New York, 2000

This thesis is dedicated to my wife, Cynthia.

ACKNOWLEDGEMENT

I am deeply indebted to Arturo Alvarez-Buylla. His enthusiasm for science and intellectual courage have been inspiring. He taught me new ways of looking at biology – perhaps allowing me to see more of its inherent beauty – and at the same time granted me the freedom to dismantle a splendid biological process. For this, I cannot thank him enough. I can only hope that someday I will be able to return the favor by passing on his fine sense of academic spirit to other students so there will always be a teacher like him.

Michael Botchan, my undergraduate research advisor, is in my mind with every experiment and every result. He was a mentor for me in the fullest sense.

I thank the following people in the order in which their contributions appear in this thesis: Jose Trevejo and Erik Falk-Pedersen for help with adenovirus production, Isabelle Caille for neurosphere work, Jose Manuel Garcia-Verdugo for EM analysis, Hynek Wichterle for help and advice with time-lapse microscopy, Richard Harland for providing the Noggin-LacZ mice, Nick Gaiano for help with retroviral production, Chisa Hidaka and Ron Crystal for the BMP7 adenovirus, Tony Tramontin for work on the Ara-C/BMP7 experiment, Kenji Adzuma for his expert advice and FPLC, Nila Patil and Coleen Hacker at Affymetrix for welcoming me into their lab and sharing critical resources and information, Steve Merlin for his expert control of the FACS machine, Felix Naef for past and continued collaborations on gene expression profile analysis, Masafumi Muritani for help with PCR cloning, and Benedicte Menn for contributing a great deal of effort towards the validation of the profile analysis data. Of course, the lab would not run without Sattie and Amy. I thank them both for making it possible to get anything done in the lab.

I thank my thesis committee Jim Hudspeth, Torsten Wiesel, and Lee Niswander for their time and insightful comments.

TABLE OF CONTENTS

ABSTRACT	1
CHAPTER 1: Introduction	2
CHAPTER 2: Type B cells (SVZ astrocytes) are neural stem cells	14
CHAPTER 3: Astrocytes provide a niche for SVZ neurogenesis	22
CHAPTER 4: Noggin antagonizes BMP signaling to create a niche for adult neurogenesis	32
CHAPTER 5: Gene expression profiling of adult SVZ stem cells and their neurogenic niche	47
CHAPTER 6: Conclusions and Perspectives	59
CHAPTER 7: Methods	65
BIBLIOGRAPHY	78

ABSTRACT

Neurogenesis persists in restricted regions of the adult vertebrate brain. The largest region of adult neurogenesis is the subventricular zone (SVZ) of the lateral ventricle wall. Neural stem cells reside in the SVZ. The SVZ cell types and molecular signals necessary for this neurogenic niche were poorly understood. Here, I first demonstrate that astrocyte-like cells in the SVZ (type B cells) can self-renew and differentiate into mature brain cells. This data contributed to the identification of type B cells as the SVZ stem cell. In vivo, all SVZ cell types are in direct contact with type B cells. By reconstituting cell-cell interactions of dissociated SVZ cells in culture, I defined an in vitro cellular environment that recapitulates SVZ neurogenesis; these cultures provided an in vitro assay for the study of external molecular signals that regulate SVZ neurogenesis.

Ependymal cells lie adjacent to the SVZ. I show that the bone morphogenetic protein (BMP) antagonist Noggin is expressed by ependymal cells and that SVZ cells express BMPs as well as their receptors. In vitro, BMP signaling potently inhibited neurogenesis. Conversely, Noggin protein in vitro promoted neurogenesis. Overexpression of BMPs in ependymal cells decreased SVZ cell proliferation and abolished type A cell regeneration. Ectopic Noggin expression in the normally non-neurogenic striatum promoted neuronal differentiation of transplanted SVZ cells. I thus propose that ependymal Noggin production creates a neurogenic niche in the adjacent SVZ by antagonizing BMP signaling.

To identify other genes with roles in the SVZ, I utilized high-density oligonucleotide arrays to determine the transcriptional profiles of the SVZ region as well as purified type B and ependymal cells. SVZ regional and cell-specific expression profiles were compared to those of other brain regions. Differential gene expression was validated by Northern blot and histological techniques. This transcriptional profile data provides new markers and candidate regulatory genes for future investigations into the SVZ neurogenic niche.

CHAPTER 1

Introduction

It is now widely accepted that new neurons are added continuously to select regions of the adult mammalian brain. Over thirty years of reports describing neurogenesis in the adult brains of fish, frogs, reptiles, birds, and rodents (Altman, 1970; Straznicky and Gaze, 1971; Birse et al., 1980; Goldman and Nottebohm, 1983; Lopez-Garcia et al., 1990; Alvarez-Buylla and Lois, 1995) have recently culminated in studies demonstrating the birth of new central nervous system neurons in primates including humans (Eriksson et al., 1998; Gould et al., 1999). Hence, the nearly century-old, dogmatic proposition of a “fixed, ended, immutable” adult brain has been refuted, spurring new investigations into the regenerative capacity of the central nervous system.

The dentate gyrus of the hippocampus (reviewed in Gage et al., 1998) and the lateral ventricle subventricular zone (SVZ) (reviewed in García-Verdugo et al., 1998; reviewed in Lim and Alvarez-Buylla, 2001) are two brain regions in which neurons are born in the adult. The SVZ is the larger of these two germinal zones, consisting of a layer of cells adjacent to the ependyma along the entire length of the lateral ventricular wall. In postnatal (Luskin, 1993) and adult rodents (Lois and Alvarez-Buylla, 1994), cells born in the SVZ migrate from the ventricular wall into the olfactory bulb (OB) where they differentiate into interneurons. Interestingly, in the monkey brain, there is

evidence that the SVZ generates new neurons for the prefrontal, inferior temporal, and posterior parietal cortex (Gould et al., 1999). In the adult human SVZ, investigators have also found proliferating cells (Globus and Kuhlenbeck, 1944; Eriksson et al., 1998), raising the intriguing possibility that we -- like rodents and other primates -- harbor a neurogenic population of cells within the walls of our brain ventricles (Goldman, 1998).

The proliferation of SVZ cells continues throughout life (Kuhn et al., 1996; Goldman et al., 1997). It has been estimated that at least 30,000 new OB neurons are born in the mouse every day to replace those that are dying (Lois and Alvarez-Buylla, 1994). This profound level of continuous neurogenesis argues for the presence of neurogenic stem cells within the SVZ. In Chapter 2, I present work that contributed to the identification of the adult mouse SVZ stem cell. The remaining chapters detail my studies of the cellular and molecular components of the SVZ that maintain this remarkable “fountain of youth” in the adult mammalian brain.

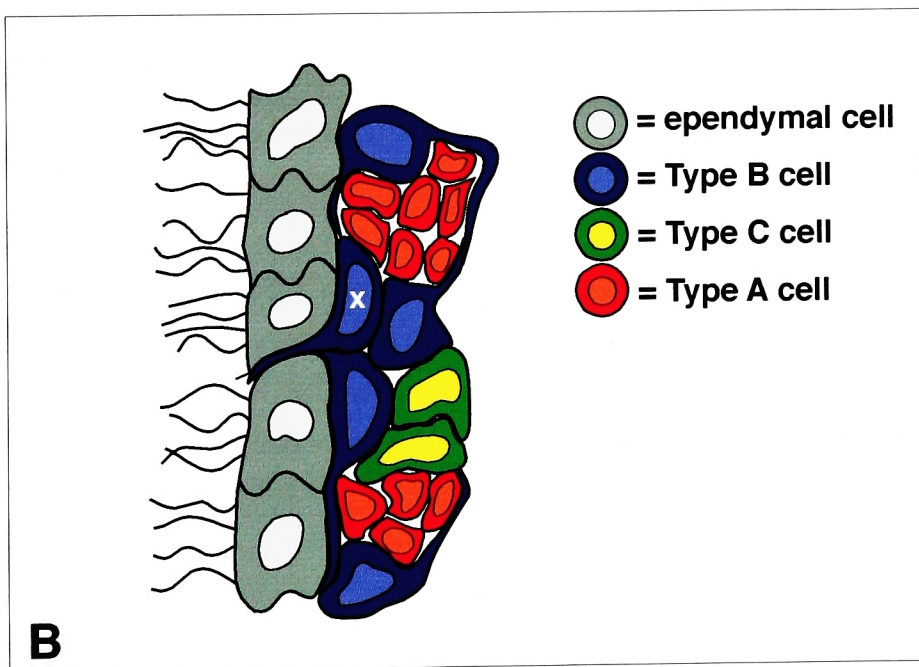
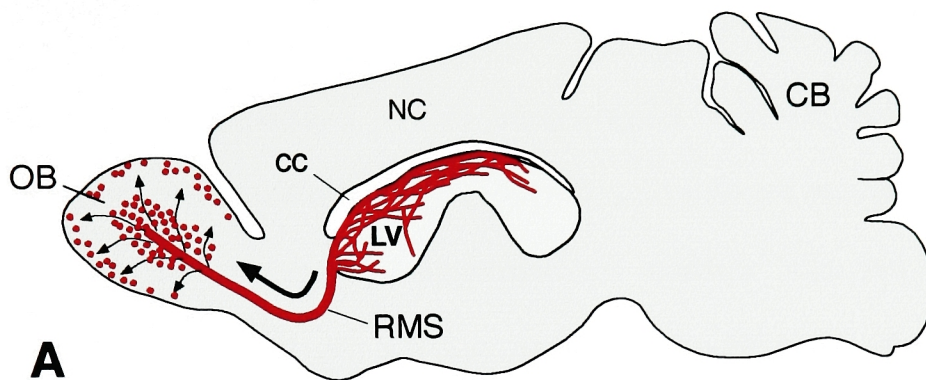
Cellular composition and organization of the adult mouse SVZ

In the adult mouse, neuroblasts born along the entire length of the SVZ migrate anteriorly to the OB. The migratory neuroblasts (type A cells) travel as chains of themselves (Lois et al., 1996; Wichterle et al., 1997) along many interconnecting paths widely distributed throughout the lateral ventricle wall (Doetsch and Alvarez-Buylla, 1996). These paths converge at the anterior SVZ where the confluence of type A cells continues along a restricted path into the OB (Fig. 1A). The chains of migrating type A cells are ensheathed by the processes of slowly dividing SVZ astrocytes (type B cells) (Lois et al., 1996). Scattered along the type A cell chains are clusters of rapidly dividing

Figure 1

(A) Chain migration of type A neuroblasts in the adult SVZ. Schematic sagittal view of the adult brain. Type A cells are born in the walls of the lateral ventricle (LV, light gray) and migrate along a network of interconnecting pathways (red lines) to the olfactory bulb (OB). In the OB, type A cells differentiate into interneurons (red dots). (adapted from Doetsch and Alvarez-Buylla, 1996)

(B) Schematic frontal cross-section of the adult SVZ. Ependymal cells (gray) are multi-ciliated and are closely apposed to the underlying SVZ cells. The ventricular lumen is to the left. Type B cells (blue) are slowly-dividing astrocyte-like cells that ensheath chains of migrating type A cells (red). In this cross-section, type A cells would be migrating out of the plane of the paper. Type C cells (green) are highly mitotic and found as clusters along the chains of type A cells. (adapted from Lim and Alvarez-Buylla, 2001)



immature cells (type C cells). Type C cell clusters are often interposed between type B and A cells (Doetsch et al., 1997). (See Fig. 1B for a schematic cross-section of the SVZ.)

SVZ cell types are defined by their morphological, immunocytochemical, and ultrastructural characteristics (Doetsch et al., 1997). Type A cells are immunopositive for a neuron-specific β -tubulin revealed by monoclonal antibody Tuj1 and express a polysialylated form of neural cell adhesion molecule (PSA-NCAM). Type B cells contain intermediate filament bundles containing glial-fibrillary acidic protein (GFAP), a marker assigned to mature astrocytes (Bignami et al., 1972). Type C cells are ultrastructurally immature and do not stain for markers of mature brain cells. Adjacent to the SVZ is the layer of multi-ciliated ependymal cells. Interestingly, all SVZ cell types and the ependyma express nestin (Doetsch et al., 1997), an intermediate filament protein found in neuroepithelial stem cells (Lendahl et al., 1990).

Ependymal cells line the luminal surface of the brain ventricle and appear highly differentiated, bearing multiple beating cilia that move cerebrospinal fluid through the ventricular system. The lateral ventricle ependyma is generally described as a layer of multiciliated epithelial cells that separate the SVZ from the ventricular lumen. However, upon closer examination using electron microscopy (EM), the ependymal layer does not appear entirely continuous. In normal mice, a small number of type B cells make direct contact with the ventricle (Doetsch et al., 1999b). Some of these type B cells contact the ventricle by extending a thin cellular process between ependymal cells while a few have a larger luminal surface (see “x”-marked cell in Fig. 1B). Thus, the boundary between the ependymal layer and the SVZ is somewhat blurred by the small number of type B cells

that are interdigitated with the ependymal cells. In addition to their unusual cellular location, some of the ventricle-contacting type B cells possess a single, thin cilium lacking the central pair of microtubules. Similar single cilium with this 9+0 microtubule arrangement have been described in embryonic neuroepithelial cells (Sotelo and Trujillo-Cenóz, 1958; Stensaas and Stensass, 1968), adult avian brain neuronal precursors (Alvarez-Buylla et al., 1998) and in cells progressing through the cell cycle (Ho and Tucker, 1989).

Which is the SVZ stem cell?

Self-renewal and production of at least one type of differentiated descendant are two defining attributes of stem cells. In vivo, proliferating SVZ cells generate OB neurons for the life of the animal (Kuhn et al., 1996; Goldman et al., 1997), suggesting the presence of a neurogenic stem cell within the wall of the lateral ventricle. Furthermore, self-renewing SVZ cells have been propagated in vitro with high concentrations of exogenous growth factors, and these cells can differentiate into neurons, astrocytes, and oligodendrocytes (Reynolds and Weiss, 1992; Gage et al., 1995; Weiss et al., 1996b; McKay, 1997). Hence, a population of cells in the SVZ satisfies the aforementioned criteria and can thus be described as stem cells. The SVZ stem cell is perhaps analogous to stem cells found in self-renewing tissues such as the skin, gut, and blood. Stem cells of the SVZ and these other tissues generate large numbers of new cells for their respective organ systems throughout the life of the animal. The constant production of new cells complements normal cell turnover, maintaining the tissue cell

population. I define the adult mouse SVZ stem cell as the self-renewing cell type responsible for the lifelong production of OB neurons¹.

One misleading notion about stem cells is that they should be undifferentiated or primitive, lacking expression of markers attributed to more mature cells. This preconception has led many researchers to ignore the "mature-looking" cells as potential stem cells. However, it is becoming increasingly clear that stem cells can bear what were thought to be the biochemical hallmarks of differentiated cells. For instance, skin stem cells express intermediate filament keratins found in mature keratinocytes (Coulombe et al., 1989; Vasioukhin et al., 1999). Intestinal crypt stem cells, which continuously replace the epithelial lining of the small bowel, have been described as being more epithelial than primitive (Fuchs and Segre, 2000). Hematopoietic stem cells, perhaps the best studied of all stem cells, can transiently express what have been considered to be lineage-restricted factors (Cheng et al., 1996; Hu et al., 1997) while still maintaining the ability to produce any blood cell lineage.

The preconception of an immature-appearing stem cell also initially misled the search for the SVZ stem cell. Based on their immature cellular appearance, proximity to the type A cells, and high mitotic activity, type C cells were hypothesized to be SVZ stem cells (Doetsch et al., 1997). However, later, experimental evidence supported the

¹ The definition of a stem cell is matter of debate (Morrison et al., 1997; Gage, 1998; Alvarez-Buylla and Temple, 1998; Watt and Hogan, 2000). It seems that the semantic difficulty arises from an attempt to provide one definition for stem cells in both development and adulthood. For instance, while the pluripotential embryonic stem cell (ES cell) commonly used to produce transgenic animals can contribute to all adult tissues, stem cells in the adult do not generate such a complete repertoire. In fact, there is evidence that in normal, uninjured adult epithelial tissues in steady state cell renewal, most stem cells are unipotent, producing only one type of differentiated cell (reviewed in Slack, 2000). Furthermore, ES cells do not self-renew for the entire life of the organism, while there is evidence that adult stem cells do. It remains to be determined how similar or dissimilar adult stem cells are to the pluripotent ES cells or those in embryonic development (a more complete discussion can be found in Lim and Alvarez-Buylla, 2001).

hypothesis that type B cells – the SVZ astrocytes – are in fact SVZ stem cells. Three lines of in vivo experimentation led to this conclusion (Doetsch et al., 1999a). First, in accord with the generally accepted view that stem cells divide infrequently, type B cells are the slowest dividing cell type of the SVZ. Second, type B cells are capable of regenerating the SVZ after chemical elimination of rapidly dividing cells. Third, cells expressing the type B cell GFAP marker are in the neurogenic lineage of OB neurons. While these experiments strongly suggested that type B cells are the SVZ stem cell, the property of self-renewal was not yet demonstrated. In Chapter 2, I present experiments demonstrating the self-renewal of type B cells in vitro. Taken together, the in vitro demonstration of self-renewal and the above in vivo evidence indicates that type B cells are the SVZ stem cell.

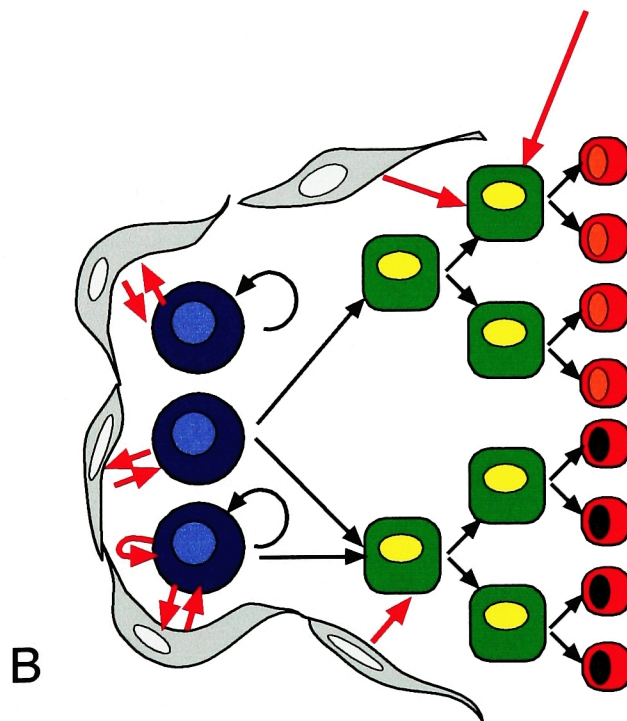
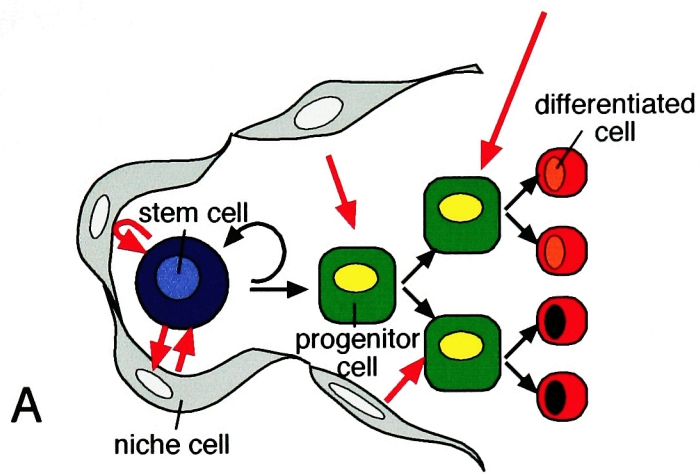
Adult stem cells and their generation of progenitors

It is generally believed that between an adult stem cell and its highly differentiated descendants, there is an intermediate population of progenitors with a limited proliferation capacity (reviewed in Watt and Hogan, 2000) (Fig 2). Stem cells and their progenitors are collectively referred to as precursor cells (reviewed in McKay, 1997). The proposed role of the intermediate progenitors is to amplify the number of differentiated cells produced by one stem cell division (reviewed in Potten and Loeffler, 1990). For instance, in the skin, progenitors can divide 3-5 times before finally becoming a keratinocyte (Jones and Watt, 1993). Hence, although stem cells have the capacity for lifelong self-renewal, they may need to divide only infrequently.

Figure 2

(A) **Strict asymmetric stem cell division.** The stem cell (blue) divides asymmetrically to give rise to itself (curved black arrow) and a progenitor cell (green). The progenitor cell has a limited capacity for proliferation and differentiates in response to external signals to give rise to differentiated cell types (red). External signals (soluble factors, extracellular matrix, and membrane bound factors) are shown as thick red arrows. For clarity, some signaling possibilities are not shown. Note that external signals can induce/select different final fates (red cells with red nuclei and red cells with black nuclei). The gray cells are “niche” cells, producing factors that control stem cell fate.

(B) **Populational asymmetry.** Stem cells can either self renew with symmetric divisions (top stem cells), divide to produce two progenitors (middle stem cell), or divide asymmetrically (bottom stem cell). (adapted from Watt and Hogan, 2000)



There are two general strategies by which stem cell self-renewal is coordinated with the production of progenitors. In one scenario, the stem cell always divides asymmetrically to give rise to one stem cell and one progenitor (Fig 2A). Evidence for this mode of stem cell behavior is abundant in unicellular organisms (Jacobs and Shapiro, 1998) and invertebrates (Lu et al., 1998) ; however examples for strictly asymmetric stem cell behavior are not found in mammals (Morrison et al., 1997). In the other strategy, dividing stem cells give rise to two descendants, both of which have a certain probability of becoming a stem cell or progenitor; asymmetry in this paradigm is thus maintained on a population basis -- not at the level of the individual stem cell (Fig. 2B). Stem cell populations utilizing the strategy of populational asymmetry can in principle expand their numbers as might be needed after injury to repopulate regenerating tissues, or to accommodate growth; such modulations of the size of the stem cell pool has been described in organs including the blood (Harrison and Lerner, 1991; Morrison et al., 1995) and intestine (Paulus et al., 1992).

Control of adult stem cell differentiation

The overall developmental potential of a stem cell and the fate of its progenitors are ultimately controlled by cell autonomous factors intrinsic to each cell. These intrinsic signals (e.g., transcription factors) are sensitive to external signals (e.g. growth factors) in cell's microenvironment. In the stem cell microenvironment there is a complex interplay of external signals between stem cells, their progenitors, and the neighboring cells (reviewed in Watt and Hogan, 2000) (Fig. 2). In this model, the final fate of cells derived

from the stem cell can be modulated by external signals acting directly on the stem cell itself or on the progenitors.

External signals can have a profound effect upon the differentiation potential of stem cells and their progenitors. For instance, bone marrow-derived cells transplanted to the adult brain appear to produce microglia and astrocytes (Eglitis and Mezey, 1997), differentiate into myocytes when introduced into injured muscle (Ferrari et al., 1998), and are a source of hepatocytes during liver regeneration (Petersen et al., 1999). Cultured adult-derived neural stem cells also display dramatic expansions of their differentiation repertoire when introduced into novel microenvironments²: they can give rise to several blood cell lineages when introduced into the bloodstream of sublethally-irradiated mice (Bjornson et al., 1999) and contribute to the development of several non-neural tissues when injected into the amniotic cavity of stage 4 chick embryos (Clarke et al., 2000). These experiments show that final fate of stem cells is strongly dependent upon the external signals in their microenvironment.

What is the nature of these external signals? The concept of a specialized microenvironment for stem cells – or “niche” – was originally developed in studies of hematopoiesis (Schofield, 1978) where it was found that soluble factors derived from

² Extensive cell culture with high concentrations of mitogens might be required for adult-derived neural stem cells to acquire the ability to differentiate into non-neural tissues. If intrinsic signals that restrict a stem cell's differentiation potential are biochemical in nature, then one can envisage how such signals can be “erased.” For example, Lewis and colleagues have proposed a mathematical model for a biological “switch” (Lewis et al., 1977). The switch has only 2 stable states (“on” or “off”), and the “on” state will persist so long as the rate of gene synthesis for the switch is sufficient to maintain the gene product concentration above a certain threshold. When the rate of cell division is outpaces the gene synthesis for the switch, the switch turns “off,” and the intrinsic signal for differentiation is lost. It is interesting that the most surprising changes in neural stem cell differentiation potential are observed in stem cell populations that have been grown with high concentrations of mitogens, stimulating a cell cycle of somewhere between 18 and 48 hours. Most stem cells have been found to have exceedingly long cell cycle times (on the order of days to months), and perhaps the in vitro mitogenic conditions have “erased” some stem cell intrinsic signals, allowing a wider diversity of fates.

cells in the bone marrow selected the final fate of the developing blood cells (reviewed in Morrison et al., 1997). Later, various components of the extracellular matrix (ECM) and certain membrane-bound molecules (Quesenberry and Becker, 1998) were demonstrated to control stem cell behavior as well. Therefore, the external signals influencing stem cell biology comprise those that are soluble and non-soluble in nature.

A niche for adult neurogenesis

For adult neurogenesis to occur, it has been hypothesized that an appropriate set of neurogenic signals needs to be present within the stem cell microenvironment (García-Verdugo et al., 1998; Gage, 2000). The notion of a niche for SVZ neurogenesis is supported by transplantation experiments. SVZ cells transplanted to the SVZ of another animal generate extensive numbers of new neurons (Lois and Alvarez-Buylla, 1994; Doetsch and Alvarez-Buylla, 1996). However, SVZ cells transplanted to non-neurogenic brain regions do not produce neurons; rather, they primarily differentiate into astrocytes (Herrera et al., 1999). Hence, it is possible that the SVZ contains instructive external signals for neurogenesis.

The signals within the SVZ microenvironment are also instructive for non-SVZ-derived neural stem cells and progenitors. Cultured hippocampal stem cells transplanted to the SVZ produce GABA-ergic interneurons for the OB, a neurotransmitter phenotype appropriate for the OB and not observed in the regenerating granule cells of the hippocampus. In addition, embryonic lateral ganglion eminence (LGE) cells transplanted to the adult SVZ migrate efficiently to the OB and differentiate into interneurons (Wichterle et al., 1999). However, it is also clear that not all pools of neural precursor

cells can respond to the SVZ microenvironment. For instance, embryonic ventricular zone (VZ) (Zigova et al., 1996) and medial ganglion eminence (MGE) cells (Wichterle et al., 1999) do not migrate to the OB when transplanted to the SVZ³.

What are the external signals in the SVZ that govern neurogenesis? Most studies of molecular signals controlling the fate of mammalian neural stem cells have been performed in vitro using stem cell populations that have been amplified with high concentrations of soluble mitogens. In one such study, it was found that platelet-derived growth factor (PDGF) instructs neuronal differentiation of adult SVZ-derived stem cells while ciliary neurotrophic factor (CNTF) and thyroid hormone (T3) induce the formation of astrocytes and oligodendrocytes, respectively (Johe et al., 1996). However, it is not clear that PDGF, CNTF, T3, or the mitogens used (EGF and FGF-2) play a role in the SVZ. Furthermore, the culture conditions used for this study may have altered the stem cell differentiation potential and responsiveness to external signals; for instance, it was recently reported that oligodendrocyte precursors can be “reprogrammed” to behave as multipotent neural stem cells by sequential exposure to PDGF, serum, and FGF-2 (Kondo and Raff, 2000 see also footnote 2). Hence, it is not clear that in vitro cultures of adult-derived neural stem cells grown with EGF and/or FGF-2 recapitulate the neurogenesis observed in the SVZ. A culture system that more faithfully reproduces SVZ neurogenesis would greatly facilitate studies of external signaling molecules.

In addition to soluble molecules, neural development is also regulated by extracellular matrix (Sanes, 1989) and membrane-bound factors (Davis and Temple,

³ LGE, MGE, and VZ may consist mainly of progenitor cells with some intrinsic restrictions to their differentiation potential. It is possible that LGE progenitors respond appropriately to the SVZ

1994) which likely mediate the influence of direct cell-cell interactions (Wang and Barres, 2000). Therefore, the cellular composition and architecture of the SVZ germinal zone is likely important for the behavior of stem cells and their progenitors. By reconstituting intercellular interactions of SVZ cell types in vitro without serum or exogenous growth factors, I defined a cellular niche for SVZ neurogenesis; these in vitro studies presented in Chapter 3 provided an in vitro assay with which to study external molecular signals that regulate SVZ stem cell behavior.

There is a need to identify the signals endogenous to the SVZ microenvironment and determine how they act within this germinal zone. Such studies require that data from experimental studies be “overlaid” onto what is known about the SVZ cellular composition, architecture, and neurogenic lineage. Hypotheses concerning the role of signaling molecules under study should incorporate both the experimental and descriptive expression data.

Strategies for neural development in the embryo may be utilized in adult neurogenesis. In the developing *Xenopus* embryo, Noggin, a secreted antagonist of bone morphogenetic proteins (BMPs), plays a role in neural induction (Lamb et al., 1993). In Chapter 4, I show that Noggin is expressed by ependymal cells. BMPs and their receptors are found in the adjacent SVZ. BMPs potently inhibited the formation of new neurons from SVZ precursors; conversely, Noggin promoted neurogenesis. Cell-autonomous BMP signaling inhibited SVZ precursors from producing neuroblasts while inducing glial cell differentiation. BMP overexpression in the ependyma reduced SVZ cell proliferation and abolished neuroblast regeneration in the SVZ. Ectopic Noggin

microenvironment because their intrinsic program may have similarities to that of adult SVZ stem cells and

expression promoted neuronal differentiation of SVZ cells transplanted into the normally non-neurogenic striatum. Collectively, the data indicate that Noggin protein derived from the ependymal cells antagonizes BMP signaling to create a neurogenic niche for the adult SVZ.

There is undoubtedly a multitude of external signals in the SVZ niche acting in concert with the intrinsic signals of the stem cells and progenitors. In order to generate new hypotheses concerning the molecular regulation of SVZ stem cell behavior, it is necessary to identify both external and intrinsic signals within the SVZ. With the advent of DNA microarray technology, it is now possible to determine the expression levels of tens of thousands of genes simultaneously. In Chapter 5, I present the expression profiles of the SVZ brain region as well as purified populations of SVZ cells. SVZ regional and cell-specific expression profiles were compared to those of other brain regions to identify genes potentially involved in adult neurogenesis. Merging the expression profiles with our knowledge of the cellular composition and architecture of the SVZ will provide new clues about the molecular secrets tucked away in our brain's neurogenic niche.

CHAPTER 2

Type B cells (SVZ astrocytes) are self-renewing neural stem cells⁴

A traditional view of adult stem cells is that they divide very slowly. For instance, to maintain hematopoiesis, blood stem cells enter the cell cycle every 1-3 months (Bradford et al., 1997; Cheshier et al., 1999). In the skin, the slowest-cycling cell has stem cell behavior (Morris and Potten, 1994). Due to their slow cell cycle, stem cells are labeled infrequently by a single pulse of nucleoside analogs such as [³H]-thymidine or bromodeoxyuridine (BrdU). Efficient labeling of stem cells requires continuous or repeated administration of [³H]-thymidine or BrdU for a prolonged duration. Once having incorporated the label, the stem cells retain the mitotic marker for an extended period of time and can thus be identified as label-retaining cells. Rapidly-dividing progenitor cells dilute out the label and/or migrate from the region. In the SVZ, type B cells are the label-retaining cells (Doetsch et al., 1999a).

Because they divide more slowly than other cell types, adult stem cells are thought to be more resistant to antimitotic agents. Thus, treatment with certain types of antimitotic drugs should be able to eliminate rapidly dividing progenitor cells while sparing a population of stem cells capable of regenerating the killed cells. Infusion of the

⁴ This chapter describes my role in the laboratory-wide effort to identify the SVZ stem cell. The in vivo experiments described in the introductory portion of this chapter were all performed by Dr. Fiona Doetsch, a former student of this lab. My role was to devise a method of vitally labeling type B cells for identification in neurosphere cultures, which, at the time, was the in vitro system of choice of studying neural stem cells. The actual neurosphere cultures were performed by a former postdoctoral fellow Dr. Isabelle Caille. The identification of the SVZ stem cell was important for the rest of this thesis.

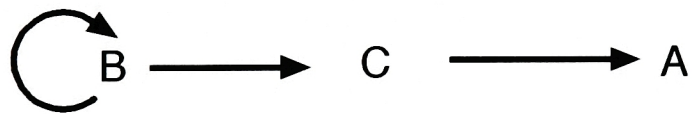
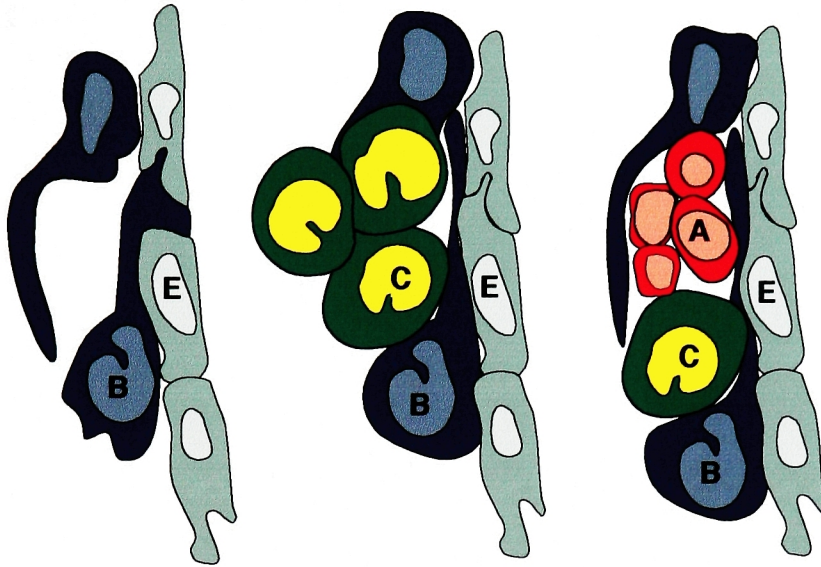
antimitotic cytosine-D-arabino-furanoside (Ara-C) into the SVZ for six days eliminates all type A and C cells (Doetsch et al., 1999b). The only cell types remaining are type B and ependyma. At the end of Ara-C treatment, no BrdU incorporation is observed in the SVZ. However, 12 hours after Ara-C removal, type B cells begin incorporating BrdU. No ependymal cells incorporate the mitotic marker. Two days later, the first type C cells appear, and by 14 days, the entire cellular and architectural composition of the SVZ is regenerated. The appearance of type C cells followed by type A cells suggests a developmental lineage of B to C to A (Fig. 3).

The fate of type B cells has been specifically followed with an avian leukemia retroviral vector (RCAS) encoding alkaline phosphatase (AP) injected into the SVZ of GFAPP-tva transgenic mice. The GFAPP-tva transgene in the recipient mice directs expression of the avian retrovirus receptor to GFAP-positive cells (Holland and Varmus, 1998). Hence, only mitotic type B cells are labeled by the RCAS vector. One day after injection, only type B cells express the RCAS marker AP gene, confirming the specificity of the initial infection. 3.5 days later, AP-positive cells are found en route to the OB, and by 14 days, many AP-positive neurons integrate into the OB. Thus, type B cells are in the neurogenic lineage.

While it was clearly shown that type B cells are the SVZ label-retaining cells, a label-retaining cell is not necessarily a stem cell. Dividing type B cells might simply represent local endogenous glial turnover. Regeneration of the SVZ after Ara-C treatment suggested that type B cells are capable of giving rise to type C and A cells, but it was not clear that type B cells had to self-renew to do so. The lineage analysis of type B cells with the RCAS virus clearly demonstrated that a GFAP-positive cell was in the

Figure 3

Model of neurogenesis in the adult SVZ. Type B cells (blue) are neuronal stem cells. Type B cells divide to give rise to type C cells (green) which likely are progenitors. Type C cells then give rise to type A cells (red), the migratory neuroblasts. After Ara-C treatment, the SVZ has only type B cells and ependyma (left). 3 days after the end of Ara-C treatment, type C cells reappear (middle), and by 5 days type A cells are regenerated (right) (Doetsch et al., 1999). (figure reprinted from Doetsch, 1999)



SVZ Astrocyte

Immature
Precursor

Migrating
Neuroblast

neurogenic lineage, but this cell was not necessarily a self-renewing stem cell. Thus, we needed another method to determine whether or not type B cells can self-renew and produce neurons.

Type B cells can self-renew and differentiate into neurons and glia

Neural stem cells isolated from the adult brain SVZ can be propagated as non-adherent clusters of cells called neurospheres (Reynolds and Weiss, 1992; Morshead et al., 1994; Gritti et al., 1996). Cell proliferation is maintained by high concentrations of epidermal growth factor (EGF). These neural stem cells can be clonally isolated, passaged in culture, and differentiated into neurons, astrocytes, and oligodendrocytes.

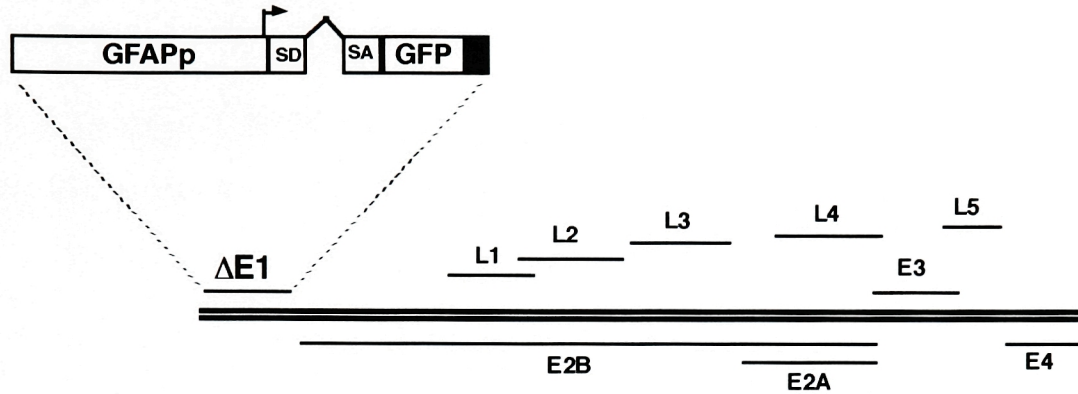
In order to vitally label type B cells for neurosphere cultures, I constructed an adenoviral vector (Ad5-GFAPp-GFP) that expresses green fluorescent protein (GFP) under control of the GFAP promoter (GFAPp) (Yoon et al., 1996; Zolotukhin et al., 1996; Baba et al., 1997). The GFAPp-GFP construct was recombined into the E1 adenovirus gene locus (see Fig. 4, top) which renders the vector incapable of replication; in this location, no adenoviral transcriptional elements lie upstream of GFAPp, ensuring that transcriptional activation of GFP depends upon GFAPp sequences. Furthermore, since the adenovirus genome remains extrachromosomal in an infected cell, no cellular genomic sequences can modify the GFAPp activity in cis⁵. To test the specificity of Ad5-GFAPp-GFP expression, SVZ-derived astrocytes were infected in culture. GFP expression was strong in GFAP-positive cells (Fig. 4A-C). In GFAP-negative HELA

⁵ A similar GFAP promoter fragment driving the expression of LacZ was used to generate several lines of transgenic mice. LacZ expression in these mice was variable among the seven different lines and not always specific to astrocytes (Galou et al., 1994). It is possible that genomic sequences flanking the integrated reporter construct was detrimental to GFAPp-specific LacZ expression (Yang et al., 1997).

Figure 4

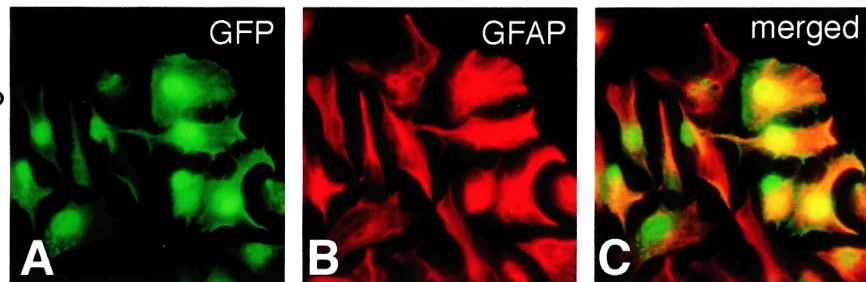
Selective expression of GFP in astrocytes with the Ad5-GFAPp-GFP vector. Top: schematic of adenoviral vector. The GFAPp-GFP construct replaces the E1 gene of Ad5. (A) SVZ astrocytes infected in vitro at 1000 viral particles/cell express high levels of GFP. Ad5-GFAPp-GFP expression is co-regulated with endogenous GFAP expression (B-C). (D-I) Ad5-GFAPp-GFP does not express in HELA cells. HELA cells do not express detectable levels of GFAP. HELA cells infected with Ad5-GFAPp-GFP at 1000 viral particles/cell do not express GFP (D-E). Infection of HELA cells with an adenovirus expressing GFP under a constitutively active CMV promoter (Ad5-CMV-GFP) express high levels of GFP at both 1000 and 100 viral particles/cell.

Ad5-GFAPp-GFP



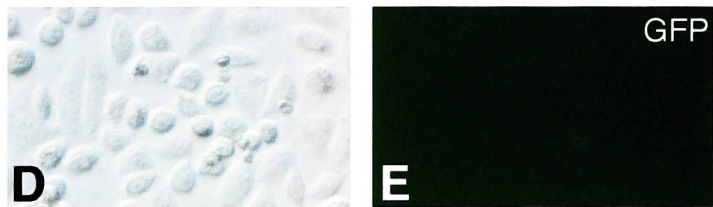
SVZ astrocytes

Ad5-GFAPp-GFP
1000 p/cell

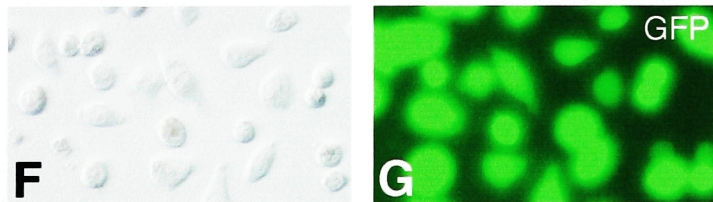


HELA cells

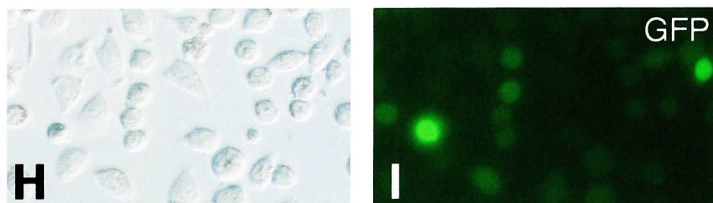
Ad5-GFAPp-GFP
1000 p/cell



Ad5-GFP
1000 p/cell



100 p/cell



cells, Ad5-GFAPp-GFP did not express GFP, demonstrating that GFP expression depends upon cellular GFAP promoter activity (Fig. 4D-E). A control adenovirus vector that expresses GFP under the constitutively active CMV promoter (Ad5-CMV-GFP) drove GFP to high levels in HELA cells (Fig. 4F-I).

When Ad5-GFAPp-GFP was injected in the SVZ and animals allowed to survive for 48 hr, type B cells became selectively labeled. Double labeling for GFAP confirmed that the GFP reporter gene was specifically expressed in GFAP-containing cells (Fig. 5A-C). Double labeling for cell-specific markers showed that GFP was not expressed in ependymal cells or in type A cells (Fig. 5D-I). Labeling of type B cells with GFP was confirmed by preembedding anti-GFP immunogold staining and EM (Fig. 5M). Ependymal cells were not labeled. Importantly, injections of Ad5-GFAPp-GFP into the lateral ventricle did not drive GFP expression in ependymal cells (Fig. 5J-K), whereas injections of Ad5-CMV-GFP labeled ependymal cells strongly (Fig. 5L)⁶.

After dissociation of the walls of the ventricle in mice that were injected with Ad5-GFAPp-GFP, 0.4%-1.2% of the total cells were brightly fluorescent. Clonal-isolation wells containing single GFP-positive cells in EGF-containing medium were marked, and these fluorescent cells followed on a daily basis (Fig 6A-F). Results of four independent experiments are shown in Fig. 6. Of the fluorescently labeled cells scored, 9%-14.3% gave rise to neurospheres. Half of the neurospheres derived from GFP-positive cells were plated for differentiation and shown to generate neurons and glia. In addition, the other half of the neurospheres were dissociated and passaged, and these

⁶ Ependymal cells have been previously considered to express GFAP (Doetsch et al., 1997). However, only polyclonal antibodies to GFAP stain ependymal cells; monoclonal antibodies to GFAP do not stain ependymal cells but do label type B cells (Doetsch et al., 1999a). It is possible that reports of GFAP

Figure 5

Ad5-GFAPp-GFP selectively labels astrocytes in the mouse brain. Panels (A-L) are 1 μ m confocal optical sections of frontal sections through the SVZ of mice infected with the Ad5-GFAPp-GFP adenovirus 48 hr earlier. (A-C) GFP-positive cells in the SVZ are GFAP positive. (D-F) CD24-positive ependymal cells are not GFP positive. (G-I) PSA-NCAM-positive type A cells are not GFP-positive. Instead, type B cells surrounding the chains of type A cells express GFP. Scale bar = 10 μ m. (J-K) Injections of Ad5-GFAPp-GFP into the lateral ventricle do not label ependymal cells. Notice that ependymal cells incorporate rhodamine beads that were co-injected with the Ad5-GFAPp-GFP virus but do not express the GFAPp-GFP construct (K, corresponding GFP image in J). With similar injections, Ad5-CMV-GFP labels ependymal cells strongly (L). (M). EM analysis of immunogold anti-GFP stained sections confirms GFP expression in type B cells. Immunogold appears as dark, electron-dense spots (indicated by red arrows). Ependymal cells were not labeled.

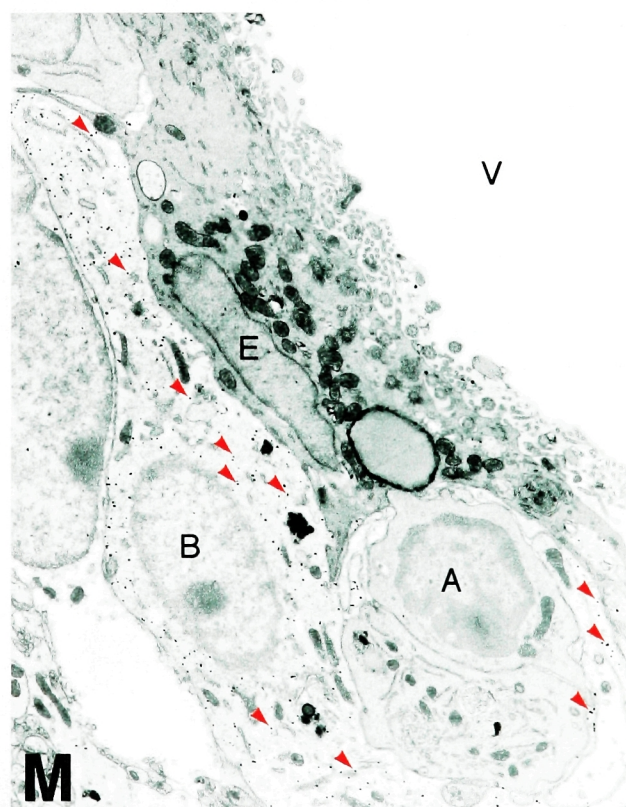
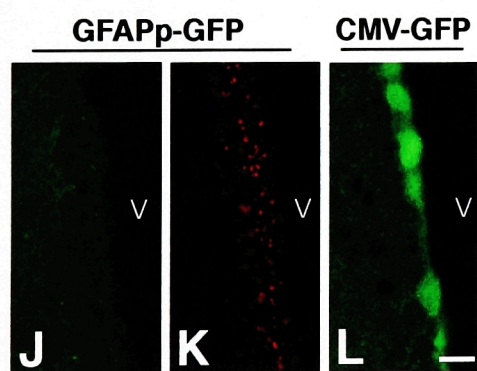
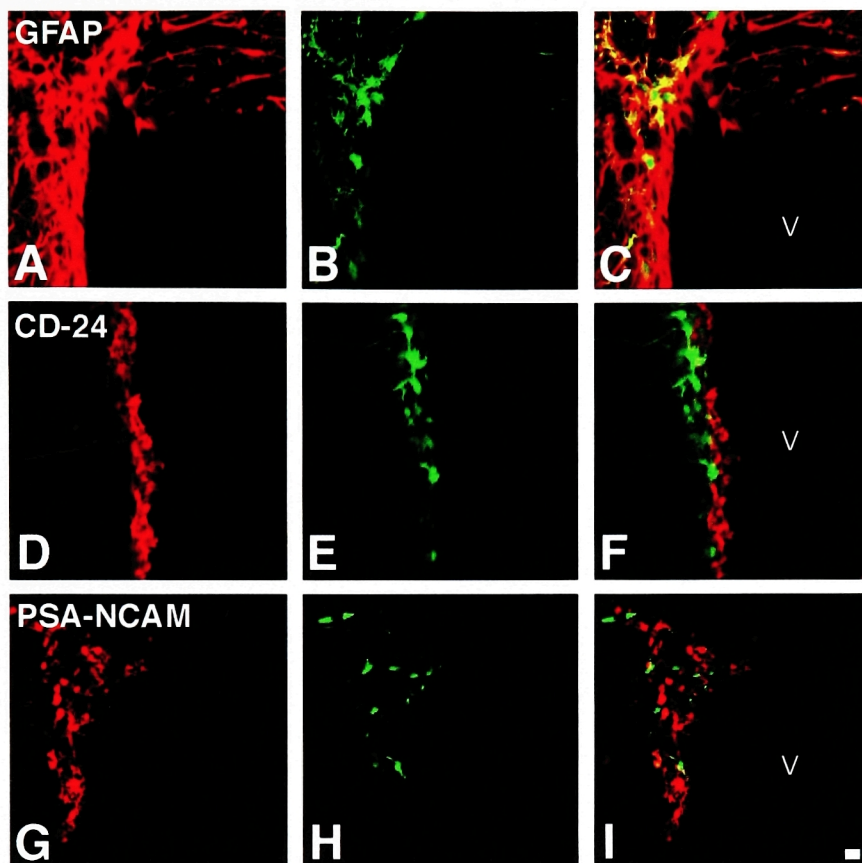
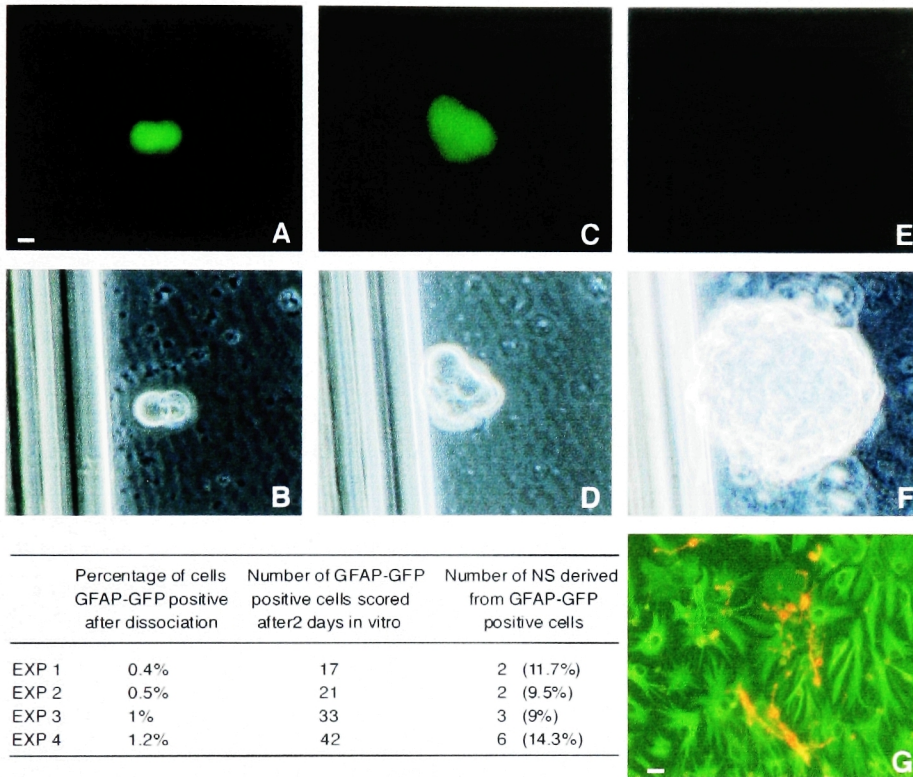


Figure 6

GFAP-GFP labeled SVZ cells give rise to neurospheres.

(A-F) SVZ cells were infected in vivo with the Ad5-GFAPP-GFP adenovirus; 48 hr later, cells were dissociated and cultured in multiwell plates. Epifluorescent (A, C, and E) and phase contrast (B, D, and F) images of a GFP-positive cell monitored as it generated a neurosphere. The GFP fluorescence is progressively reduced as the neurosphere grows due to dilution of the adenovirus genome or promoter inactivation (E). (A-B), 3 DIV; (C-D), 5 DIV; (E-F), 8 DIV. (G) Double-staining with Tuj1 (red) and GFAP (green) of a secondary neurosphere derived from the one in (F) differentiated into neurons and glia upon removal of EGF. Scale bars: (A-F), 25 μ m; (G), 50 μ m. The table shows the percentage of GFP-positive cells after dissociation and the proportion of these cells that gave rise to neurospheres in four independent experiments.



secondary neurospheres also differentiated into neurons and glia after plating (Fig. 6G). Hence, cells derived from type B cells can self-renew and produce differentiated cell types under the neurosphere culture conditions. Taken together with the *in vivo* experiments described above, the data indicate that type B cells are the SVZ stem cell.

Discussion

It is classically believed that stem cells possess a very immature and undifferentiated phenotype. Furthermore, the lineages of neurons and glia have long been thought to diverge early in embryonic development. In the shadow of these dogmatic beliefs, the suggestion that a glial-like cell gives rise to neurons in the adult brain seems extraordinary.

Recently, Johansson et al. (Johansson et al., 1999) suggested that ependymal cells are multipotent neural stem cells. While the results of Johansson et al. and those presented in this chapter (and in Doetsch et al., 1999a) agree in that they describe a neural stem cell with mature cellular characteristics, they disagree upon the exact identity of the SVZ stem cell. The experimental foundation of the controversial claims about SVZ stem cell identity has received careful appraisal (Barres, 1999; Momba et al., 2000; Lim and Alvarez-Buylla, 2001). Johansson et al. claim that the ependymal cells are SVZ label-retaining cells. However, EM was not used to definitively demonstrate the mitotic marker in ependymal nuclei. Type B cells sometimes have their nuclei separated from the ventricular lumen by only a thin process of an adjacent ependymal cell, and such a nuclei could be easily mistaken as belonging to an ependymal cell (Doetsch et al., 1999a;

expression in ependymal cells is due to the use of polyclonal antibodies that may cross-react with related intermediate filament proteins.

Doetsch et al., 1999b) (Fig. 1B). In addition, some type B cells are interposed between ependymal cells and actually contact the ventricle; these type B cells may have their nuclei directly in the ependymal layer.

Do ependymal cells ever divide in vivo? Previous reports are also conflicting. A survey of the literature reveals reports concluding that the lateral ventricle ependyma do not divide and others that claim to have evidence of ependymal proliferation in the same area (Bruni, 1998). It is difficult to come to any conclusion from the earlier reports, as EM was not used to confirm ependymal cell identity in the lateral ventricle wall. There are also reports of ependymal cell proliferation in the 4th ventricle and central canal of the spinal cord. However, more detailed EM analysis is required to confirm that the proliferating cells in these caudal regions correspond to multiciliated ependymal cells. Johansson et al. show by EM a ventricle contacting cell in anaphase in the central canal, however this cell appears unciliated; furthermore, the disposition of the chromatin in the nucleus is not characteristic of a cell that has recently divided. Perhaps the ependymal cells along the neuraxis are not all equivalent. In children, ependymal tumors occur most frequently in the 4th ventricle, and this may reflect such intrinsic differences (Anonymous1998).

Epithelial layers with a stem cell component often display a remarkable regenerative capacity in pathological conditions. If the ependyma contains a stem cell, then one might expect this epithelium to regenerate after injury. However, there is presently no convincing evidence of ependymal regeneration after injury (Bruni et al., 1985). Interestingly, injury to the ependymal cells stimulates the subependymal

astrocytes to proliferate and form a gliotic scar which appears to substitute for the missing ependyma (Bruni et al., 1985; Grondona et al., 1996).

To determine if ependymal cells can give rise to OB neurons, Johansson et al. performed experiments that were designed to follow the fate of ependymal cells in vivo. To label ependymal cells, they injected either the fluorescent lipophilic label DiI or adenovirus carrying the β -galactosidase marker into the lateral ventricular lumen. One day after injection, labeled cells appeared restricted to the ependymal layer. Ten days after injection, a large number of labeled cells were found either en route to the OB or in the OB. The interpretation of this data is difficult. Intraventricular injections of tracer substances label all cells that contact the ventricle. Since some type B cells contact the ventricle, it is possible that the DiI injection labeled B cells as well as the ciliated ependyma. Transfer of DiI from the ependyma to other cell types is also difficult to rule out. Johansson et al. employed the adenoviral vector in an attempt to exclude these possibilities. They found that only ependymal cells express the adenovirus receptor CXADR and thus assumed that this would restrict adenoviral infection to the ependyma. This assumption is, however, not correct as adenoviral vectors have been reported to infect multiple brain cell types (Davidson et al., 1993) including astrocytes and other SVZ cells (Yoon et al., 1996; Doetsch et al., 1999a and this thesis). Furthermore, the fact that type B cells contact the ventricle complicates the adenovirus result in the same way it renders the DiI experiment difficult to interpret.

Johansson et al. also tested ependymal cells for their ability to produce multipotent neurospheres. From a population of dissociated SVZ cells, multiciliated ependymal cells were micromanipulated into single culture wells. About 6% of these

cells form neurospheres. The provocative results of Johansson et al. have not been yet confirmed by other groups. In similar experiments, Doetsch et al. were not able to grow neurospheres from ependymal cells. Chiasson et al. (Chiasson et al., 1999) reports that while ependymal cells can divide in culture, the proliferation is independent of EGF, and the EGF-grown ependymal cells cannot be passaged and do not differentiate into neurons.

Although it is tempting to relate EGF-responsive cells in vitro to the in vivo stem cell, a more conservative viewpoint is that the neurosphere assay reveals cell types that can self-renew in response to EGF signaling and can give rise to differentiated cell types. Understanding the signals endogenous to the SVZ neurogenic niche is a fundamental next step in explaining adult neurogenesis.

CHAPTER 3

Astrocytes provide a niche for SVZ neurogenesis

The description of the SVZ cellular architecture provides important clues about the regulation of SVZ neurogenesis. In vivo, type A cells and putative type C cells are in intimate contact with the SVZ astrocytes (type B cells). Type B cells also contact each other. Immunocytochemistry of forebrain sections shows that the highest density of GFAP-positive astrocytes is found in the SVZ. Astrocytes produce a variety of intercellular signals, both soluble and membrane associated, that influence central nervous system (CNS) development (Zaheer et al., 1995). Since astrocytes are in intimate contact with all of the SVZ cell types in vivo, I explored the possibility that astrocytes provide a neurogenic microenvironment for SVZ cells.

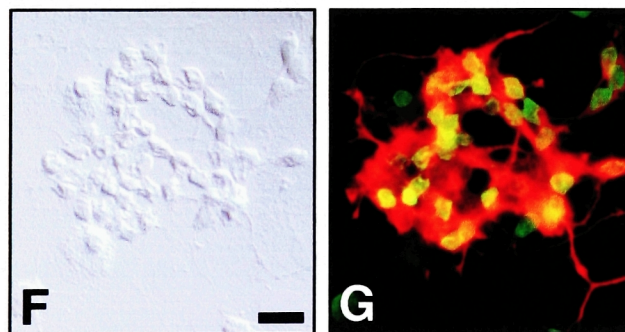
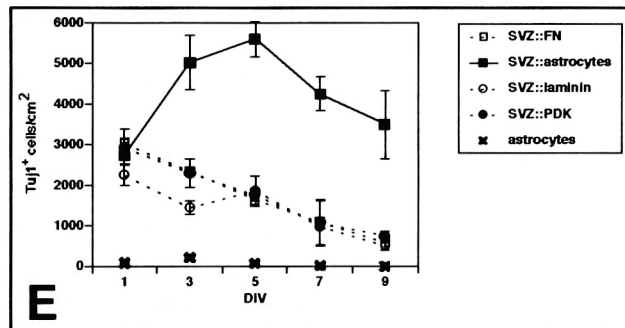
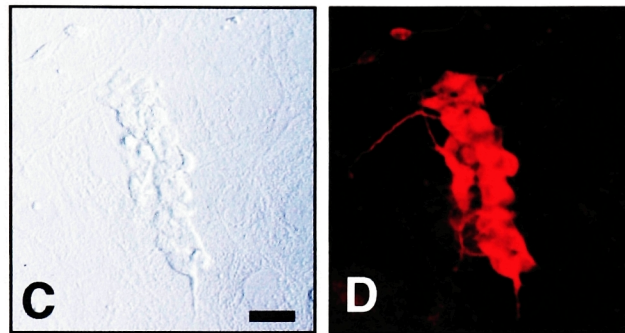
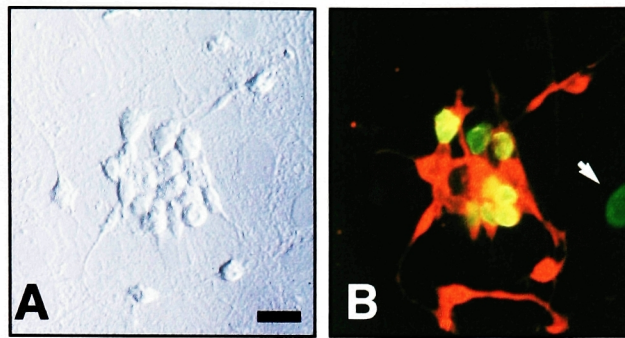
Astrocyte monolayers support neurogenesis of dissociated postnatal and adult SVZ cells

Confluent astrocyte monolayers were prepared from neonatal brains. Onto these monolayers, I plated dissociated SVZ cells from postnatal day-6 to day-10 mice at 5000 cells/cm² in serum-free medium. After one day in vitro (1 DIV), single, well-isolated SVZ cells were observed on top of the astrocytes by phase-contrast microscopy. By 3 DIV, clusters of 3-5 cells having a rounded, phase-bright morphology appeared in the astrocyte co-culture, and these clusters continued to form larger colonies (Fig. 7A). SVZ

Figure 7

Astrocyte monolayers support the proliferation and differentiation of SVZ cells.

(a) and (c) Differential interference contrast (DIC) images of typical colonies from postnatal SVZ precursors. (b) and (d) Epifluorescent images of (a) and (c), respectively. (b) Colonies are immunopositive for the Tuj1 neuronal marker (red) and have incorporated BrdU (green) between 4 and 5 DIV. (d) Colonies are also immunopositive for neuronal marker MAP-2. (e) Time course of SVZ neurogenesis. Tuj1+ cell density in co-culture v. culture on different substrates is reported at 2 day intervals. Error bars = SEM of triplicate cultures. Astrocyte monolayers alone did not produce Tuj1+ cells at any time point. (f) DIC image of a neuronal colony from the adult SVZ. (g) Respective epifluorescence showing BrdU incorporation (green) and Tuj1 immunoreactivity (red). All above cultures were photographed at 5 DIV. Bar = 20 μ m.



cells plated onto poly-D-lysine (PDK), laminin, or fibronectin substrates remained as single cells and did not form colonies at any time point.

Colonies that formed on astrocytes were immunopositive for both a neuron-specific β -tubulin revealed by monoclonal antibody Tuj1 (Fig. 7B), and the neuron-specific microtubule associated protein MAP2 (Fig. 7C,D). Furthermore, SVZ-derived colonies were immunopositive for PSA-NCAM (Fig. 10G,H). The presence of the above markers and the small ($<10\mu\text{m}$ diameter) rounded somas with one or two processes identified the cells in the colonies as SVZ Type A neuroblasts. To confirm that these neuronal colonies arise by proliferation, a nucleotide analog, bromodeoxyuridine (BrdU) was added to co-cultures at 4 DIV. Within 24 hours, many of the Tuj1⁺ cells were labeled (Fig. 7B).

The supporting astrocyte monolayers were initially prepared from SVZ cell dissociates. However, SVZ astrocyte preparations alone gave rise to a small number of neuronal colonies, supporting the view that the type B cells are neurogenic. I therefore used cortically-derived astrocytes, which were morphologically and immunocytochemically (GFAP⁺ and S100⁺) similar to SVZ Type B cells. Cortical astrocytes alone never gave rise to neuronal colonies but supported SVZ neurogenesis. To confirm that the colonies arose from SVZ-derived cells, I used transgenic SVZ cells that constitutively express β -galactosidase (Tan and Breen, 1993). All Tuj1⁺ colonies on non-transgenic astrocyte monolayers were X-Gal⁺ (data not shown).

I performed a time course of SVZ neurogenesis on astrocyte monolayers, poly-D-lysine, laminin, and fibronectin substrates (Fig. 7E). There was no difference of SVZ-cell plating efficiency among the different conditions. The density of Tuj1⁺ cells in

astrocyte co-culture increased rapidly, reaching a maximum at 5 DIV. On the other culture substrates tested, the density of Tuj1+ cells decreased linearly. This decline was attributed to Tuj1+ cell death as Tuj1+ cell debris increased with time.

Astrocyte monolayers also supported neurogenesis of adult-derived SVZ cells. SVZ cells dissociated from 3-month-old CD-1 mice were plated onto astrocyte monolayers or PDK substrate. Neuronal colonies identical in appearance to those derived from postnatal cells formed in astrocyte co-culture (Fig. 7F); none were observed on the PDK substrate. Staining for Tuj1 and BrdU incorporation between 4 and 5 DIV and confirmed the neuronal nature and proliferative origin of these adult-derived colonies (Fig. 7G).

Culture medium continuously conditioned by astrocytes did not support SVZ neurogenesis on PDK substrate (data not shown). A 20-fold concentration of this astrocyte-conditioned medium was also incapable of stimulating neurogenesis of SVZ cells on PDK, laminin, fibronectin, membranes isolated from cultured astrocytes, or killed astrocyte monolayers (data not shown, see Methods). Hence, it is possible that direct cell contact between SVZ precursors and live astrocytes is necessary for neurogenesis. 3T3 fibroblast monolayers did not support SVZ neurogenesis (data not shown), indicating that the neurogenic cell-cell interaction is specific to astrocytes.

SVZ cell types can be fractionated by differential adhesion to poly-D-lysine treated plastic substrates

SVZ dissociates were pre-plated onto PDK-treated plastic culture dishes for 16-20 hours, separating SVZ cells into two populations: flat, phase-dark tightly-adherent cells,

and rounded, phase-bright loosely-attached cells. The loosely-attached cells were first removed from the pre-plate culture by serial rinses of culture medium. The first fraction of cells (Fraction 1) was essentially homogeneous as assessed by both morphology (Fig. 8A) and immunocytochemistry (Fig. 8B,C). Fraction 1 reproducibly consisted of Tuj1+, PSA-NCAM+ cells with less than 1% contamination by GFAP+ glial cells (see inset, Fig. 9); hence, I designated Fraction 1 the Type A cell fraction. Type A cell identity was further confirmed in a chain migration assay. After six hours in vitro, aggregated Type A cells (Fig. 8D) began forming chains and migrated away from the aggregate (Fig. 8E). The migratory A cells were homogeneously Tuj1+ (Fig. 8F), and GFAP- (Fig. 8G). These results confirm a previous report that SVZ cells can migrate in chains in the absence of glia (Wichterle et al., 1997).

Fraction 1 contained the greatest number of cells (Fig. 9A). Fractions 2 and 3 were collected with continued and more vigorous rinsing of the pre-plate. Fraction 4 was collected after a brief treatment of trypsin. The yield of Fraction 4 was much greater than that of Fraction 3, suggesting that the last collection was selective for those cells tightly adherent to the pre-plate. Fraction 4 cells were mostly flat and phase-dark (Fig. 8I-K), and most were immunonegative for Tuj1 and PSA-NCAM (inset, Fig. 9). About one-third of these cells expressed GFAP. Because Fraction 4 was enriched for cells whose morphological and immunocytochemical profile resembled Type B (astrocytes) and Type C (immature) cells, I designated this fraction the B/C cell fraction.

Each fraction was tested for Tuj1+ colony formation in astrocyte co-culture. The neuronal colony forming precursors were found mostly in Fraction 4. About 25% of the Fraction 4 cells plated formed neuronal colonies. In other experiments in which the

Figure 8

Fractionation of SVZ cells by differential adhesion yields populations of cells with distinct characteristics.

(a-c) are of Fraction 1, Type A cells. See text and Fig. 3 for details. (a) DIC image of isolated Type A cells (b) epifluorescent image revealing Tuj1 staining (red). Although most fields did not include contaminating glia, this field was selected to show rare GFAP⁺ cells (arrow, green). (c) Purified Type A cells are PSA-NCAM⁺ (red). Purified Type A cells can migrate in chains. (d) Aggregate of Type A cells immediate after embedding in Matrigel. (e) Chain migration from aggregates after 6 hr in culture. The culture in (e) was double-stained for Tuj1 (f) and GFAP (g). (h) shows a positive control for GFAP staining (green) in Matrigel culture. (i-k) are of Fraction 4, B/C cells. Most of the adherent cells had a flattened, spread, phase-dark appearance. ~30% of these cells were GFAP⁺ (see inset, Fig. 3). Nuclei are counterstained with Hoechst 33258 (blue). Bar = 20 μ m.

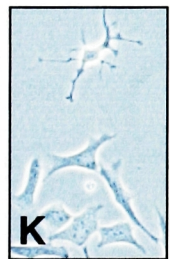
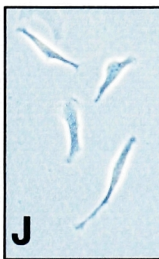
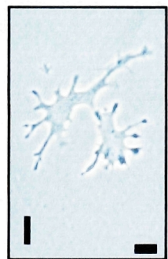
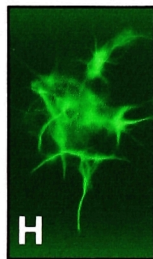
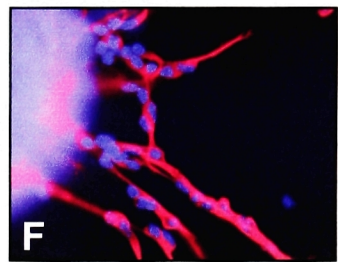
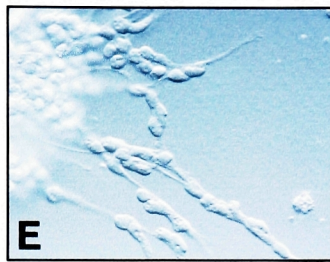
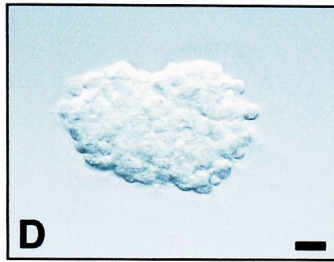
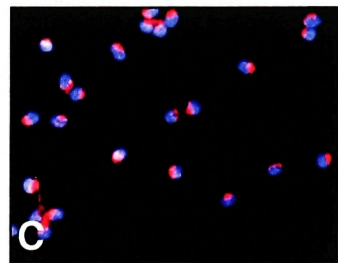
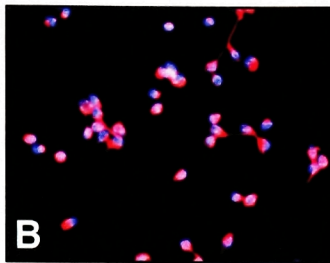
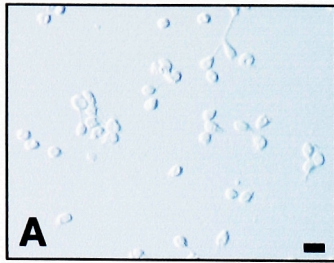
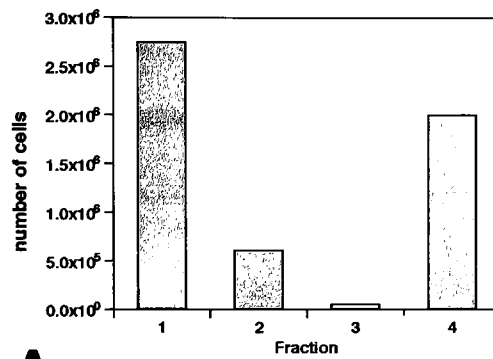


Figure 9

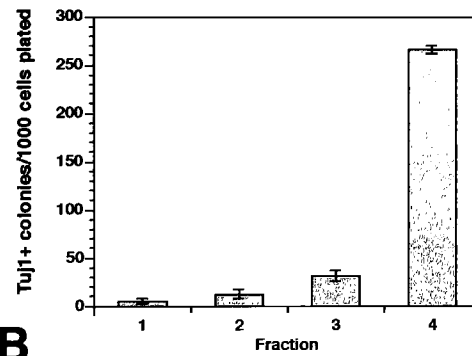
The four fractions of SVZ cells have different yields and abilities to generate Tuj1+ colonies.

(a) Fractionation yield. Fraction 4 was collected after treatment with trypsin. (b) Equal numbers of cells from the different fractions were plated onto astrocyte monolayers. Cultures were fixed at 5 DIV. Clusters of more than 4 Tuj1+ cells were counted as colonies. Error bars = SEM of triplicate cultures.

(Inset) Immunocytochemistry of Fraction 1 (Type A cells) and Fraction 4 (Type B/C cells) purity. For every SVZ fractionation, an aliquot of each fraction was plated for immunostaining for Type A markers (Tuj1 and PSA-NCAM) and a Type B marker (GFAP). Between 500 and 1000 cells were counted in each fraction. Standard deviation is indicated in parentheses. Note that in Fraction 4, almost half of the cells were immunonegative for any of the three markers; these are putative Type C cells.



A



B

	<u>%Tuj1+</u>	<u>%GFAP+</u>	<u>% PSA-NCAM+</u>
Frac. 1	98.8 (±0.789)	0.484 (±.408)	98.9 (±0.545)
Frac. 4	14.2 (±4.58)	36.1 (±20.6)	18.3 (±1.13)

SVZ-derived cells were first labeled with a lipophilic fluorescent dye PKH26, many Fraction 4 cells were observed to attain a flat, astrocyte morphology. Thus, Fraction 4 cells give rise to both glia and neurons. The small number of cells in Fractions 2 and 3 had cellular compositions and colony forming potentials intermediate to those of Fractions 1 and 4, therefore these fractions were not studied further.

Type A cells do not proliferate to form colonies in astrocyte co-culture

In vivo (Menezes et al., 1995) and in vitro studies (Luskin et al., 1997) have shown that Type A cells undergo mitosis, but whether these cells have the potential to proliferate extensively is not known. Previous studies in vivo (Lois and Alvarez-Buylla, 1994; Doetsch et al., 1997) left open the possibility that Type A cells divide symmetrically to provide a continuous supply of themselves. To investigate whether co-culture with astrocytes can stimulate Type A cells to produce greater numbers of themselves, I plated purified Type A cells at 5000 cells/cm² onto astrocyte monolayers or PDK substrate. On astrocytes, Type A cells did not form colonies but instead remained as single cells, extended neurites (Fig. 10B), and did not incorporate BrdU (data not shown). While astrocyte co-culture did not stimulate proliferation and colony formation, type A cell survival was enhanced. At 3 and 5 DIV, nearly all of the type A cells were surviving on astrocytes (Fig. 10A compare 1 DIV to 3 and 5 DIV, black boxes) whereas on PDK, only 74% and 66% were surviving at 3 and 5 DIV, respectively (Fig. 10A, open boxes). Enhancement of survival was not seen at 7 and 9 DIV.

The Type B/C cell fraction contains precursors capable of proliferating to form colonies of Type A cells

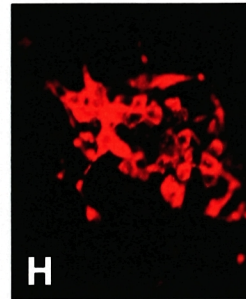
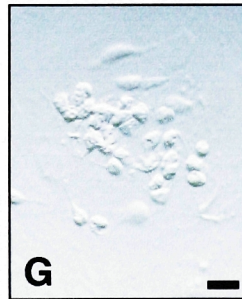
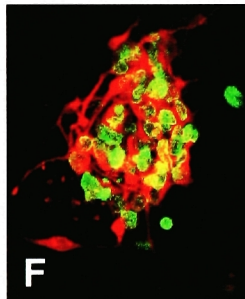
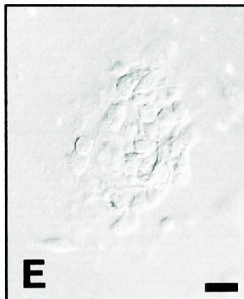
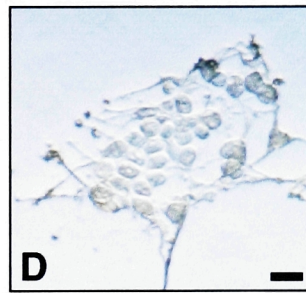
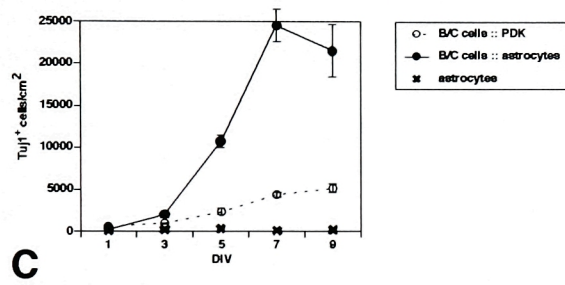
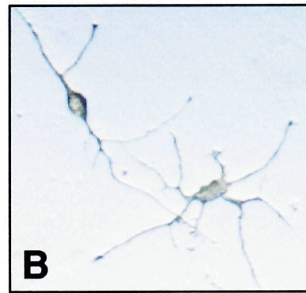
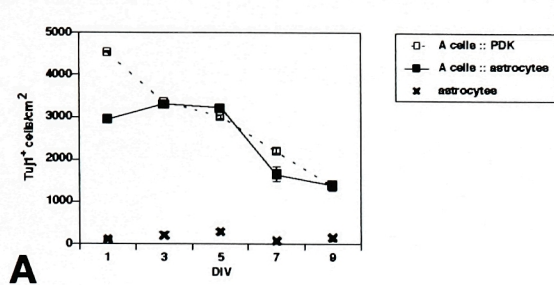
It has been proposed that the Type C cells are the immediate precursors of Type A cells (Doetsch et al., 1997), and that Type B cells are the precursor of either Type A or C cells (García-Verdugo et al., 1998; Doetsch et al., 1999a). I plated B/C cells at 5000 cells/cm² onto either astrocyte monolayers or PDK substrate. At 1 DIV, there were fewer than 600 Tuj1+ cells/cm² in both culture conditions (Fig. 10C). By 3 DIV, phase-bright colonies of fewer than 8 rounded cells were observed by phase-contrast microscopy in the astrocyte co-cultures, and these colonies continued to grow (Fig. 10D, 5 DIV). The cells proliferated until reaching a plateau of 23,000 Tuj1+ cells/cm² at 9 DIV (Fig. 10C), a nearly 40-fold increase in neuronal cell number. To confirm that most Tuj1+ cells counted in the B/C-astrocyte co-culture arose from proliferation, I labeled dividing cells with BrdU between 2 and 4 DIV. Double-staining for Tuj1 and BrdU at 4 DIV revealed that 87% (SEM=4%, n=3) were double-labeled (Fig. 10E,F). Thus, most Tuj1+ cells counted in this neurogenesis assay were born in culture. Colonies at 5 DIV were also immunopositive for PSA-NCAM, another marker of Type A cells (Fig. 10G, H).

There was a modest increase in Tuj1+ cell number when Fraction 4 B/C cells were cultured on PDK (Fig. 10C). However, I noticed that in these cultures, some SVZ astrocytes had proliferated, and the Tuj1+ colonies were always on top of the flat SVZ-derived astrocytes. From this, I inferred that astrocytes from Fraction 4 proliferated on the PDK substrate and served as a substrate for the neuronal precursors, inducing the formation of a few Type A cell colonies.

Figure 10

Fraction 1 (Type A cells), and Fraction 4 (Type B/C cells) in astrocyte co-culture.

(a) Time course of A cell-astrocyte co-culture v. culture on poly-D-lysine. Error bars = SEM of triplicate cultures. (b) Tuj1+ cells stained with DAB in A cell-astrocyte co-culture at 5 DIV. (c) Time course of B/C cell-astrocyte co-culture v. culture on poly-D-lysine. (d) Typical colony of Tuj1+ cells stained with DAB in astrocyte co-culture at 5 DIV. (e and f) co-cultures were exposed to BrdU from 2 to 4 DIV. (e) DIC image of a neuronal colony. (f) Same colony double-stained for Tuj1 (red) and BrdU (yellow-green). DIC (g) and epifluorescent (h) images of a neuronal colony stained for PSA-NCAM. Bars = 20 μ m.



Type B cells in vitro give rise to colonies of type A cells

Adult SVZ cells from hPAP transgenic mice (Deprimo et al., 1996) were plated at low density onto astrocyte monolayers such that fewer than 10 type A cell colonies formed per cm². hPAP mice express human placental alkaline phosphatase in the membrane of all cells. To identify SVZ-derived cells, cultures were stained with NBT/BCIP to reveal the hPAP marker gene product (Fig. 11A, purple stain). At 1DIV, single SVZ-derived cells were isolated from one another by hundreds of microns. Some of these single cells had flattened-morphology (Fig 11A, 1DIV). About 25% of SVZ cells with this flattened morphology in vitro can be double labeled with GFAP (inset, Fig. 9). At 2 DIV, doublets of these flattened cells were observed, suggesting their division. By 5 DIV, colonies also contained smaller cells with a rounded soma (type A cells) as well as those with the flattened morphology. At 5 DIV, colonies can contain all three SVZ cell types as determined by immunostaining in other experiments (Fig. 11B). At 7, 9, and 11DIV, the colonies were larger and contained a greater proportion of the small, rounded, type A neuroblasts (Fig. 11A). Notice that in these later colonies, the flat cells are still present, suggesting their self-renewal.

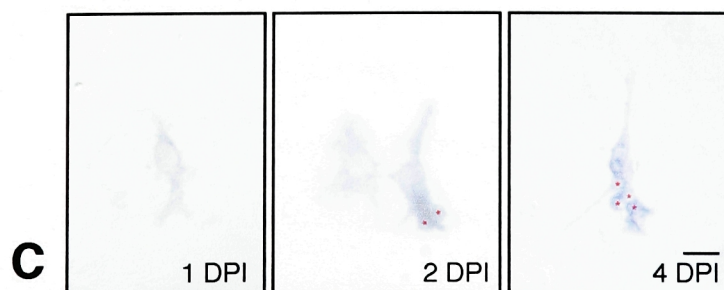
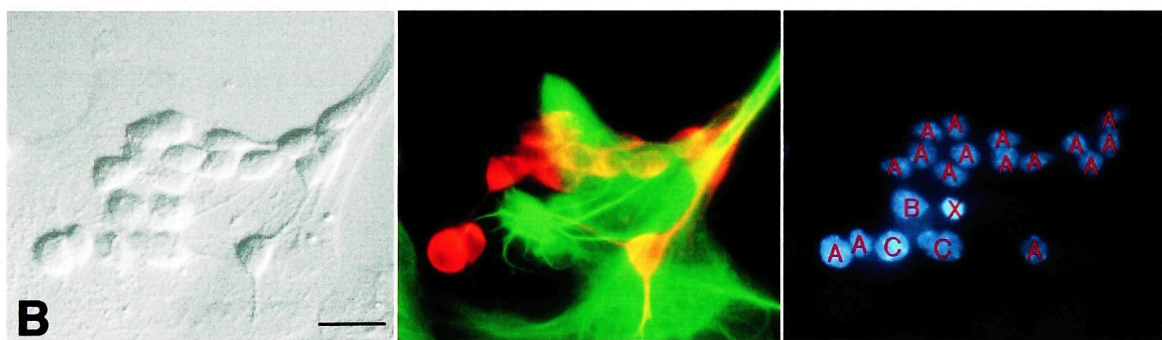
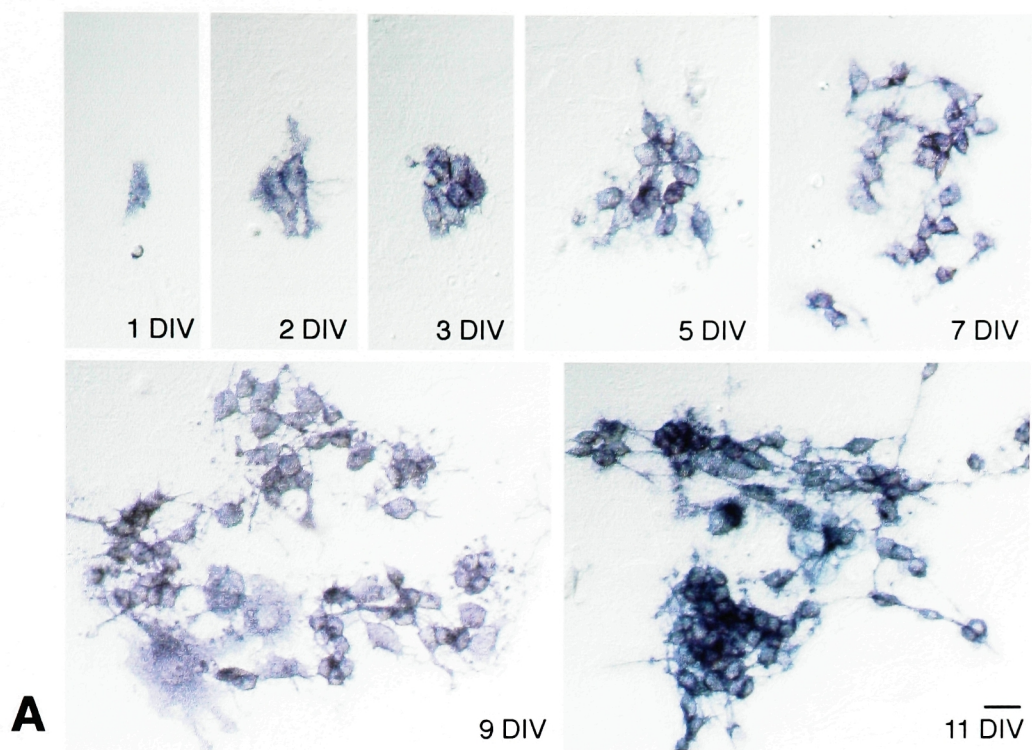
To specifically follow the fate of type B cells in culture, I infected SVZ cells from GFAPP-tva transgenic mice (Holland and Varmus, 1998) (see Chapter 2) with an RCAS-alkaline phosphatase (AP) marker retrovirus. Only mitotic GFAP-positive cells can incorporate the AP marker into their genome. One day post infection (1DPI), AP-positive cells with the flattened-morphology were observed (Fig. 11C, 1DPI); this cell is derived from a dividing type B cell. At 2DPI, clusters of AP-positive cells now contained type A cells (Fig. 11C, 2DPI), and the number of type A cells in these clusters

Figure 11

(A) Single adult SVZ cells can give rise to colonies containing multiple cell types.

Time course of adult hPAP SVZ cells in astrocyte co-culture. The hPAP marker stains purple. At 1 DIV, isolated SVZ cells are observed. At 2 DIV, doublets of flat SVZ cells arise. Later, at 5 – 11 DIV, colonies contain flat cells and round type A cells. (B)

Colonies at 5 DIV can have all three SVZ cell types. Left: DIC image of SVZ cell colony. Middle: Tuj1 (red) stains type A cells and GFAP (green) stains type B cells and the monolayer below. Notice that some cells do not stain for either Tuj1 or GFAP; these are likely type C cells. Right, nuclear counterstain of the colony at left and middle. The nuclei of the monolayer cells are very large and faint and thus easily distinguishable from those of SVZ-derived cells. Cell types are indicated in red letters. (C) **Type B cells can give rise to colonies of type A cells.** The fate of type B cells was followed in vitro with an RCAS virus that can label only dividing type B cells. At 1 day post-infection (1 DPI), solitary flat cells are seen. These have morphologies similar to those in (A) and (B). At 2 DPI, some colonies contain both flat cells and rounded type A cells (indicated by red dots). The number of type A cells increases with time (4 DPI). Scale bar = 10 μ m.



increased with time (Fig. 11C, 4DPI). These experiments show that colonies of type A cells are derived from dividing type B cells.

Discussion

Culturing dissociated postnatal or adult SVZ cells on astrocyte monolayers – but not other substrates – recapitulated the extensive neurogenesis observed *in vivo*. In a serum-free medium free of exogenous growth factors, SVZ precursors proliferated rapidly on astrocytes to form colonies containing up to a hundred Type A neuroblasts. Pure Type A cells could migrate but themselves did not give rise to neuronal colonies. Colonies of type A cells were shown to be derived from dividing type B cells, and the neuronal colony-forming precursors could be isolated by differential adhesion to plastic.

Although the continued presence of the flat, putative type B cells in colonies with type A cells suggests that type B cells are self-renewing, it is not clear if this self-renewal occurs through asymmetric division or through populational asymmetry. It would be ideal to directly observe the self-renewing behavior of type B cells in these astrocyte co-cultures using time lapse video microscopy. Using the GFAPp-GFP adenovirus to vitally identify dissociated type B cells, I was able to record the cellular behavior of these neural stem cells. However, currently, my time lapse cultures (similar to those of Wichterle et al., 1997) become unhealthy within 3 days. Furthermore, as has been previously reported (Liu et al., 1999), it appears that in these cultures the GFP protein may be somewhat toxic to type B cells⁷. I had also engineered an RCAS-GFP retrovirus for use with the GFAPp-

⁷ It is not clear why GFP toxicity was not observed in the neurosphere cultures (Chapter 2). I can only speculate that EGF induces "protective" signals that can compensate for the GFP toxicity.

tva mice, however expression levels of GFP in mouse cells were not sufficient for standard epifluorescent detection.

Direct contact between astrocytes and SVZ precursors may be necessary for the neurogenesis. Soluble factors produced by astrocytes may be necessary for SVZ neurogenesis but not sufficient. Direct contact with astrocytes also regulates neurogenesis of other precursors in vitro. Olfactory receptor precursors cultured on cortical astrocytes proliferate extensively and differentiate into mature olfactory receptor neurons (Pixley, 1992; Grill and Pixley, 1997). Cortical neuron precursors from the embryo are maintained in division by contact with astrocytes (Davis and Temple, 1994). Although astrocytes are not present in either the PNS olfactory epithelium where olfactory precursors reside, or in the developing ventricular zone, contact with astrocytes stimulates neurogenesis of precursors from these germinal zones. In contrast, neuronal precursors from the external germinal layer of the developing cerebellum cease neurogenesis when in contact with astrocytes (Gao et al., 1991). Hence, different precursors respond differently to the astrocyte microenvironment.

Astrocytes may present a neurogenic microenvironment at their cell surface with a combination of growth factors, extracellular matrix (ECM), and membrane-bound molecules. It is possible that the extracellular milieu at the interface between astrocytes and precursors concentrates and/or stabilizes soluble factors. Growth factors are often bound to ECM or membrane-bound molecules (reviewed in Flaumenhaft and Rifkin, 1991). Temple et al. (Temple, 1989) found that embryonic cortical precursors continue to divide in conditioned medium supplemented with membranes prepared from cultured astrocytes or glial cells. I attempted similar experiments in which I cultured SVZ

precursors in conditioned medium on astrocyte membrane preparations or killed astrocyte monolayers; however, such cultures did not recapitulate the in vitro neurogenesis. SVZ neurogenesis may require cell-cell interaction with live astrocytes. An intriguing possibility is that contact with SVZ precursors induces astrocytes to generate a neurogenic microenvironment at their cell surface. Most importantly, this study reveals that for the brain, as for other tissues, the cell-cell interaction within the stem cell niche is a critical factor for neurogenesis.

SVZ precursors cultured on astrocytes undergo extensive neurogenesis, generating an in vitro model of the adult SVZ. This model is not unlike the cultures used to study blood cell development in which precursors cultured on bone marrow stromal cells undergo hematopoiesis. Hence, this colony-forming assay can be exploited in the same way that hematopoiesis models have been used to discover the signals that direct proliferation and differentiation.

CHAPTER 4

Noggin antagonizes BMP signaling to create a niche for adult neurogenesis.

SVZ cells transplanted to non-neurogenic brain regions differentiate primarily into astrocytes (Herrera et al., 1999). In the adult SVZ, the vast majority of cells born in the SVZ migrate to the OB where they become interneurons in the granule or periglomerular layer (Lois and Alvarez-Buylla, 1994; Doetsch and Alvarez-Buylla, 1996). No cells migrating from the SVZ have been traced to an astrocytic fate. One interpretation of these findings is that there are instructive signals for a neuronal lineage in the SVZ, and that these signals are absent from non-neurogenic regions of the brain. Another notion is that outside of the SVZ there are instructive cues for astrocytic differentiation, and that these cues are not present in the SVZ niche. These two views, of course, are not mutually exclusive. I sought to identify the external signals that promote neurogenesis in the SVZ and determine the mechanisms by which they act.

Noggin belongs to a class of polypeptides that bind to bone morphogenetic proteins (BMPs) and consequently prevent their activation of BMP receptors (BMPRs) (reviewed in Wilson and Hemmati-Brivanlou, 1997). In *Xenopus* gastrula stage embryos, Noggin is secreted by the Spemann organizer (Smith and Harland, 1992) and induces neural tissue from dorsal ectoderm (Lamb et al., 1993) by inhibiting ectodermal BMPs (Wilson and Hemmati-Brivanlou, 1995; Zimmerman et al., 1996). In the mouse embryo, Noggin is not required for neural induction, however it is essential for the later

development of the neural tube, somite (McMahon et al., 1998), and cartilage morphogenesis (Brunet et al., 1998). Recently it was shown that double homozygous mutants of the BMP antagonists Noggin and Chordin have defects in the development of the prosencephalon (Bachiller et al., 2000). Noggin has also been shown to negatively regulate neuronal differentiation of neocortical precursors in vitro (Li and LoTurco, 2000).

BMPs have multiple roles in embryonic brain development. BMPs promote astroglial lineage of epidermal growth factor (EGF)-amplified cells from the embryonic SVZ (Gross et al., 1996), induce neuronal differentiation of cortical ventricular zone (Li et al., 1998), inhibit neurogenesis of embryonic olfactory epithelial progenitors (Shou et al., 1999), and regulate cortical cell number and phenotype (Mabie et al., 1999).

While the functions of Noggin and BMPs in development have been studied, their roles in the adult brain have not been described. Noggin (Valenzuela et al., 1995), BMPs (Gross et al., 1996), and BMPRs (Soderstrom et al., 1996a; Zhang et al., 1998) continue to be expressed in the adult brain. In this chapter, I show that Noggin is expressed by ependymal cells and provide evidence indicating that Noggin protein antagonizes BMP signaling to create a neurogenic niche for SVZ cells.

Noggin is expressed by adult brain ependymal cells

Reverse-transcription-polymerase chain reaction (RT-PCR) analysis of microdissected SVZ tissue including the adjacent ependyma showed that Noggin transcripts are present in this region (Fig. 12A). To determine the cell type that expresses Noggin protein, I immunostained brain sections with Noggin antibodies. Confocal image

Figure 12

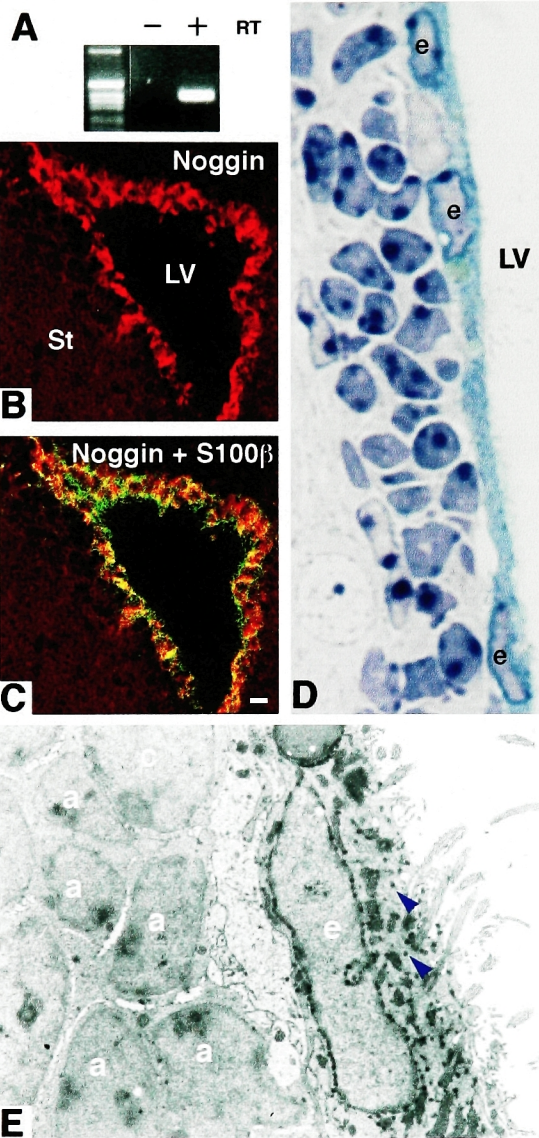
Noggin expression in adult ependymal cells

RT-PCR detects Noggin transcripts in SVZ dissections that include ependymal cells. (A) Noggin-specific primers amplified a single band of expected size (343nt). Omission of reverse-transcriptase (RT-minus lane) resulted in no amplification.

Monoclonal antibody to Noggin protein stains ependymal cells. Noggin staining (A, red fluorescence) co-localized with ependymal marker S100 β (C, yellow fluorescence = co-localization). Bar = 10 μ m.

Noggin gene expression is localized to ependymal cells. Mice heterozygous for Noggin-LacZ gene-replacement were analyzed for LacZ expression. In these animals, LacZ expression parallels Noggin gene expression. (D) Semi-thin (1.5 μ m) section stained with X-Gal revealed Noggin-LacZ expression (sky blue deposit) in ependymal cells (marked with "e"). Underlying SVZ cells (nuclei are revealed by the toluidine blue counterstain) do not express Noggin-LacZ. (E) Ultrathin sections reveal the X-Gal deposit as dark, electron dense particles (blue arrowheads) in the cytoplasm of ciliated ependymal cells. SVZ cell types identified by ultrastructural characteristics are labeled and do not have X-Gal deposits.

LV= lateral ventricle, St = striatum, a = type A cell, b = type B cell cytoplasm, c = type C cell, e = ependymal cell



analysis revealed strong Noggin immunoreactivity in the cells that line the ventricle lumen (Fig. 12B, red fluorescence). S100 β , a marker of ependymal cells (Didier et al., 1986), co-localized with the Noggin staining (Fig. 12C, yellow fluorescence = co-localization), indicating that Noggin protein is expressed by the ependymal cells.

To confirm the ependymal Noggin expression and to obtain a higher cellular resolution, I utilized the Noggin-LacZ "knock-in" heterozygous mice (McMahon et al., 1998). Noggin-LacZ heterozygotes develop normally and express the LacZ marker in parallel with Noggin (McMahon et al., 1998). Brains from adult heterozygous Noggin-LacZ mice were sectioned, stained with X-Gal, and prepared for electron microscopy. 2 μ m thick plastic sections of the lateral ventricle wall revealed a dense, blue X-gal cytoplasmic reaction deposit in ependymal cells (Fig. 12D). Brain sections from wild-type littermates did not stain with X-gal. Electron microscopy of ultrathin sections confirmed the ependymal localization of the X-gal deposit (seen as dark, black granules in the cytoplasm, Fig. 12E, blue arrowheads).

BMPs and their cognate receptors are expressed in the SVZ.

To determine if BMP and BMPRs are present in the SVZ, I performed RT-PCR on microdissected SVZ tissue (Fig. 13A). Transcripts for BMP2 and 4, BMPR IA, BMPR IB, and BMPR II were amplified from SVZ-derived cDNA. Dissociated SVZ cells can be separated by differential adhesion to poly-lysine coated plastic into two fractions, one consisting of >98% type A cells and the other enriched for type B and C cells (Chapter 3, Lim and Alvarez-Buylla, 1999). I performed semi-quantitative RT-PCR on the two fractions of SVZ cells (Fig. 13B). Expression of BMP2 and 4 was higher by

Figure 13

BMP and BMP receptor expression in SVZ cells

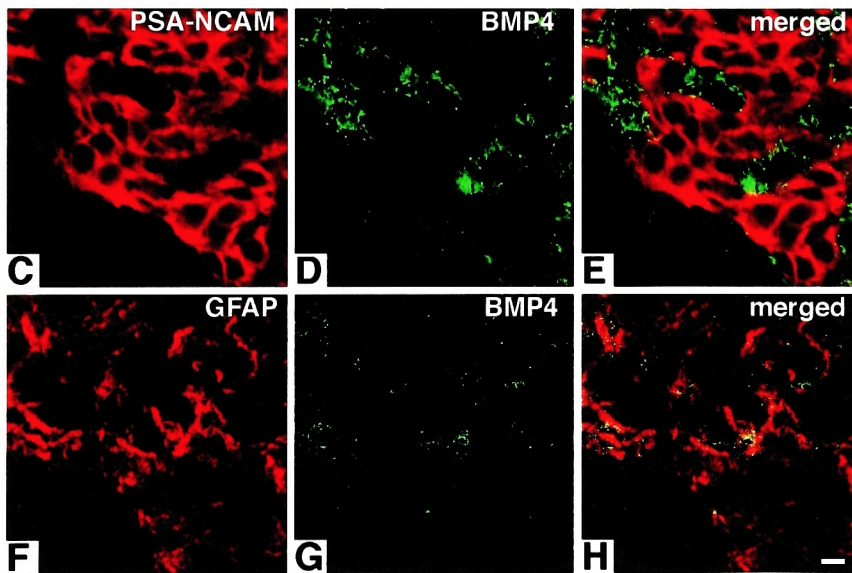
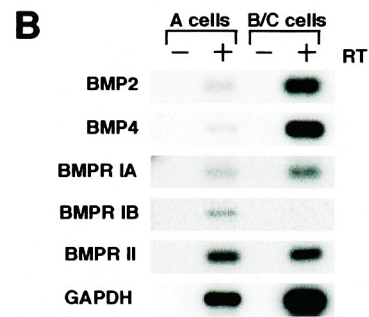
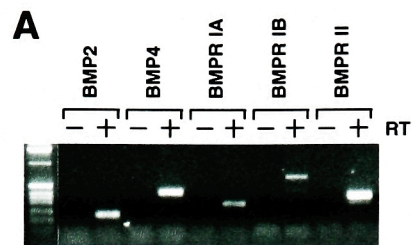
(A) RT-PCR analysis of SVZ tissue detected transcripts for BMP ligands 2 and 4 and receptors BMPR IA, BMPR IB, and BMPR II. Omission of reverse-transcriptase (RT-minus lanes) resulted in no amplification. Amplified bands were cloned and sequenced to verify the specificity of the PCR reaction.

Semi-quantitative RT-PCR analysis of purified type A cells and type B/C cell population.

(B) BMP2 and 4 were predominantly expressed by B/C cells. BMPR IB was expressed only in type A cells. BMPR IA and BMPR II receptors were detected in both SVZ cell populations.

SVZ type B cells express BMP4 protein. (C-E) BMP4 protein (green fluorescence) was not detected in type A cells (PSA-NCAM staining, red fluorescence) BMP4 staining was largely found around the chains of type A cells in the position expected for type B cells.

(F-H) BMP4 protein staining (G and H, green fluorescence) co-localized with a type B cell marker, GFAP (F, red fluorescence; H, yellow = co-localization). Images are of 1 μ m confocal optical sections. Bar = 5 μ m



20- and 25-fold, respectively, in the B/C cell fraction as compared to the type A cell fraction. BMPR IA and BMPR II were detected in both fractions. Interestingly, BMPR IB was detected only in the A cells. To localize BMP4 in vivo, I immunostained coronal brain sections with an anti-BMP4 antibody. BMP4 staining was not found in PSA-NCAM-positive type A cells (Fig 13C-E). Instead, GFAP and BMP4 co-localized (Fig. 13F-H), suggesting that BMP4 is produced by type B cells.

BMPs inhibit neurogenesis of SVZ cells

Since adult SVZ cells express BMPs and their receptors, I determined the effect of BMP ligands on SVZ neurogenesis. As described in Chapter 3, dissociated SVZ cells cultured on astrocyte monolayers in medium free of serum or exogenous growth factors generate large colonies of type A cells (Lim and Alvarez-Buylla, 1999). These neurogenic colonies arise from type B and C cells and not type A cells. Figure 14A-B shows a typical colony in these co-cultures. These colonies express markers of type A cells including the neuron-specific β -tubulin revealed by Tuj1 staining (red, Fig. 14B). Proliferating cells (green nuclei, Fig. 14B) were marked with the nucleotide analog bromodeoxyuridine (BrdU) between 4 and 5 days in vitro (DIV), demonstrating that type A cells were born in vitro.

BMPs greatly reduced adult SVZ cell neurogenesis in SVZ co-cultures. 50 ng/ml of BMP4 decreased the number of neurons born between 4 and 5DIV by over 10-fold as compared to controls (Fig. 14C). 50ng/ml of BMP2 had a similar effect on SVZ neurogenesis, nearly abolishing the birth of new neurons (Fig. 14D). The addition of BMPs did not change the initial SVZ cell survival as measured by plating efficiency at 24

Figure 14

BMPs inhibit SVZ neurogenesis

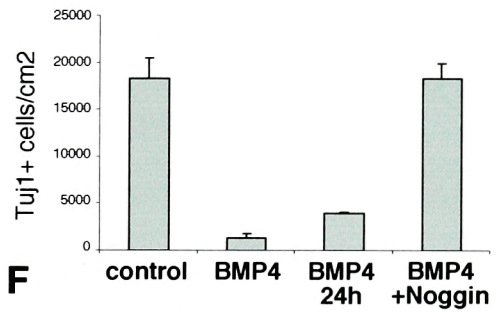
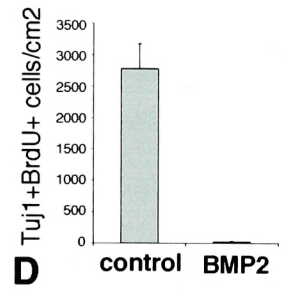
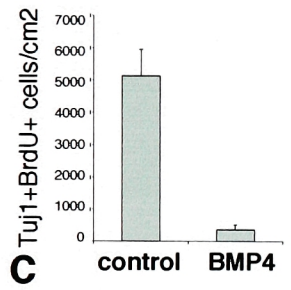
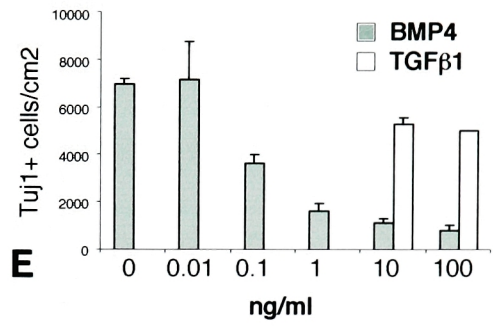
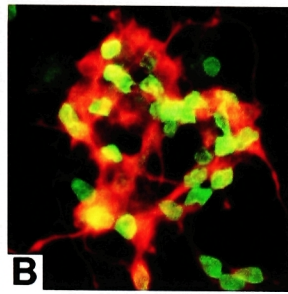
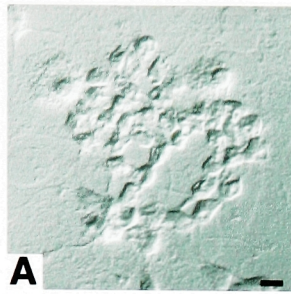
(A-B) Neurogenic colony derived from an adult SVZ precursor cell at 5DIV in astrocyte co-cultures. BrdU was added at 4DIV. Nearly all of the cells in this colony are immunopositive for the type A cell neuronal marker Tuj1 (B, red) and have incorporated the BrdU mitotic marker (B, green). In (C-D), neurogenesis was quantified by direct cell counting of Tuj1-positive, BrdU-positive double-stained cells. Scale bars = 5 μ m.

(C) BMP4 inhibits neurogenesis of adult SVZ cells. BrdU was added at 4DIV and cultures analyzed at 5DIV. 50ng/ml of BMP4 decreased the number of Tuj1-positive, BrdU-positive cells by over 10-fold. (D) BMP2 at 50 ng/ml nearly abolished the birth of new neurons.

(E) BMP4 inhibits SVZ type B/C cells production of type A cells in a dose-dependent manner. SVZ type B/C cells were co-cultured on astrocyte monolayers in increasing concentrations of BMP4. All Tuj1+ type A cells counted at 5DIV in this assay are born in vitro (Lim and Alvarez-Buylla, 1999). 50% inhibition of type A cell production was achieved by 0.1ng/ml of BMP4. TGF β did not significantly reduce neurogenesis (open bars).

(F) Continuous exposure to BMP4 is not necessary for inhibition of SVZ neurogenesis. Transient, 24h exposure to BMP4 (BMP4 24h) inhibited B/C cell neurogenesis by 4-fold. Continuous exposure to BMP4 reduced neurogenesis by 7-fold. Preincubation of BMP4 with the BMP antagonist Noggin (BMP4 + Noggin) abolished BMP4 activity.

Data shown are from experiments performed in triplicate. Error bars = SEM.



hours, and did not increase cell death in the co-cultures (see next section). In co-cultures of type B/C cells on astrocytes, the production of new neurons is linear at 5DIV, with peak production occurring between 7 and 9DIV (Lim and Alvarez-Buylla, 1999). BMP4 inhibited neurogenesis 5DIV in a dose-dependent manner, with 50% inhibition occurring at 0.1ng/ml (Fig. 14E). In this assay, BMP4 at 100ng/ml inhibited neurogenesis by 7-fold. Thus, BMP4 can inhibit type B/C cells from generating type A cells. TGF β (Fig. 14E) or GDNF (not shown), molecules related to the BMPs, did not significantly inhibit neurogenesis at the two highest concentrations (10 and 100ng/ml) tested.

I next tested whether continuous exposure to BMP4 is required for inhibition of neurogenesis. Type B/C cell co-cultures were exposed to 50ng/ml of BMP4 for 24h, after which the BMP ligand was removed with three changes of medium. The 24h exposure to BMP4 result in a 4-fold reduction of neurogenesis at 5DIV as compared to controls that underwent a similar medium change at 24h (Fig. 14F). Continuous exposure to BMP4 reduced neuronal production by 7-fold in this experiment. This result suggests that continuous BMP signaling is not required to inhibit neurogenesis. Rather, a transient episode of BMP signaling is sufficient to reduce the neurogenic capacity of early SVZ precursors. BMP4 preincubated with 1 μ g/ml of Noggin protein was ineffective at inhibiting SVZ neurogenesis (Fig. 14F), confirming that the BMP ligand was responsible for the inhibitory activity in cultures.

BMPs promote survival of SVZ type A cells

In embryonic telencephalic (Furuta et al., 1997; Mabie et al., 1999), neural crest cell (Graham et al., 1996), and limb development (Merino et al., 1999), BMPs can induce

apoptosis. It was therefore possible that BMPs induce cell death of type A cells. To address this possibility, I tested the effect of BMP4 on purified type A cells. Type A cells were isolated by differential adhesion to poly-lysine coated plastic and cultured in the presence of different concentrations of BMP4 as well as brain-derived neurotrophic factor (BDNF), GDNF, and basic fibroblast growth factor (FGF2). BDNF is a known survival factor for many classes of neurons (reviewed in Barde, 1994) including type A cells which express the TrkB BDNF receptor (Kirschenbaum and Goldman, 1995; Zigova et al., 1998 and D. Lim, data not shown). Cell survival was assessed at 10DIV. Without additional factors, 36% of the initially plated type A cells survive at 10 DIV (Lim and Alvarez-Buylla, 1999 and this experiment). As expected, BDNF enhanced the survival of type A cells by approximately 40% at 10 and 100ng/ml, while neither GDNF nor FGF2 significantly altered cell survival (Fig. 15A). BMP4 enhanced type A cell survival by 40-50% at concentrations as low as 1ng/ml. Similar neurotrophin-like effects of BMPs have been described for CNS neurons (Jordan et al., 1997; Hattori et al., 1999; Espejo et al., 1999).

Since it was possible that BMPs indirectly induce cell death by acting on cell types other than type A, I measured the extent of cell death in SVZ co-cultures that contained all SVZ cell types. SVZ cell colonies were allowed to form for 5DIV and cultured for an additional 24h in the presence or absence of 50ng/ml of BMP4. Cell death was quantified by terminal transferase mediated dUTP nick end-labeling (TUNEL) staining, which detects DNA fragmentation associated with apoptosis, and by nuclear pyknosis. By both measures, BMP4 decreased the extent of cell death in cultures by 10-15% as compared to controls (Fig. 15B). Hence, BMPs do not inhibit SVZ neurogenesis

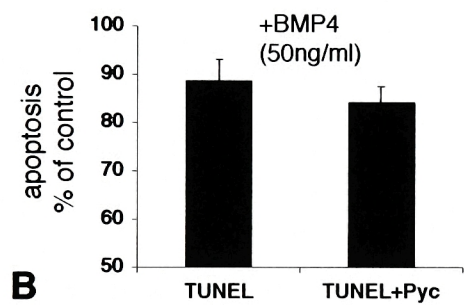
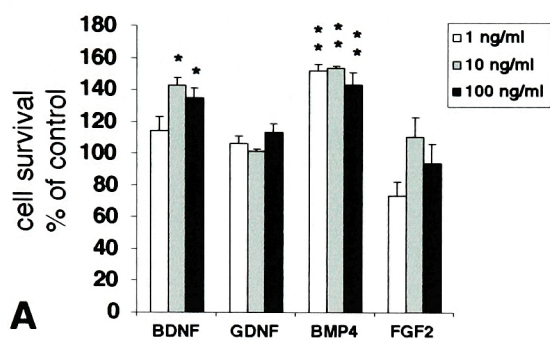
Figure 15

BMP4 promotes the survival of type A cells

Cell survival of pure type A cell cultures is enhanced by BMP4 or BDNF but not GDNF and FGF2. (A) Cell survival at 10DIV is represented as percentage of control. Factors were used at 1, 10, and 100ng/ml. BDNF increased survival by about 40% at 10 and 100ng/ml (* = $p < 0.05$, t-test). BMP4 was more potent, increasing survival by about 50% at all concentrations tested (** = $p < 0.01$, t-test).

(B) Cell death in SVZ cell colonies as measured by TUNEL and nuclear pycnosis (pyc) was decreased in the presence of BMP4.

Data shown are from experiments performed in triplicate. Error bars = SEM.



by inducing cell death of type A cells. Rather, BMP4 promotes the survival of SVZ-derived neurons.

BMP signaling cell-autonomously inhibits SVZ B/C cell neurogenesis

BMPs could exert their neurogenic-inhibitory effect either directly on the SVZ precursors or indirectly through the monolayer astrocytes. To demonstrate that BMP signaling can cell-autonomously inhibit SVZ neurogenesis, I constructed retroviral vectors that transduce BMPRs harboring point mutations that allow receptor signaling in the absence of ligand (Zou et al., 1997 and references therein). These constitutively active receptors directly activate the downstream mediator of BMP activity, SMAD1, in a cell-autonomous manner (Kretschmar et al., 1997). As controls, wild-type BMPRs and vector alone were used. Since the retroviral vectors also carry the alkaline-phosphatase (AP) marker gene, infected cells were identified with AP staining. See Fig. 16, inset for a schematic of the retroviruses.

Type B/C cell co-cultures were infected with each retroviral vector at 1DIV and analyzed at 5DIV. Cultures were stained for AP expression and Tuj1-immunopositivity. Fig. 16A and B show representative AP-positive, Tuj1-positive double-labeled cells. The ratio of neurons to glia produced by retrovirally-infected cells varied with the retroviral vector used. The retroviral vector alone, pCLE, produced 4 AP-positive, Tuj1-positive neurons, which were small and round, for every 1 AP-positive, Tuj1-negative cell, which was generally large and flat (example in Fig. 16C). The Tuj1-negative flat cells were GFAP-positive as assessed by double immunocytochemistry (Fig. 16D). Wild-type receptors (BMPR IA wt and BMPR IB wt) produced similar Tuj1-positive/Tuj1-negative

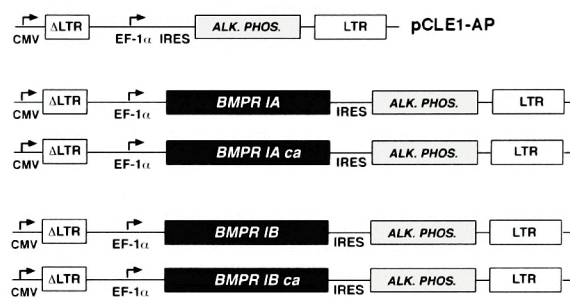
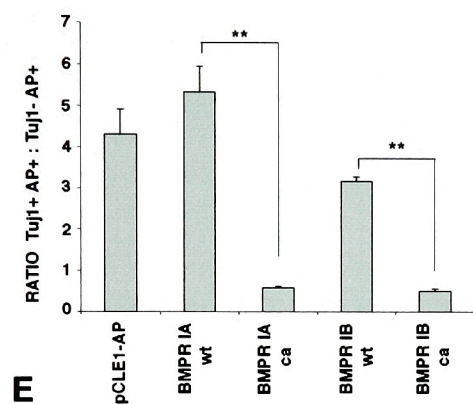
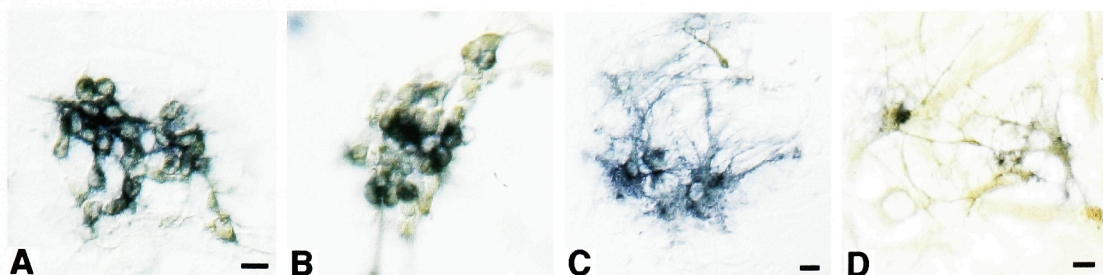
Figure 16

BMP signaling cell-autonomously inhibits neurogenesis of type B/C cells by directing glial differentiation

Lower right: Schematic of retroviral constructs. BMPR expression in infected cells is driven by the EF-1 α promoter. The point mutations are described in the Experimental Procedures. The AP marker gene is translated from an internal ribosome entry site (IRES).

Type B/C cells in co-culture were infected with retroviral vectors at 1DIV and analyzed at 5DIV. (A-B) Typical AP-positive, Tuj1-positive colonies. AP staining is purple and Tuj1 staining is brown (diaminobenzidine). Note that nearly all cells in the colony in (A) are AP-positive. In (B), approximately half of the cells are AP-positive. Tuj1-positive, AP-positive cells (type A cells) were typically small and round. (C) AP-negative cells were generally large and flat and stained for GFAP (D). Scale bars = 10 μ m.

(E) Quantification of the effect of retrovirally transduced BMPRs. Cultures were processed for AP and Tuj1 immunocytochemistry, and AP-positive cells counted. The ratio of AP-positive, Tuj1-positive neurons to AP-positive, Tuj1-negative cells is shown in the chart. Constitutively active BMPRs (BMPR IA ca, BMPR IB ca) decreased the proportion of neurons. Error bars = SEM (n=4), $p < 0.01$, t-test.



cell ratios, 5 and 3, respectively (Fig. 16E). However, constitutively active receptors (BMPR IA ca and BMPR IB ca) reduced the Tuj1-positive/Tuj1-negative cell ratio 10-fold to about 0.5 (Fig. 16E). Although BMPR IB is not expressed at detectable levels in type B/C cells (Fig. 13B), BMPR IB ca has been found to produce a similar phenotype as BMPR IA ca in cells that normally do not express BMPR IB (Akiyama et al., 1997). Thus, BMP signaling in the SVZ B/C cell population cell-autonomously inhibited neurogenesis and promoted glial differentiation.

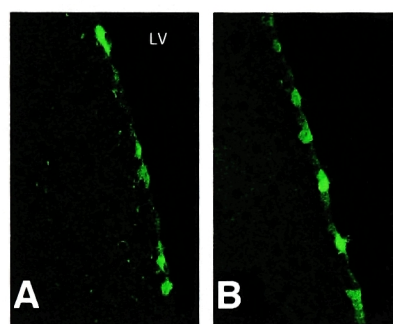
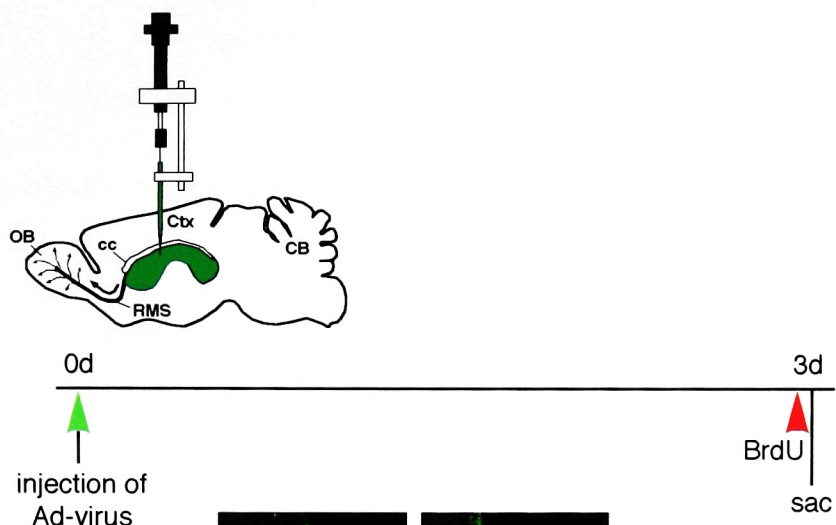
BMP overexpression in vivo inhibits SVZ proliferation and type A cell production

The in vitro data predicts that increasing BMP signaling in the SVZ would decrease neurogenesis. To test this hypothesis, I utilized an adenoviral vector to overexpress BMPs in ependymal cells adjacent to the SVZ. Adenoviral vectors injected into the lateral ventricle efficiently infect ependymal cells (Johansson et al., 1999; Doetsch et al., 1999a). Fig. 17A shows expression of green fluorescent protein (GFP) in lateral ventricle ependymal cells infected by the control Ad5-GFP adenovirus. Ad5-BMP7 overexpresses BMP7 in infected cells. BMP7, like BMP2 and 4, signals through the BMPR IA, BMPRIB and BMPR II receptor subtypes present in the SVZ (reviewed in Massague, 1998) but is at least 10-fold less sensitive to Noggin antagonism than BMP2 and 4 (Zimmerman et al., 1996). To confirm the targeting of the Ad5-BMP7 injections, Ad5-GFP virus was co-injected into the ventricles resulting in ependymal cell GFP labeling (Fig. 17B). Three days after infection, recipient animals received an injection of BrdU. One hour later, animals were sacrificed and brain sections processed for BrdU

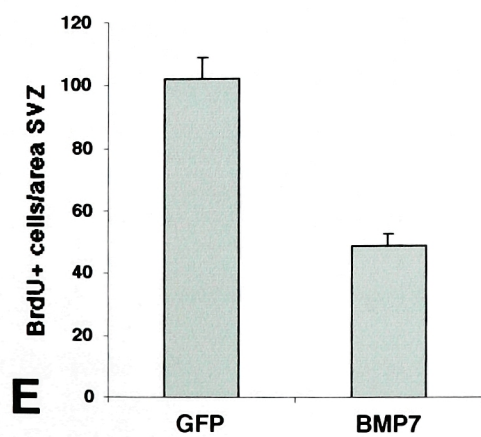
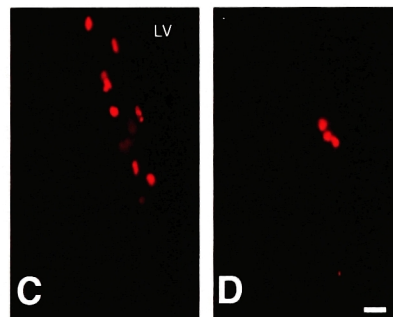
Figure 17

BMP overexpression in ependymal cells in vivo inhibits SVZ proliferation

Ad5-GFP control virus alone or Ad5-BMP7 + Ad5-GFP together was injected into the lateral ventricles (Ad5-GFP was co-injected with Ad5-BMP7 to monitor the extent of infection). Three days later, animals received an injection of BrdU 1 hour before sacrifice. Experimental design is shown at top. Viral infection was revealed by GFP expression in ependymal cells (A,B). (C,D) BrdU immunohistochemistry revealed proliferating SVZ cells. Significantly fewer BrdU-positive SVZ cells were seen in Ad5-BMP7 injected animals (compare C with D). BMP7 decreased SVZ proliferation by 50% (E). Error bars = SEM (n=3), $p = 0.006$. Bar = 20 μm .



Ad5-GFP Ad5-BMP7



immunohistochemistry. Expression of BMP7 in ependymal cells inhibited SVZ cell proliferation (Fig. 17D compared to control, Fig. 17C) by 50% (Fig. 17E).

To demonstrate that BMP overexpression can inhibit the birth of type A cells, I evaluated the effect of BMP7 on SVZ regeneration after antimitotic drug delivery. Cytosine-arabinoside (Ara-C) administered by osmotic pump to the surface of the brain for 6 days results in the elimination of type A cells in the SVZ, leaving behind type B and ependymal cells (Doetsch et al., 1999b). After pump removal, type B cells proliferate and repopulate the SVZ with migratory type A neuroblasts. To test the effects of BMPs in a SVZ depleted of type A and C cells, I injected Ad5-BMP7 or Ad5-GFP into the lateral ventricle after six days of Ara-C delivery.

Regeneration of type A cells was assessed by whole mount dissection of lateral ventricle walls and immunostaining for PSA-NCAM (Doetsch and Alvarez-Buylla, 1996; Doetsch et al., 1999b). Adenoviral injections were confirmed by observation of GFP expression in the whole mounts (Fig. 18A). 5 days after pump removal/viral injection, clusters of PSA-NCAM-positive cells were observed in the SVZ of control Ad5-GFAP injected animals (Fig. 18B and C). However, Ad5-BMP7 prevented the reappearance of PSA-NCAM-positive type A cells after Ara-C treatment (Fig. 18D and J). These results demonstrate that BMPs decrease SVZ proliferation and prevent neurogenesis in vivo.

Endogenous BMPs are antagonized by Noggin protein

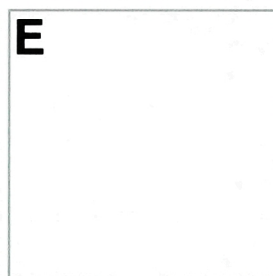
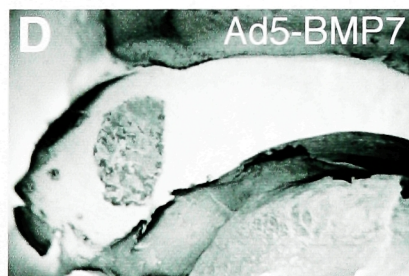
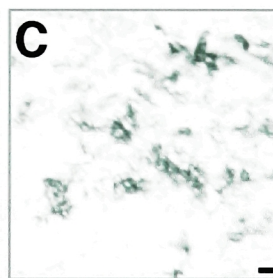
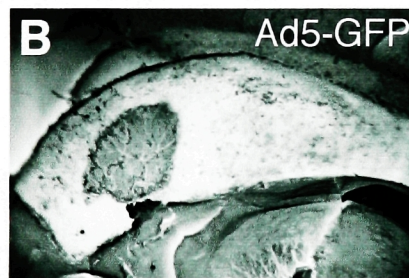
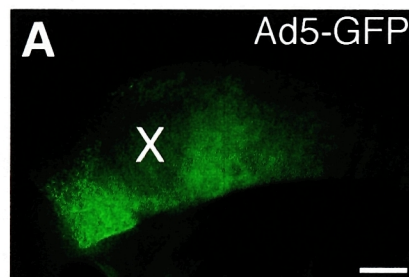
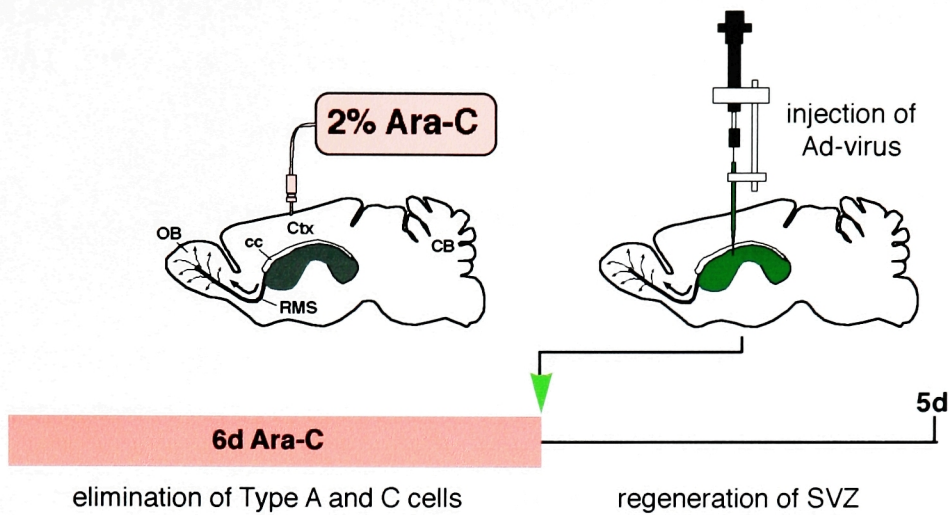
Noggin is a potent antagonist of BMPs (Zimmerman et al., 1996). I purified mouse Noggin protein from HELA cells infected with Ad5-Noggin (see Methods). Homogeneity of the Noggin protein was assessed by silver stain SDS-PAGE analysis

Figure 18

BMP7 overexpression in ependymal cells abolished type A cell production.

Anti-mitotic Ara-C treatment eliminates type C and A cells from the SVZ. 5 days after Ara-C treatment is terminated, type C and A cells are regenerated (Doetsch et al., 1999b). Ara-C treated brains were intraventricularly injected with Ad5-GFP or Ad5-BMP7. 5 days after viral infection, lateral wall whole mounts were immunostained for PSA-NCAM to identify the regenerating type A cells. Experimental design is shown at top. (A) GFP expression in infected ependymal cells is seen in whole mount dissections before immunostaining. A region of the lateral wall that is fused with the medial wall in vivo was not infected by the adenoviral vectors (GFP-negative area marked with “x”). The same whole mount in (A) stained for PSA-NCAM revealed small clusters of type A cells seen as dark foci in (B) and dark cellular clusters in a higher magnification in (C). (D,E) Ad5-BMP7 abolished the regeneration of type A cells. No foci of PSA-NCAM-positive cells were seen.

White bar in (F) = 500 μm . Black bar = 20 μm .



(Fig. 19A). Purified mouse Noggin protein cross-reacted with the monoclonal antibody to human Noggin (Fig. 19B), inhibited BMP4 (Fig. 19F), and could dorsalize ventral *Xenopus* embryo tissue (D. Weinstein, A. Hemmati-Brivanlou, unpublished observations).

Adult SVZ cells were co-cultured on astrocytes in the presence or absence of purified Noggin protein at 3 $\mu\text{g/ml}$. BrdU was added at 4.5DIV or 7.5DIV, and analyzed at 5 and 8DIV, respectively. The number of Tuj1-positive, BrdU-positive cells were counted to quantify neurogenesis. Noggin increased the birth of new neurons by nearly 20% at 5DIV and 50% at 8DIV (Fig. 19C). Although BMPs enhance type A cell survival (Fig. 15), a large increase in cell death was not noted in Noggin-treated cultures; the observed increase in neurogenesis indicates that the change in the rate of neurogenesis dominated any potential increase in the rate of cell death.

It has previously been shown that endogenous BMPs signal most effectively within cellular aggregates (Wilson and Hemmati-Brivanlou, 1995). SVZ cell aggregates were cultured in the presence or absence of 3 $\mu\text{g/ml}$ of Noggin. After 2.5-3DIV, cultures were enzymatically dissociated to single cells. Noggin did not significantly change the number of cells. Equal numbers of cells were lysed and protein extracts analyzed by Western blot. Noggin increased the expression of neuron-specific beta tubulin by an average of 20% while concomitantly reducing GFAP expression by nearly 50% (Fig. 19D). In another experiment, the Western blot results paralleled direct counts of plated, immunostained cells (not shown). Since endogenous BMPs would be expected to reduce Tuj1-positive and increase GFAP protein expression, the above results are consistent with

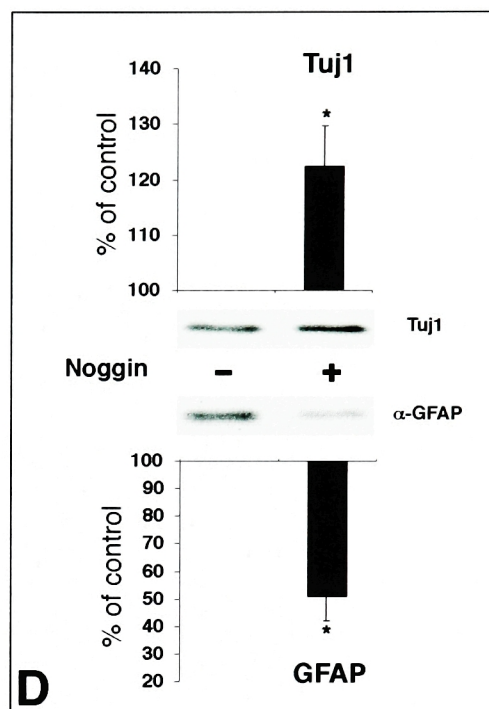
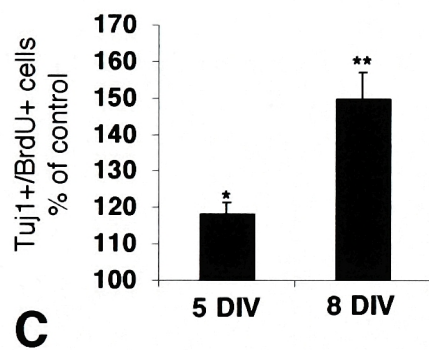
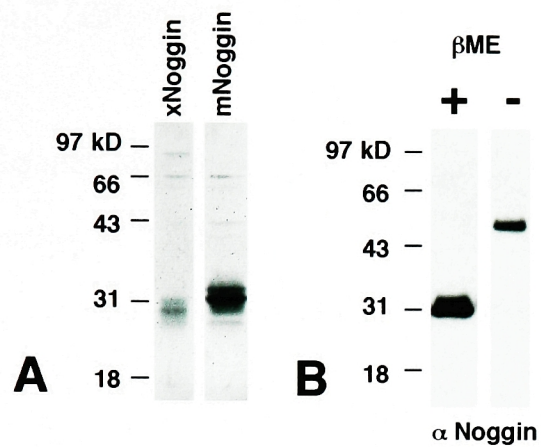
Figure 19

Noggin protein inhibits endogenous BMP signaling.

(A-B) Purification of mouse Noggin protein from Ad5-Noggin infected HELA cells. (A) SDS-PAGE silver stain analysis of purified Noggin protein. Reduced Noggin appears as a blurry band at 31kD due to heavy glycosylation (Smith et al., 1993). Purified mouse Noggin (mNoggin) has a slightly retarded mobility as compared to purified *Xenopus* Noggin (xNoggin). No significant contaminating bands were detected even though the gel was intentionally overloaded. (B) Western blot analysis of mouse Noggin protein. A monoclonal antibody to human Noggin protein recognized mouse Noggin. As expected, under non-reducing conditions, Noggin had a mobility consistent with dimerization (β ME-negative lane). β ME = beta-mercaptoethanol.

Noggin increases neurogenesis in adult SVZ cultures. (C) 3ug/ml of purified Noggin protein increased the number of neurons born at 5DIV and 8DIV by about 20 and 50%, respectively, as compared to control cultures. Data shown are the means from 3 independent experiments each performed in triplicate. (* = $p < 0.05$, ** = $p < 0.01$).

Noggin increases neuronal differentiation while inhibiting glial differentiation in aggregates of SVZ cells. (D) 600,000 P3 SVZ cells/cm² were cultured 2.5-3DIV in the presence (+) or absence (-) of 3ug/ml of Noggin. Equal numbers of cells were lysed and protein extracts analyzed by Western blot. Tuj1 and GFAP immunoreactive protein bands were detected by ECL on the same blot. Exposed films were scanned for density analysis by NIH Image 1.62. The bands shown are from one typical experiment. Noggin increased the Tuj1+ protein levels by 20% while concomitantly decreasing GFAP expression by 50%. The charts represent data from three independent experiments performed in either duplicate or triplicate. (* = $p < 0.05$).



the interpretation that Noggin increases neurogenesis by reducing endogenous BMP signaling.

Ectopic Noggin expression in the striatum promotes neuronal differentiation of grafted SVZ cells

The above data support the notion that Noggin is a part of the SVZ neurogenic microenvironment. Directly under the SVZ lies the striatum. Noggin is notably absent from the striatum (Valenzuela et al., 1995), and BMP2 and 4 are expressed in adult striatal dissections (Gross et al., 1996). SVZ cells grafted into the striatum are not neurogenic and differentiate primarily into astrocytes (Herrera et al., 1999). Hence, the BMPs from the striatum and/or grafted SVZ cells may be inducing astrocytic differentiation of SVZ cells transplanted into this region. To test the hypothesis that Noggin can create a neurogenic compartment, I used Ad5-Noggin to produce ectopic Noggin expression in the striatum and transplanted SVZ cells into this region.

Ad5-Noggin or Ad5-GFP control virus was injected into the striata of mice. Animals were allowed to recover for two days, a time sufficient for ectopic Noggin protein to be immunohistochemically detected. To identify grafted SVZ cells I used as SVZ donors transgenic hPAP mice which express human placental alkaline phosphatase in the cell membrane of all cells (Deprimo et al., 1996). Dissociated hPAP SVZ cells were stereotactically injected into the same site as the prior adenoviral injections, and animals were allowed to survive for seven days after transplant.

A focus of GFP expression was seen at the striatal injection site (Fig. 20A, C). Noggin immunohistochemistry demonstrated a high level of ectopic Noggin protein

Figure 20

Ectopic Noggin expression in the striatum promotes neuronal differentiation of transplanted SVZ cells

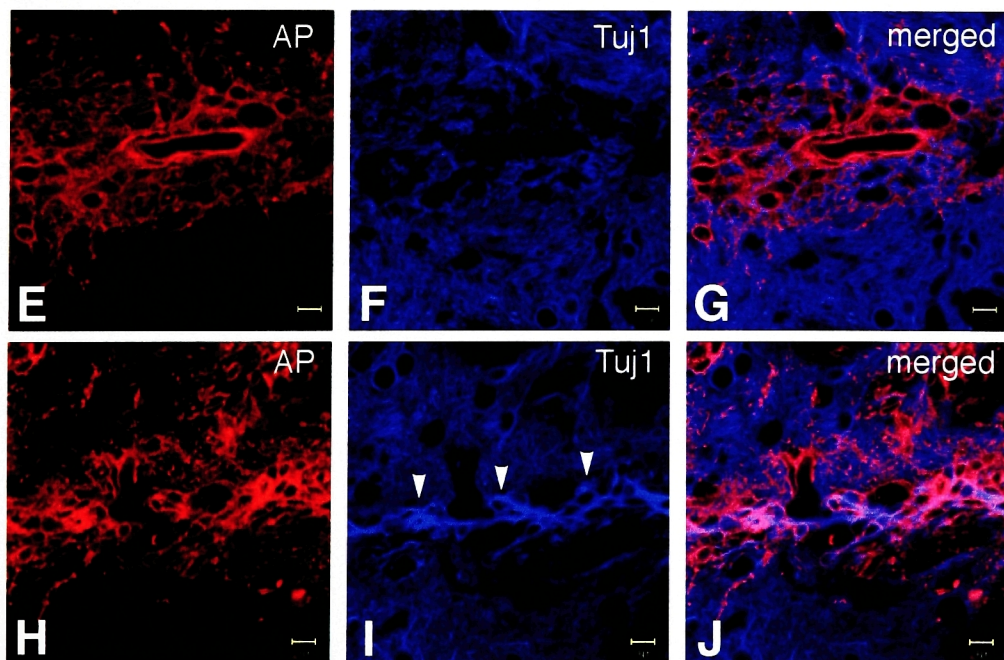
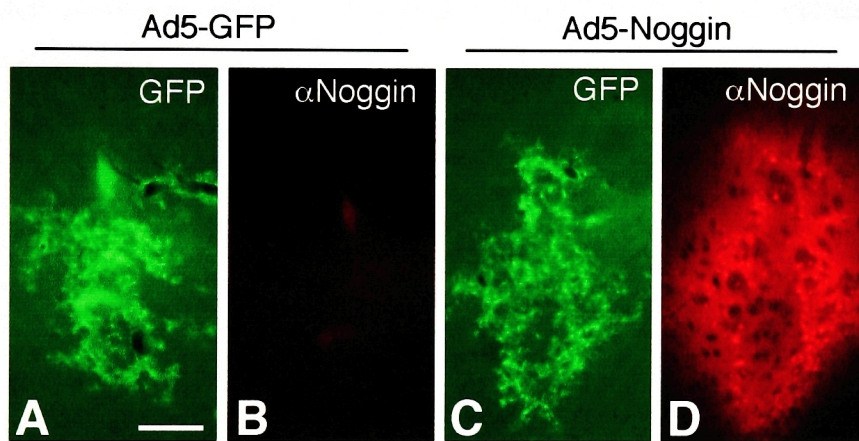
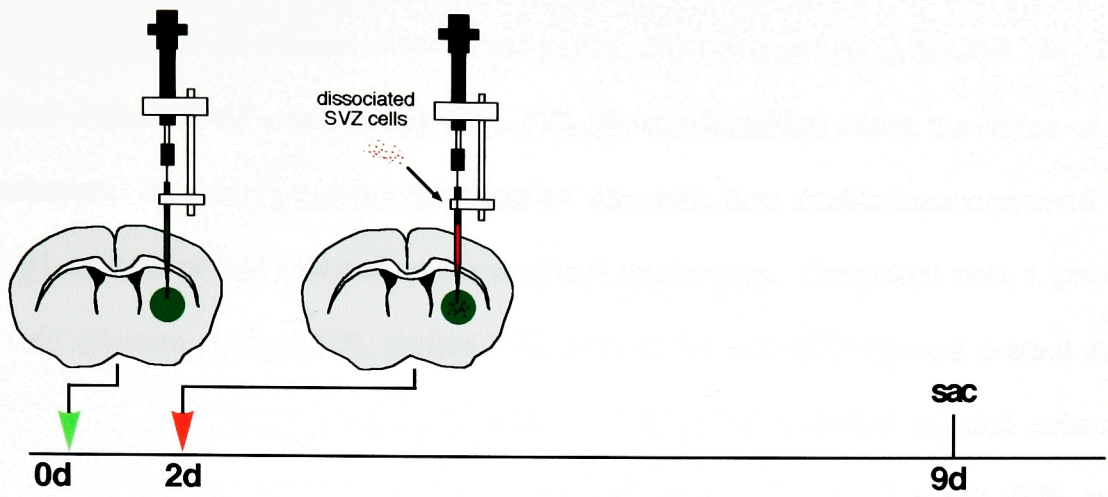
Experimental design is shown at top. (A-D) Injection of Ad5-Noggin into the striatum generates an ectopic region of Noggin expression. Photos of brain sections 4 days after viral infection. (A) GFP fluorescence of Ad5-GFP control virus infected striatal cells and (B) corresponding epifluorescent photomicrograph of Noggin immunostaining. No striatal Noggin expression was observed in Ad5-GFP injected animals. Strong Noggin expression around the injection site was obtained with the Ad5-Noggin vector (D, red fluorescence. The corresponding GFP image is C). White bar = 500 μ m.

Two days after adenoviral infection, dissociated SVZ cells from transgenic donors expressing AP in all cells were injected into the site of the viral infection. Seven days after SVZ cell transplants, graft-derived cells were identified by immunostaining for the AP marker gene product that localizes to cellular membranes (E,F,G,H, red fluorescence).

(E-F) Transplant-derived SVZ cells in Ad5-GFP injected striatum are primarily astrocytic and not Tuj1-positive. (E) AP-positive cells have a highly branched astrocytic morphology and are not Tuj1-positive (F, G).

(H-J). Clusters of transplant-derived Tuj1-positive cells are found in Ad5-Noggin injected striatum. (H) Small, rounded AP-positive cell bodies are found within a field of branched cells. The small rounded cells are Tuj1-positive (I-J). The size, morphology, and elongated chain-like structures of the Tuj1-positive cells are consistent with their being type A cells.

Images in (E-J) are of 1 μ m optical confocal sections. Yellow bar = 10 μ m.



expression by Ad5-Noggin infected cells (Fig. 20D) and not by Ad5-GFP (Fig 20B). Graft-derived hPAP-positive cells (Fig. 20E, H) were identified within the region of viral infection. Sections harboring the injection site were then double-immunostained with Tuj1 antibodies and analyzed at the confocal microscope. Consistent with a previous study (Herrera et al., 1999), grafted SVZ cells in the Ad5-GFP injected control striata were mostly Tuj1-negative (Fig 20E-G). In 4 out of 6 Ad5-GFP injected striata, no clusters of Tuj1-positive type A cells were observed. 2 out of 6 Ad5-GFP striata contained a small number of graft-derived Tuj1-positive cells. In contrast, 4 out of 4 Ad5-Noggin injected striata contained large clusters of graft-derived Tuj1-positive cells with the size and morphology of type A cells (Fig. 20H-J). These ectopic type A cells formed extensive chain-like structures similar to those observed in the SVZ. This experiment indicates that Noggin can create an environment in the striatum for neuronal differentiation of SVZ precursor cells.

Discussion

Unlike the embryonic brain, where neurogenesis is a transient phenomenon, the adult SVZ must retain the neurogenic environment for an extended period of time, probably for the entire life of the animal (Kuhn et al., 1996; Goldman et al., 1997). During development, Noggin and BMPs are thought to act in temporally restricted inductive events. Here I show that BMP and Noggin are retained in the SVZ region in adult life and that these molecules are important regulators of adult neurogenesis.

Previous work shows that BMPs and their receptors are expressed in the adult brain (Gross et al., 1996; Soderstrom et al., 1996b; Ebendal et al., 1998; Zhang et al.,

1998). This widespread presence of BMPs may in part restrict neurogenesis to regions expressing BMP antagonists. However, Noggin is expressed in other adult brain regions where neurogenesis has not been observed (Valenzuela et al., 1995). Other signals and/or the presence of a stem cell possessing a certain pattern intrinsic signals are likely necessary for neurogenesis observed in the SVZ.

BMPs have been found to have distinct effects in different neural precursor populations. In the developing neocortex (Li et al., 1998) and for neural crest cells (Shah and Anderson, 1997), BMPs stimulate neuronal differentiation. In contrast, BMPs inhibit neurogenesis of embryonic neural stem cells propagated in vitro (Gross et al., 1996) and embryonic PNS olfactory epithelial precursors (Shou et al., 1999). The apparent discrepancies could be due to BMPs acting on different cell populations. In the adult SVZ, BMPs prevented the formation of new neurons, but increased the survival of neuroblasts. My data suggest that in the SVZ BMPs have distinct effects on cells at different stages within the same lineage. To determine the effects of BMPs on the earliest population of SVZ precursors in vivo, I used the regeneration assay following antimitotic treatment (Fig 18). Under these conditions, neuroblasts (Type A cells) and transit amplifying precursors (Type C cells) are eliminated (Doetsch et al., 1999b) at the time of BMP overexpression. These in vivo experiments, together with the in vitro data indicating that a brief early exposure to BMPs is sufficient to dramatically reduce neurogenesis (Fig. 14F), suggest that BMPs inhibit neurogenesis by acting on SVZ stem cells or early precursors within the neurogenic lineage. BMPs have also been found to have stage-specific effects on cells in the oligodendrocyte lineage (Grinspan et al., 2000). Cell-specific responses to BMPs could be due to the expression of different BMPRs (Zou

et al., 1997; Chen et al., 1998) and/or the presence of distinct Smad binding partners in different cells (Hata et al., 2000). Interestingly, type A cells that responded to BMPs with increased survival express BMPR IB, IA and II while earlier SVZ precursors express only the IA and II receptor subunits (Fig. 13).

My transplantation studies (Fig. 20) demonstrate that Noggin can create a neurogenic microenvironment for SVZ cells. BMPs expressed in the striatum (Gross et al., 1996) may create an environment that promotes astrocytic differentiation of SVZ cells grafted to this region (Herrera et al., 1999). High levels of ectopic Noggin expression promoted neuronal differentiation of SVZ cells grafted to the striatum, supporting the notion that the SVZ neurogenic compartment has low BMP signaling. Although neural stem cells have been propagated in vitro from brain regions that are normally not neurogenic (Weiss et al., 1996a; Palmer et al., 1999), ectopic Noggin expression alone under these conditions was not sufficient to induce ectopic neurogenesis (Lim and Alvarez-Buylla, unpublished observations). This suggests that other neurogenic signals are required to promote neurogenesis of non-SVZ neural stem cells.

The pattern of Noggin and BMP expression in the SVZ, together with the functional data presented here support a model in which Noggin from ependymal cells creates a neurogenic environment for SVZ stem cells. Type B cells are intimately associated with the ependymal cell layer, and a fraction of type B cells make direct contact with the ventricle (Doetsch et al., 1999b). Some of these ventricle-contacting type B cells extend a thin cellular process between ependymal cells, and other B cells have a larger luminal surface (Fig. 21). The formation of these projections into the ventricle and the tight interaction with ependymal cells has been suggested to be related

to the neurogenic activation of type B cells during SVZ regeneration (Doetsch et al., 1999b). The intimate association between type B cells and the Noggin producing ependymal cells may be important for BMP antagonism in vivo: because of this cellular arrangement, Noggin produced by the ependyma would have immediate access to BMPs in the microenvironment of type B cells, promoting the neuronal lineage (Fig 21).

My hypothesis of ependymal Noggin function predicts that in the absence of the ependyma, gliogenesis would increase in the SVZ. Intraventricular injections of neuraminidase result in ependymal cell detachment from the ventricular walls. Interestingly, after ependymal cell denudation, the SVZ becomes a glial scar (Grondona et al., 1996). This result, of course, is a result of a complex experimental manipulation, and an adult ependymal cell-specific Noggin knockout would more directly answer the question of Noggin function near the SVZ. As there are other BMP antagonists that can function in a redundant manner (Bachiller et al., 2000), it will be important to determine if other BMP antagonists contribute to the SVZ neurogenic environment. In addition, other BMPs and related molecules may play a role in adult SVZ function.

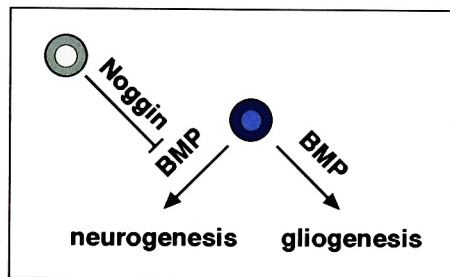
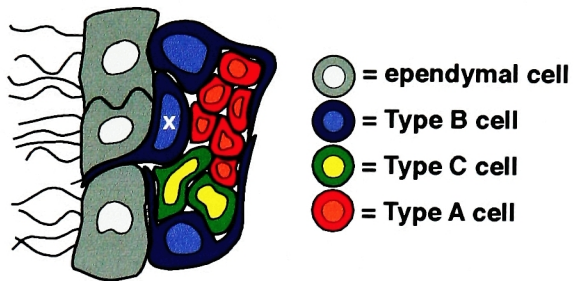
My model of an interaction between the ependyma and adjacent SVZ is reminiscent of neural induction in the embryo. This similarity between adult and embryonic neurogenic strategies suggests a more general hypothesis, that particular paradigms observed in development continue to reverberate later in life. Future work characterizing SVZ stem cells and their niche may reveal more similarities between adult neurogenesis and embryonic development, not only in the identity of the molecules, but also in the logic of their interaction.

Figure 21

Schematic of SVZ architecture and proposed role of Noggin and BMPs

(top) Architecture of the SVZ. Type B cells (SVZ astrocytes) are closely apposed to ependymal cells. Some type B cells (marked with “x”) extend a process between ependymal cells; these intercalating type B cells have been proposed to be cells activated for the neurogenic lineage (Doetsch et al., 1999). Clusters of type C cells are found along the chains of migratory type A cells (neuroblasts).

(bottom, in box) Proposed role of Noggin in promoting the neuronal lineage of SVZ cells. Type B cell BMP signaling blocks the neurogenic pathway, directing type B cells to gliogenesis (right pathway). Noggin produced by ependymal cells antagonizes type B cell BMP signaling, promoting neurogenesis of SVZ cells (left pathway). The close association of type B cells and ependyma schematized above may be important for this inductive event.



CHAPTER 5

Gene expression profiling of adult SVZ stem cells and their neurogenic niche

From the analysis of Noggin and BMP signaling in the previous chapter, it is apparent that SVZ neurogenesis is in part regulated by molecular signals present in their microenvironment. While the model for a neuronal-glial “switch” mediated by Noggin and BMPs is compelling in its simplicity, there are undoubtedly a multitude of other external factors that determine this and another aspects of SVZ biology. Furthermore, a study of the external factors in the SVZ niche is only half of the story: SVZ cell behavior is likely restricted by intrinsic signals. Supporting this notion are experiments I performed earlier (not included in this thesis, but data can be reviewed in Lim et al., 1997). I observed that postnatal SVZ cells grafted into the embryonic day 15 mouse brain ventricle (a time during which neurogenesis is underway in nearly all brain regions) most commonly incorporated into the SVZ or OB of the recipient animals. Certain engraftment sites (cortex, hippocampus) were never observed. SVZ cells found in ectopic brain regions all had morphological and size characteristics of interneurons, suggesting that by early postnatal development, SVZ cell neurogenesis is intrinsically restricted to particular neuronal lineages and microenvironments⁸. The remainder of this thesis concerns the identification of external signals and intrinsic factors regulating SVZ

⁸ Admittedly, I am emphasizing the negative results of these studies. The incorporation of SVZ-derived cells in one particular ectopic location (inferior colliculus) was actually quite robust. Based on genechip

biology. To accomplish this, I utilized high density oligonucleotide expression arrays to analyze the transcriptional profile of adult neurogenic cells. Initial data analysis has revealed genes that are potentially important for SVZ biology.

It is now possible to determine the expression levels of tens of thousands of genes simultaneously, and the analysis of these gene expression profiles provides a powerful means of understanding complex cellular behaviors. Specific transcriptional patterns revealed on a whole genome level have been correlated with cellular processes ranging from wound healing (Iyer et al., 1999) to yeast sporulation (Chu et al., 1998), and it thus follows that neurogenesis – in particular, that of the adult brain – would present a transcriptional profile that can be distinguished from that of non-neurogenic cellular behaviors.

A simple approach to identifying interesting sets of genes is comparing the expression profiles of two or more samples. For instance, Lee et al. (Lee et al., 1999) applied this method to identify differentially expressed genes in the skeletal muscle of adult (5 months) and old (30 months) mice. Of over 6300 genes examined by microarray, over 100 were found to be differentially expressed greater than two-fold. The identity of differentially regulated genes allowed the formation of a hypothesis about the aging of muscle that was tested and confirmed in the same study.

To identify gene expression associated with SVZ neurogenesis, I first compared the gene expression profile of the SVZ with that of five other adult brain regions: whole cerebellum (Cb), cerebral cortex (Ctx), hippocampus (Hp), striatum (St), and olfactory bulb core (ObC). 26 of 11,000 genes analyzed were specific to the SVZ, indicating their

data presented later, I speculate that the microenvironment of the developing inferior colliculus may be similar to that of the SVZ and hence permit incorporation of grafted cells and promote their neurogenesis.

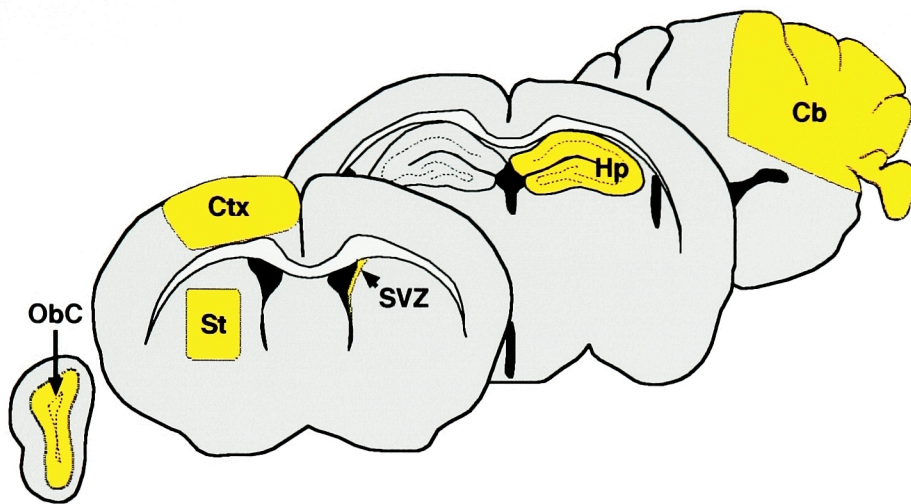
potential role in SVZ neurogenesis. 16 genes were expressed in both the SVZ and ObC; 4 of these 16 were expressed highest in the ObC, suggesting a role for these genes in the later stages of neuronal differentiation. Type B and ependymal cells were purified by fluorescent-activated cell sorting (FACS) using known antibody markers, and their individual transcriptional profiles were examined. Of the 42 genes expressed in the SVZ-ObC compartment, 29 were differentially expressed between type B and ependymal cells; 17 of the 29 were at least 3-fold higher in type B cells as compared to ependyma, and seven were more than 100-fold increased in the stem cell population. Expression array data were substantiated by Northern blot analysis and confirmed by localization of gene products in brain sections.

Identification of gene expression enriched in an adult neurogenic region

Six brain regions were selected for expression profile analysis (Fig 22). The SVZ is the largest neurogenic region in the adult mouse brain, and a certain pattern of gene expression in SVZ cells may reflect this. Dissections of SVZ tissue contain a small amount of contaminating striatal tissue, therefore, the expression profile of the striatum (St) was also obtained to filter the SVZ expression profile for potential striatal contamination. The olfactory bulb core (ObC) is enriched for the descendants of SVZ stem cells (granule interneurons) and also contains a large number of migratory type A cells both in chains as well as those migrating radially into different layers (see Fig. 1A for schematic). Gene expression shared between the SVZ and ObC -- and especially those that are increased in the ObC -- may have roles in the later stages (migration and final differentiation) of OB interneuron genesis. The cortex (Ctx), cerebellum (Cb) and

Figure 22

Brain regions for transcriptional profile analysis. (Top) The SVZ contains a large number of neurogenic stem cells. Cerebellum (Cb), cortex (Ctx), and striatum (St) are non-neurogenic regions. The olfactory bulb core (ObC) is enriched for SVZ-derived granule interneurons and type A cell migratory neuroblasts. The hippocampus (Hp) is another neurogenic brain region; many fewer neurons are born in the Hp as compared to the SVZ. (Bottom) Method of target production for hybridization. Purified mRNAs were converted to double-strand T7 cDNA libraries from which biotinylated aRNA targets were produced.



regions dissected
liq. N₂ frozen

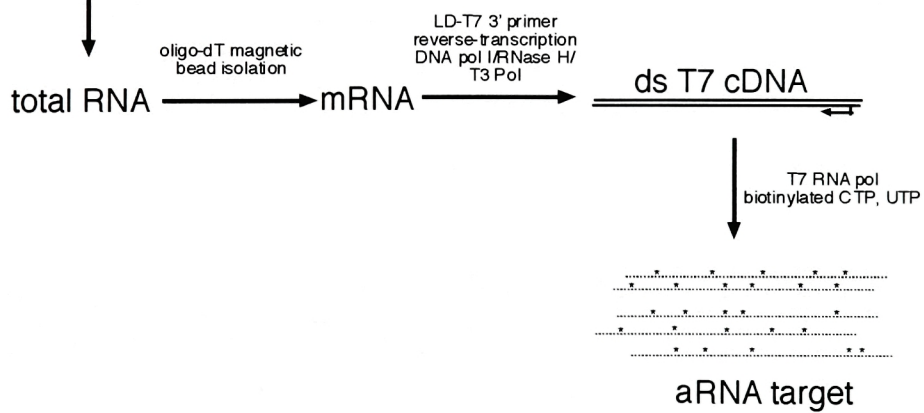
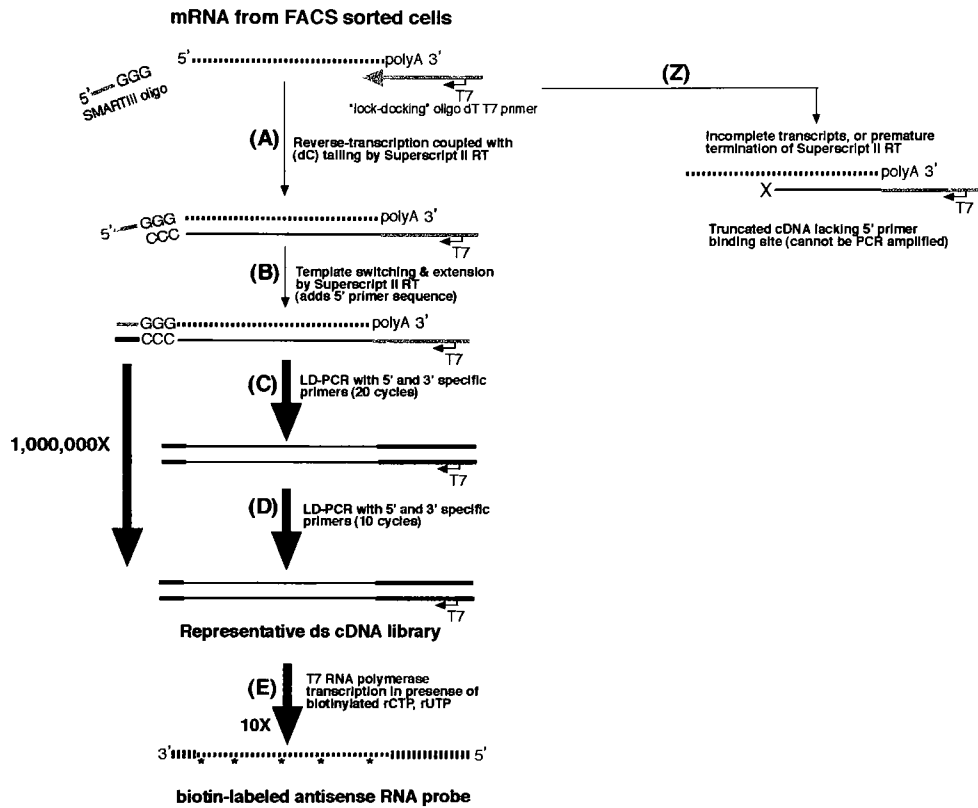


Figure 23

Method of target production for hybridization from small numbers of FACS purified SVZ cells. mRNAs were reverse transcribed from a “lock-docking” T7-oligo(dt) primer, eliminating the reverse-transcription of long stretches of poly-A. The reverse-transcriptase (RT) used is RNaseH deficient. When the RT reaches the 5’ end of the mRNA, the terminal transferase activity adds a few deoxycytidines (A). Included in the reaction is a specific 23-base pair primer with a short stretch of deoxyguanocines. The dG stretch on the primer hybridizes with the dC stretch of the 3’ end of the cDNA, and the RT switches template strands and copies the specific primer onto the end of the cDNA (B). Single-strand cDNAs were used in two rounds of LD-PCR reactions. After the first round of LD-PCR (C), double-strand cDNAs were purified by column chromatography to remove unused primers and small PCR products that were found to interfere in later PCR cycles. The amplification after the second round of LD-PCR (D) is estimated to be 1,000,000-fold. LD-PCR reactions were monitored for linear amplification (Fig. 24). The ds cDNA libraries were used to produce biotinylated aRNA for hybridization. mRNAs that are incompletely reverse transcribed are not amplified by this method (Z).



striatum (St) are all brain regions in which neurogenesis is not observed. The gene expression profiles of non-neurogenic regions serve as a reasonable initial filter to identify genes that are involved in SVZ biology. The hippocampus (Hp) expression profile was also determined. Neurogenesis also occurs in the dentate gyrus of the adult Hp, however, the relative number of new neurons born in that region are significantly less than the SVZ. Therefore the gene expression involved in adult neurogenesis in general is likely to be significantly higher in the SVZ as compared to the Hp.

The preparation of target⁹ for the expression arrays is schematized in Fig. 22. Duplicate double-strand T7-promoter cDNA libraries were prepared independently for each brain region. Quality of aRNA target was assessed on agarose gels (Fig. 24A, top), Northern blot (Fig. 24A, bottom), and hybridization quality analysis (see Methods). Visual inspection of fluorescent signals on arrays revealed no major defects in the array surface (Fig. 25A-C).

The similarity of expression data among the duplicate samples and divergence among different brain regions was evident in scatter plots of relative gene expression levels (representative plots in Fig. 25D-F). Similar expression patterns are visualized by the tendency of each point to fall on the diagonal intercepting the origin with a slope of 1 (Fig. 25D and F). When 2 different brain regions were compared (Fig. 25E), the divergence of gene expression profiles was evident by the greater degree of scatter (more points falling off of the diagonal and at greater distances)¹⁰.

⁹ Though perhaps confusing, researchers using high-density oligonucleotide arrays refer to the labeled nucleic acid molecules applied to the arrays as "target." "Probe" describes the covalently attached oligonucleotides of known sequences that interrogate the target for the presence of gene expression. In Northern blots and other DNA microarrays, "target" refers to the immobilized nucleic acid chains and "probe" are the labeled molecules.

¹⁰ A quantitative measure of this scatter utilizing correlation coefficients is in progress.

Figure 24

(A) aRNAs from the different brain regions are of appropriate size distribution (top). Northern analysis for GAPDH demonstrates that this message was maintained in its full length and is represented in equal proportions to other transcripts among the different brain regions (bottom). GAPDH levels were consistent not only among the different brain regions, but also among the independently prepared duplicate samples.

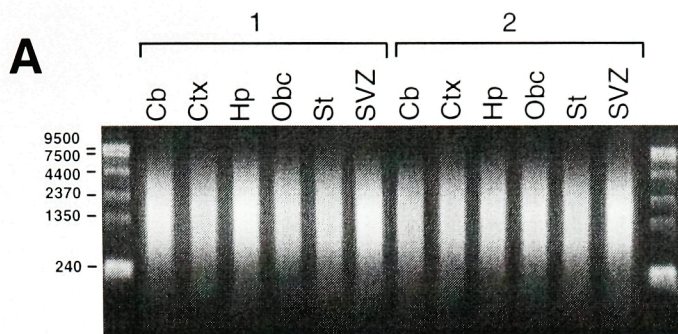
(B) FACS of SVZ cells. Left: SVZ cells stained only with secondary antibodies. Cross-bars shown isolate >99% of the non-specific signal in the lower left quadrant. Right: SVZ cells stained for CD24 and GFAP. Immunostained SVZ cells are brightly fluorescent when observed under epifluorescent microscopy, which accounts for the 1-2 order of magnitude fluorescent intensities over background seen in FACS analysis. The FACS sorting gates for GFAP-positive, CD24-negative (R1) and CD24-positive cells, GFAP-negative (R2) were set such that >99.5% of non-specifically stained cells are excluded.

(C) Cellular RNAs are stable through the immunostaining protocol. 1×10^6 SVZ cells were double immunostained for GFAP and CD24. Omission of 0.1% Tween-20 results in no GFAP staining. 1% Tween-20, Rnasin, and DTT were added to the staining solutions where indicated (+). After staining, cells were incubated at 4°C for an additional 1.5 hr. Total cellular RNA was then extracted and analyzed on agarose gel. No RNA degradation was detected in any staining protocol. Note that if SVZ cells are freeze-thawed and incubated at 37°C, all of the 28S and 18S RNAs are degraded (right lane).

(D) Analysis of ds cDNA libraries from FACS SVZ cells. A portion of the ds cDNAs after the first round of LD-PCR was used as the template in a second round of control LD-PCR reactions in which aliquots were taken after 6, 8, 10, and 12 cycles. The cDNA aliquots were analyzed on agarose gels (left panel). The size distribution of the amplified cDNAs was not biased toward smaller products by the LD-PCR. Southern blot signal for GAPDH was a single band, indicating that the initial mRNA was not heavily degraded. The linear range of amplification was determined by both the GAPDH signal intensity and visual inspection of the ethidium bromide stained cDNA population.

(E) Semi-quantitative RT-PCR confirms the separation of SVZ cells by FACS. R1-derived cDNAs contain GFAP transcripts and R2 cDNAs contain CD24 transcripts and not vice versa.

(F) Agarose gel and Northern analysis of aRNAs from FACS-derived ds cDNAs. Size distributions were as expected for brain tissue and GAPDH messages did not show signs of mRNA degradation.



GAPDH

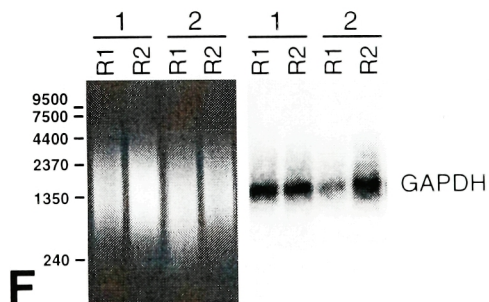
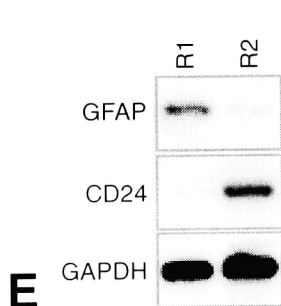
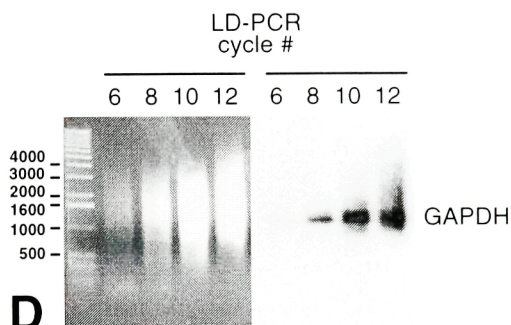
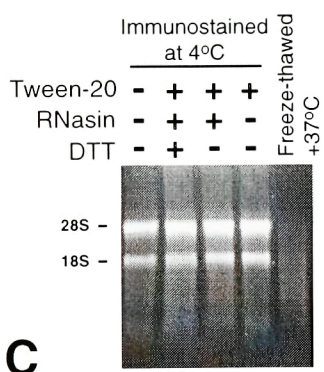
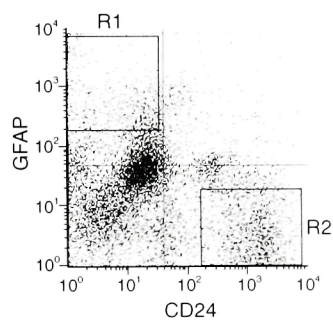
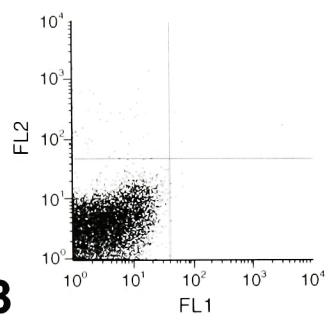
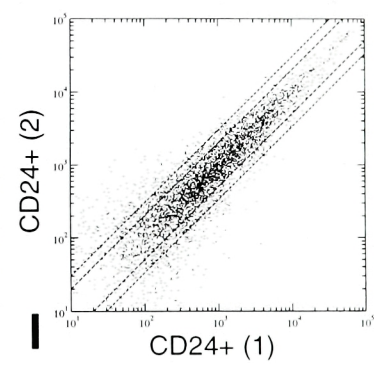
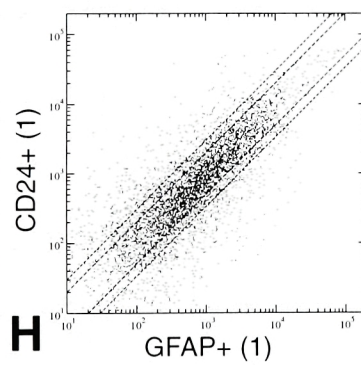
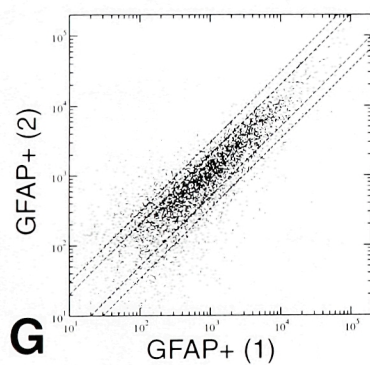
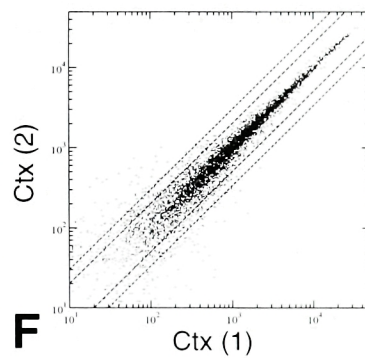
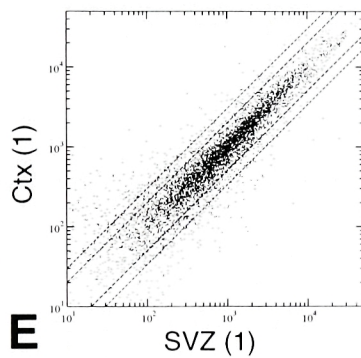
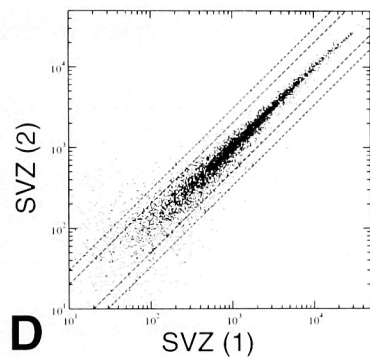
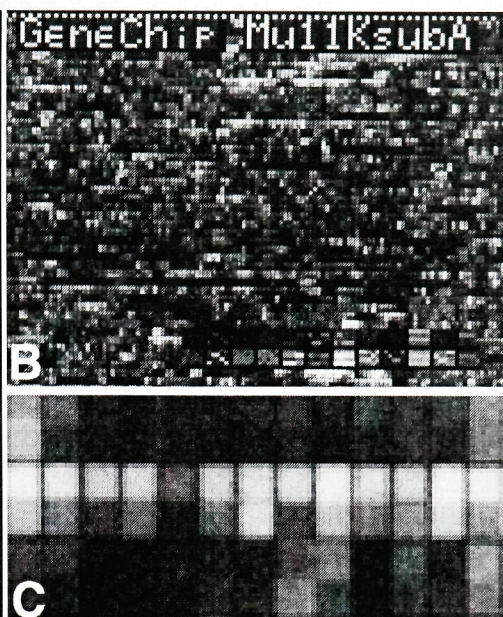
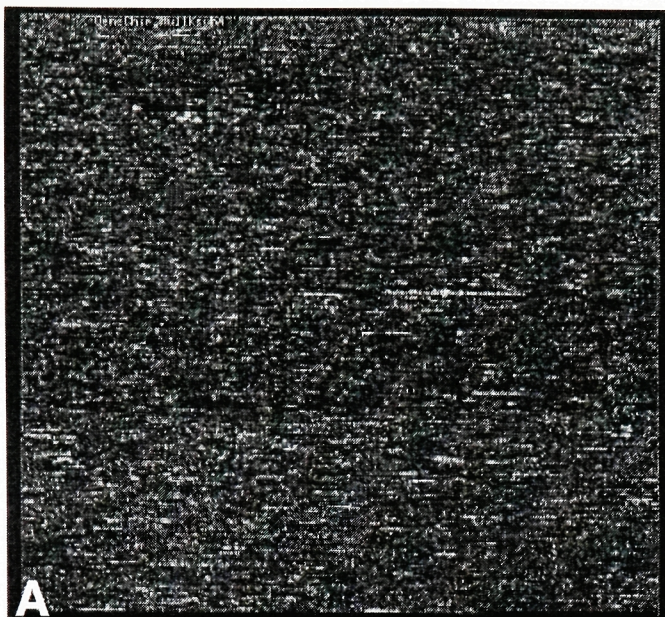


Figure 25

Representative images of hybridization signals. (A) The entire 11K subA array. (B) Higher power image of (A). (C) Detail of the probe features. (D-E) **Representative scatter plots comparing brain region expression profiles.** X and Y axes plot the relative expression levels of genes analyzed (dots). (D and E) Gene expression profiles of independently prepared duplicate samples are similar. Similarity is visualized by the tendency of the dots to fall on the diagonal. The inner bars along this diagonal represent 2-fold differences. The outer bars represent 3-fold differences. Differential gene expression is seen as increased scatter as in the comparison of SVZ and Ctx (F). (G-H) **Representative scatter plots comparing type B and ependymal cell expression profiles.** (G and I) Gene expression profiles of independently prepared duplicate samples are similar. There is more scatter in (G and I) than in (D and F), perhaps reflecting the noise introduced by the transcript amplification. Large differences in gene expression can still be detected between type B cells and ependyma (H).



The arrays employed in this study determine the relative expression levels of over 11,000 mouse genes. To identify genes that might be specifically involved in SVZ neurogenesis, the expression profile database was filtered for those genes expressed in the SVZ at greater than 2-fold higher levels than the Cb, Ctx, Hp, and St. This filter was combined with another filter for those genes having hybridization signals in the SVZ profile at least 10% of the average signal. The results of the combined filters are shown in Table 1. Most of the 42 different genes identified had fold-differences of much greater than the 2-fold criteria applied. For 19 of the 42, fold-difference increases could not be calculated for comparisons to the Cb, Ctx, Hp, and St because of a lack of reliable positive signal¹¹ in the denominator of the ratio. The arrays interrogate the expression of some genes more than once; for CD24, ribonucleotide reductase, and Sox4, the fold-difference determinations of these redundant inquiries were in close agreement, increasing the validity of the expression data. To substantiate the array data with another measure of transcript levels, the aRNA target used for hybridizations was analyzed by Northern blot (Fig. 26). Northern blot results correlate well with the fold-difference determinations from array analysis¹².

Expression profiles of type B cells and ependyma

While comparative gene expression profile analysis of whole tissue samples has revealed interesting differences between different tissues and tumor types (Perou et al.,

¹¹ The determination of a "reliable positive signal" is confidential and may not be explicitly set forth here. A fold-change number is reported by the GeneChip software (v3.1) but is accompanied by a "~," indicating that the quantification of this measure may not be reliable. Since I am intimately aware of the flaws in the GeneChip software algorithms, I am now in collaboration with Affymetrix and Felix Naef from the RU Center for Physics and Biology to devise new analytic software that will less frequently require the use of the "~."

Table 1

Genes with increased expression in the SVZ

Duplicate SVZ samples were compared with duplicate samples from each brain region (e.g., SVZ1vCb1, SVZ1vCb2, SVZ2vCb1, and SVZ2vCb2). The SVZ is the numerator of these ratios. The fold-difference between the SVZ and the region compared is shown in the columns below the region's headings. The data have been converted so that 1 or -1 is equal to no difference. The means and error were calculated in log10. ME = multiplier for error. (ME)(fold-difference) gives the upper bound and (fold-difference)/(ME) gives the lower bound for the standard deviation as it was calculated in log10. The relative level of expression in the SVZ is indicated in the AvgDiff column with the range of the two measurements in parentheses. All array hybridization intensities were scaled so that the average signal was equal to 1000.

Probe Set	Description	AvgDiff	range	Cb	ME	Ctx	ME	Hp	ME	ObC	ME	St	ME
AF026537_at	prodynorphin, complete cds.	3501	(530)	na	-	na	-	na	-	na	-	4.8	(1.3)
x53825_s_at	mRNA for heat stable antigen (HSA/CD24)	2888	(653)	6.7	(1.3)	9.2	(1.3)	4.5	(1.3)	-1.2	(1.5)	10.7	(1.4)
aa002925_s_at	cDNA clone 426274 5', mRNA sequence.	2394	(354)	12.2	(1.3)	10.6	(1.9)	19.4	(1.3)	1.5	(1.7)	5.8	(1.2)
x66405_s_at	mRNA for collagen alpha1(VI)-collagen.	2155	(480)	8.6	(1.3)	6.8	(1.8)	9.4	(1.6)	1.0	(1.5)	4.8	(1.3)
Msa.3088.0_s_at	X70298 sox-4 mRNA	1986	(295)	8.9	(1.2)	3.1	(1.2)	2.9	(1.2)	-2.8	(1.3)	3.6	(1.2)
u51000_s_at	Dix-1 gene, complete cds.	1892	(57)	na	-	3.7	(1.1)	4.6	(1.1)	-4.6	(1.2)	na	
U51167_s_at	isocitrate dehydrogenase, complete cds.	1600	(48)	2.6	(1.)	2.5	(1.1)	2.1	(1.1)	1.6	(1.2)	2.3	(1.)
m83749_s_at	D-type cyclin (CYL2), complete cds	1556	(159)	na	-	na	-	5.4	(1.3)	na	-	4.1	(1.1)
Msa.1095.0_at	X66603 brain-4 POU-domain protein, complete cds	1522	(448)	na	-	na	-	na	-	8.2	(1.8)	2.6	(1.4)
Msa.21704.0_s_at	AA028273 Homol. to IPP-2	1318	(635)	na	-	na	-	na	-	na	-	na	-
Msa.2451.0_s_at	X94322 melanoma-inhibitory-activity protein	1088	(206)	na	-	na	-	na	-	na	-	na	-
aa522093_s_at	cDNA clone 903988 5', [tazarosine-induced gene2]	1083	(93)	na	-	na	-	na	-	na	-	na	-
Z46757_s_at	mRNA for high mobility group 2 protein.	918	(345)	na	-	na	-	na	-	na	-	na	-
I15443_s_at	L6 antigen, complete cds.	852	(22)	na	-	na	-	na	-	na	-	na	-
L13204_s_at	HNF-3/forkhead homolog-4 (HFH-4), complete cds.	838	(34)	na	-	na	-	na	-	2.0	(1.4)	na	-
m35153_s_at	Mouse lamin B, complete cds.	797	(34)	2.5	(1.1)	4.5	(1.1)	6.4	(1.1)	1.1	(1.3)	4.9	(1.1)
m80540_s_at	Tes-1 homeobox protein, complete cds.	787	(9)	na	-	na	-	4.9	(1.2)	-3.8	(1.1)	na	-
Msa.30.0_at	D90242 Mouse mRNA for nPKC-eta	767	(148)	na	-	na	-	na	-	na	-	3.0	(1.6)
C81593_rc_f_at	cDNA clone J0101H11 3' sim. to ribonuc. reduct. M2	740	(84)	6.2	(1.1)	5.3	(1.2)	na	-	na	-	na	-
U88566_s_at	secreted frizzled related protein sFRP-1, complete cds.	713	(52)	na	-	3.0	(1.3)	4.9	(1.7)	2.3	(1.8)	5.9	(1.2)
ET62444_f_at	Sox4, partial cds.	693	(101)	na	-	4.3	(1.1)	2.8	(1.4)	-2.6	(1.4)	4.2	(1.1)
AF009414_g_at	Sox11, complete cds.	681	(181)	na	-	na	-	3.7	(1.3)	-1.0	(1.5)	4.0	(1.3)
Z26580_s_at	cyclin A.	670	(10)	3.9	(1.3)	na	-	na	-	2.0	(1.3)	2.8	(1.6)
aa268341_s_at	cDNA clone 733722 5' sim. to UBIQUITIN-CONJ. ENZ.	606	(38)	2.3	(1.2)	3.1	(1.2)	3.4	(1.1)	3.5	(1.1)	2.8	(1.1)
m14223_s_at	ribonucleotide reductase M2 subunit, complete cds.	572	(28)	3.5	(1.3)	3.7	(1.1)	3.6	(1.1)	2.9	(1.2)	3.2	(1.2)
Msa.24364.0_s_at	W35058 Homol. to FRIZZLED PRECURSOR.	457	(16)	na	-	na	-	na	-	na	-	na	-
d16847_s_at	stromal cell derived protein-1, complete cds.	449	(17)	na	-	na	-	3.1	(1.1)	na	-	2.9	(1.3)
x83562_s_at	N-glycan alpha 2,8-sialyltransferase.	437	(87)	na	-	na	-	na	-	1.2	(1.8)	2.6	(1.5)
AA426917_s_at	cDNA clone gb836311 similar to cyclin B1	406	(63)	na	-	4.0	(1.1)	na	-	3.6	(1.1)	na	-
Msa.740.0_at	M95603 Mouse HLH protein homol. to rat ASH1	332	(69)	na	-	na	-	na	-	na	-	na	-
aa592163_s_at	cDNA clone 1050367 5', [prot. reg. cytokinesis 1]	289	(27)	na	-	na	-	na	-	na	-	na	-
aa267055_at	cDNA clone 720860 5', mRNA sequence.	279	(1)	na	-	na	-	na	-	na	-	na	-
Msa.13177.0_f_at	W53461 Homol. to CD24 PRECURSOR.	270	(74)	na	-	na	-	na	-	-1.4	(1.9)	na	-
L22218_at	KV1.5 delayed rectifier K+ channel, complete cds.	249	(46)	na	-	na	-	na	-	na	-	na	-
U22829_s_at	P2Y purinoceptor, complete cds.	237	(31)	na	-	na	-	na	-	na	-	na	-
Msa.2695.0_s_at	Z46299 Sp17 gene for sperm specific protein	230	(62)	na	-	na	-	na	-	na	-	na	-
Msa.403.0_at	M84120 activin receptor (ActR IIB), complete cds	228	(54)	na	-	na	-	na	-	1.2	(1.3)	na	-
C78640_rc_at	cDNA clone J0052E03 3', mRNA sequence.	219	(56)	na	-	na	-	na	-	na	-	na	-
m12848_s_at	myb proto-oncogene, complete cds.	192	(26)	na	-	na	-	na	-	na	-	na	-
D26089_s_at	mRNA for mcdc21, complete cds.	181	(19)	na	-	na	-	na	-	na	-	na	-
aa198316_at	cDNA clone 658379 5', mRNA sequence.	178	(7)	na	-	na	-	na	-	na	-	na	-
Msa.27633.0_s_at	AA067092 Homologous to SREBP-1.	154	(31)	na	-	na	-	na	-	na	-	na	-
X57437_s_at	L-histidine decarboxylase.	150	(72)	na	-	na	-	na	-	na	-	na	-
aa289122_s_at	cDNA clone 750657 5' sim. to human CDK reg. sub.2	134	(7)	na	-	na	-	na	-	na	-	na	-
I02333_s_at	bilirubin/phenol family UDP glucuronosyltransferase	118	(2)	na	-	na	-	na	-	na	-	na	-

1999; Tanaka et al., 2000), the analysis of such data is enriched by knowledge of the expression patterns of individual cell types within the tissue specimen. For instance, a comparison of gene expression patterns in individual cell lines to those seen in normal breast tissue and breast tumor samples revealed features of the tumor expression profile that had discernable counterparts in specific cell lines, representing the tumor, stromal and inflammatory components of the tumor tissue (Ross et al., 2000). Correlating expression profiles with specific SVZ cell types would not only allow an analytical dissection of the whole SVZ expression profile, it also reveals new cell specific markers and potential intrinsic signals. I utilized fluorescent activated cell sorting (FACS) to purify the populations of SVZ type B cells and ependyma for gene expression profile analysis.

CD24 (heat stable antigen) antibodies strongly recognize a cell-surface epitope on ependymal cells and, to a lesser degree, on type A cells (Calaora et al., 1996). However, there are no markers available that allow the FACS of live type B cells. The Ad5-GFAPP-GFP adenoviral vector described in Chapter 2 labels only about 1% of SVZ cells (Doetsch et al., 1999a) and therefore does not yield sufficient quantities of type B cell specific mRNA for reliable amplification. Antibodies to GFAP strongly label SVZ type B cells, however GFAP is intracellular. Immunocytochemistry for intracellular antigens requires the permeabilization of the outer cell membrane to allow antibodies access to their epitopes. Other studies have demonstrated that representative cDNA libraries can be generated from cells that have been disrupted by sectioning, alcohols, and immunostaining (Crino et al., 1996; Goldsworthy et al., 1999; Fend et al., 1999; Luo et

¹² Northern blot data is being quantified and can be also represented on scatter plots with the array data to assess the agreement between the two assays.

al., 1999). The stability of SVZ cellular RNA through an immunostaining protocol including a mild, non-ionic detergent (Tween-20) is demonstrated in Fig. 24C and inferred from results of described below (Fig. 24F). Both CD24 and GFAP staining was performed with Tween-20 so that any potential changes in the gene expression profile induced by the detergent would be present in each. Strongly CD24-positive cells maintained the multiciliated morphology through the immunostaining protocol, providing a verification of staining specificity; labeled non-ciliated cells were not observed, suggesting that the enzymatic dissociation removed the CD24 epitope from type A cells. GFAP-positive cells were generally round or elliptical and not ciliated.

SVZ cells immunostained for CD24 and GFAP were sorted at 4°C according to their respective fluorescent intensities (Fig. 24B). Cells were sorted directly into an RNA extraction buffer that inactivates endogenous RNases. Total RNA from 5000-10,000 sorted cells for both type B and ependymal cell populations was isolated, and mRNAs were amplified as schematized in Fig. 23. The linearity of amplification and preservation of mRNA size distribution is shown in Fig. 24D. Amplified cDNAs were analyzed for GFAP and CD24 messages by semi-quantitative RT-PCR to verify the separation of SVZ cell types (Fig. 24E). The GFAP message was more than 10-fold enriched in the cDNA library prepared from the R1 gated GFAP-positive, CD24-negative cell populations as compared to the R2 GFAP-negative, CD24-positive population. Conversely, the CD24 message was more than 20-fold enriched in the cDNAs from the R2 population in comparison with the that of the R1 population. Thus RT-PCR demonstrates the success of both the FACS separation and the maintenance of transcriptional differences between the two populations of cells.

Duplicate libraries for both population of cells were generated independently. Scatter plots comparing expression profiles of the duplicate samples show similarity. The greater degree of scatter seen in Fig. 25 (G) and (I) as compared to (D) and (F) may represent the noise introduced by the amplification protocol. Despite this noise, strong gene expression differences between the type B cells and ependyma can be visually detected on scatter plots (Fig. 25H).

Of these 42 genes identified as having potential roles in the SVZ (Table 1), 29 were differentially expressed between type B and ependymal cells. 17 were increased by at least 3-fold in type B cells (Table 2, description in italics), and 7 were type B cell specific by over 100-fold (Table 2, description in bold). This data suggests a number of potential cell-specific markers for both type B and ependymal cells. Furthermore, the knowledge of the identity of the differentially expressed factors and their spatial expression pattern allows new hypothesis to be formed concerning both extrinsic and intrinsic signaling for SVZ stem cells.

Confirmation of differential gene expression.

Both CD24 and HNF3/HFH4 expression in the SVZ have been previously described. Ependymal cells, type A cells, and ObC granule cells express CD24 (Calaora et al., 1996 and data not shown) which correlates well with the expression data in Tables 1 and 2. Type B cells are not immunoreactive for CD24, which is also observed in the expression profiles of the FACS purified cells, further confirming the success of the FACS and transcript amplification. HNF3/HFH4 is a transcription factor expressed in ependymal cells (Blatt et al., 1999) and here was found in the CD24-positive cell

Table 2

Differential expression between type B cells and ependyma of SVZ increased genes

Boldface type indicates a greater than 100-fold difference, underlined indicates at least a 10 to 100-fold difference, and italics indicate a 3 to 10-fold difference. The average AvgDiff score is shown with the range of the two measurements in parentheses.

Probe Set	Description	AvgDiff		AvgDiff		enriched in
		GFAP+	range	CD24+	range	
AF026537_at	prodynorphin, complete cds.	-371	(420)	-889	(267)	-
x53825_s_at	mRNA for heat stable antigen (HSA/CD24)	880	(454)	15693	(1867)	CD24+
aa002925_s_at	cDNA clone 426274 5' mRNA sequence.	5399	(1044)	220	(303)	GFAP+
x66405_s_at	mRNA for collagen alpha1(VI)-collagen.	11164	(6088)	36	(45)	GFAP+
Msa.3088.0_s_at	X70298 sox-4 mRNA	1312	(193)	198	(98)	GFAP+
u51000_s_at	Dlx-1 gene, complete cds.	18913	(2415)	1171	(17)	GFAP+
U51167_s_at	isocitrate dehydrogenase, complete cds.	3042	(269)	5566	(54)	
m83749_s_at	D-type cyclin (CYL2), complete cds	6112	(129)	724	(5)	GFAP+
Msa.1095.0_at	X66603 brain-4 POU-domain protein, complete cds	825	(465)	8	(120)	GFAP+
Msa.21704.0_s_at	AA028273 Homol. to IPP-2	-2596	(575)	-3526	(395)	
Msa.2451.0_s_at	X94322 melanoma-inhibitory-activity protein	12	(515)	17275	(3246)	CD24+
aa522093_s_at	cDNA clone 903988 5', [tazarosine-induced gene2]	-657	(423)	22019	(88)	CD24+
Z46757_s_at	mRNA for high mobility group 2 protein.	517	(312)	204	(34)	
I15443_s_at	L6 antigen, complete cds.	-227	(101)	19118	(3956)	CD24+
L13204_s_at	HNF-3/forkhead homolog-4 (HFH-4), complete cds.	-628	(95)	126	(141)	CD24+
m35159_s_at	Mouse lamin B, complete cds.	73	(111)	82	(9)	
m80540_s_at	Tes-1 homeobox protein, complete cds.	129	(40)	-91	(86)	GFAP+
Msa.30.0_at	D90242 Mouse mRNA for nPKC-eta	-537	(21)	-463	(67)	
C81593_rc_f_at	cDNA clone J0101H11 3' sim. to ribonuc. reduct. M2	3012	(87)	1331	(343)	
U88566_s_at	secreted frizzled related protein sFRP-1, complete cds.	424	(10)	709	(207)	
ET62444_f_at	Sox4, partial cds.	67	(47)	-41	(20)	GFAP+
AF009414_g_at	Sox11, complete cds.	63	(29)	30	(17)	
Z26580_s_at	cyclin A.	3354	(268)	667	(204)	GFAP+
aa268341_s_at	cDNA clone 733722 5' sim. to UBIQUITIN-CONJ. ENZ.	336	(322)	212	(14)	
m14223_s_at	ribonucleotide reductase M2 subunit, complete cds.	4377	(33)	1126	(305)	GFAP+
Msa.24364.0_s_at	W35058 Homol. to FRIZZLED PRECURSOR.	6843	(3433)	1591	(1025)	GFAP+
d16847_s_at	stromal cell derived protein-1, complete cds.	67	(35)	-45	(6)	GFAP+
x83562_s_at	N-glycan alpha 2,8-sialyltransferase.	524	(586)	1472	(277)	
AA426917_s_at	cDNA clone gb836311 similar to cyclin B1	451	(233)	103	(2)	GFAP+
Msa.740.0_at	M95603 Mouse HLH protein homol. to rat ASH1	-181	(268)	-541	(48)	
aa592163_s_at	cDNA clone 1050367 5', [prot. reg. cytokinesis 1]	707	(74)	6	(3)	GFAP+
aa267055_at	cDNA clone 720860 5', mRNA sequence.	2208	(423)	18646	(1072)	CD24+
Msa.13177.0_f_at	W53461 Homol. to CD24 PRECURSOR.	-274	(53)	1129	(452)	CD24+
L22218_at	KV1.5 delayed rectifier K+ channel, complete cds.	-199	(41)	-113	(8)	
U22829_s_at	P2Y purinoceptor, complete cds.	-61	(107)	-6	(6)	
Msa.2695.0_s_at	Z46299 Sp17 gene for sperm specific protein	-23	(40)	2303	(997)	CD24+
Msa.403.0_at	M84120 activin receptor (ActR IIB), complete cds	4735	(1695)	931	(261)	GFAP+
C78640_rc_at	cDNA clone J0052E03 3', mRNA sequence.	925	(71)	834	(337)	GFAP+
m12848_s_at	myb proto-oncogene, complete cds.	-51	(21)	643	(326)	CD24+
D26089_s_at	mRNA for mcdc21, complete cds.	933	(593)	850	(575)	
aa198316_at	cDNA clone 658379 5', mRNA sequence.	2208	(423)	18646	(1072)	CD24+
Msa.27633.0_s_at	AA067092 Homologous to SREBP-1.	330	(58)	2774	(116)	CD24+
X57437_s_at	L-histidine decarboxylase.	443	(578)	16046	(8361)	CD24+
aa289122_s_at	cDNA clone 750657 5' sim. to human CDK reg. sub.2	81	(51)	-58	(44)	GFAP+
I02333_s_at	bilirubin/phenol family UDP glucuronosyltransferase	420	(55)	304	(9)	

expression profile. Interestingly, HNF3/HFH4 expression in the SVZ is only 2-fold greater than that in the ObC. HNF3/HFH4 expression in the ObC was not analyzed in previous studies (Blatt et al., 1999). While the role of HNF3/HFH4 has been established for the development of ciliated epithelial cells (Brody et al., 2000), potential roles for neurogenesis have not yet been investigated.

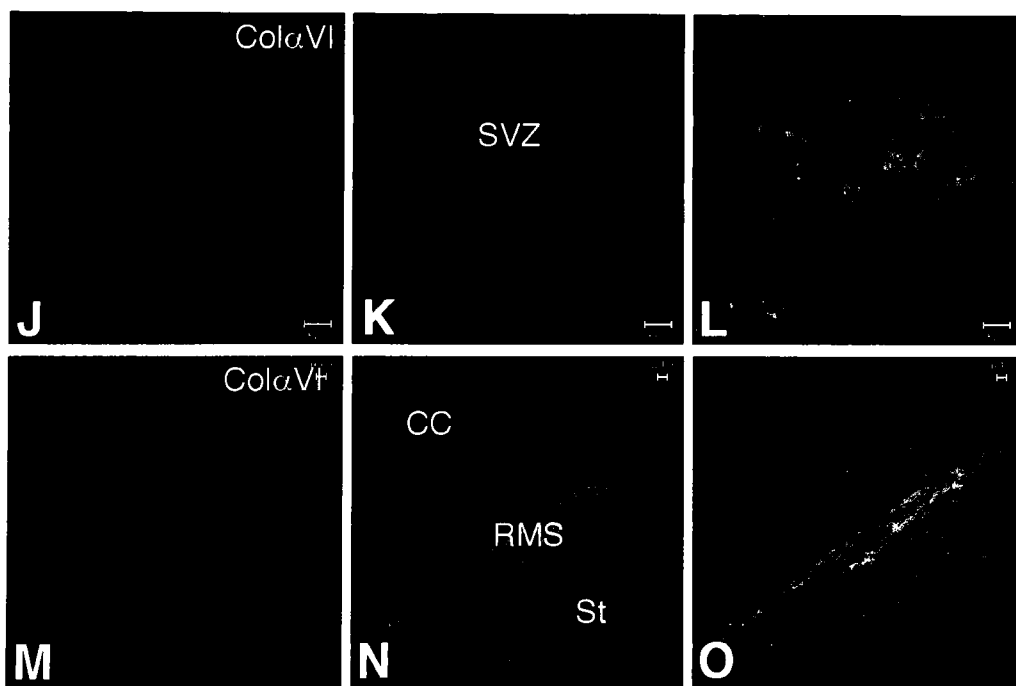
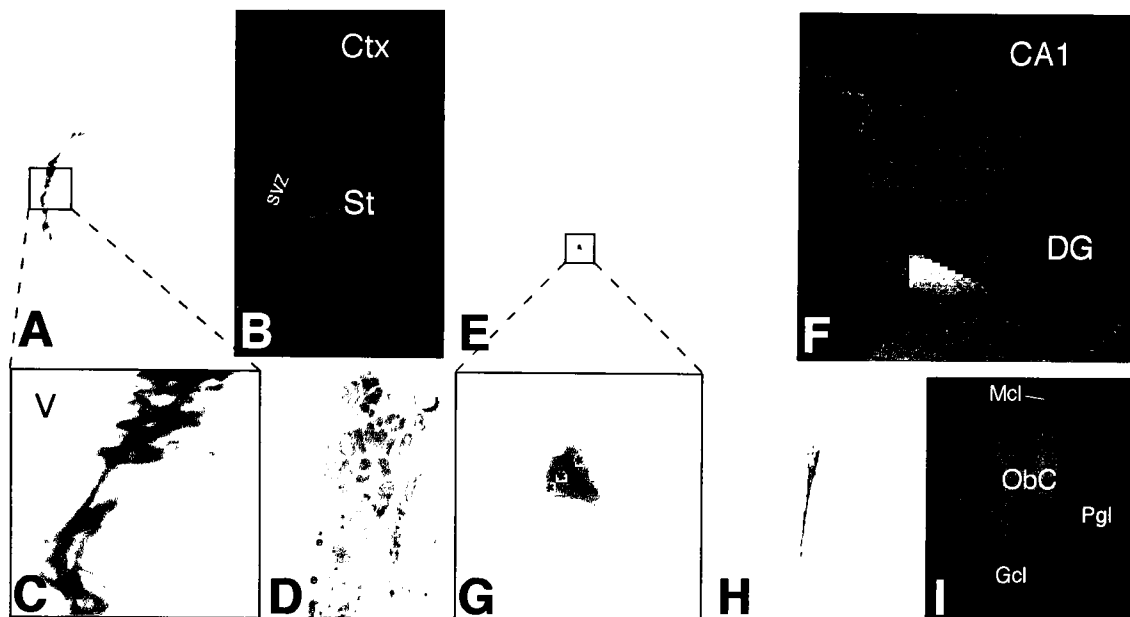
Dlx-2 (also known as Tes-1 as it is described in Tables 1 and 2) is a transcription factor important for the genesis and migration of interneurons born in the embryonic ganglionic eminences (Anderson et al., 1997a; Anderson et al., 1997b). Antibody staining for the Dlx-2 gene product was previously localized to type C and A cells (Doetsch, 1999c). Heterozygous “knock-in” mice expressing the LacZ marker from the Dlx-2 promoter (gift of G. Fishell, unpublished) was used to confirm both the previous antibody staining and the expression profile data. Fig. 27 (A-H) shows strong Dlx-2 expression in the SVZ, Hp, and ObC as predicted by data in Table 1. Furthermore, 2 μ m semi-thin sections shows that SVZ Dlx-2 expression is limited to cells in the SVZ and excluded from the ependyma (Fig. 27D) as predicted in Table 2 and previously described (Doetsch, 1999c). While antibody staining for Dlx-2 protein was not described in type B cells, EM analysis of the Dlx-2-LacZ brain sections detects moderate levels of Dlx-2 expression in this cell population (T. Tramontin, personal communication). In the Hp, small clusters of cells expressed Dlx-2 (Fig. 27G). These clusters are potentially neurogenic foci that have been recently described (Palmer et al., 2000).

Expression profile and Northern blot analysis (Fig. 26) determined that collagen α type VI (ColVI) is expressed to high levels in the SVZ and ObC. Furthermore, type B cells had over 100-fold more expression of ColVI than did ependyma. The SVZ was

Figure 27

Dlx-2 LacZ expression analysis confirms array data. Brain sections from Dlx-2 LacZ mice were stained with X-gal. (A) High levels of Dlx-2 expression (sky-blue deposit) was detected in the lateral ventricle wall. Higher power is shown in (C). Corresponding nuclear counterstained image is in (B). 2 um semi-thin sections show that Dlx-2 is restricted to the SVZ and is not detected in ependymal cells. (E) Dlx-2 is expressed in the neurogenic subgranular layer of the hippocampus dentate gyrus. Higher power magnification (G) reveals small clusters of cells similar to neurogenic clusters previously described (Palmer et al., 2000). Corresponding nuclear counterstained image is in (F). Dlx-2 is strongly expressed in the central core of the OB (H and I). This narrow strip of cells likely corresponds to arriving type A cells.

The SVZ and migratory paths are rich in ColVI. Expression profile data predicts high levels of ColVI in the SVZ and ObC. (J-K) show ColVI immunoreactivity in the SVZ and (M-O) reveal a path of ColVI in the rostral migratory stream (RMS) of type A cells.



strongly immunoreactive for ColVI (Fig. 27J-L). Since ColVI is extracellular, it was difficult to confirm that type B cells express ColVI and ependymal cells do not. However, the high levels of ColVI expression in the ObC correlates well with the intense staining of migratory type A cells en route to the OB (Fig. 27M-O).

Discussion

With this initial analysis of the expression profile data, I have identified 29 potential cell specific markers for the SVZ brain region and 42 genes that may play a roles in the biology of this germinal zone. This primary set of data provides new starting points from which to investigate molecular regulation within the SVZ.

Some of gene expression highlighted by this analysis likely contributes directly to the SVZ microenvironment. For example, melanoma inhibitory activity protein (MIA) is a secreted inhibitory growth factor that was originally identified in melanoma cell lines (Blesch et al., 1994); MIA expression is predicted to be localized to the ependyma and may influence the biology in the adjacent SVZ. ColVI is also extracellular. ColVI is an important ECM component for corneal precursor (Andresen et al., 2000) and neural crest cell migration (Perris et al., 1993); in the brain, ColVI expression has been correlated with brain tumor migration and invasiveness (Han et al., 1995). The strong expression of ColVI in the SVZ and migratory path taken together with the aforementioned studies suggests a role for this ColVI in type A cell migration. Furthermore, ColVI has also been shown to drive cells through S-phase and block apoptosis (Ruhl et al., 1999). Frizzleds are putative receptors for the Wnt family of signaling molecules (reviewed in Wodarz

and Nusse, 1998). Frizzled 2 or 10¹³ was detected specifically in the SVZ. Wnt signaling plays a critical role for stem cells in the skin (Zhu and Watt, 1999) and small intestine (Wong et al., 1998; Korinek et al., 1998). The roles of MIA, ColVI, and Wnts can be tested in vitro in the culture system presented in Chapter 2 and in a migration assay previously described (Wichterle et al., 1997).

By their being transcription factors, *Dlx-1*, *Dlx-2*, *HNF3/HFH4*, *Sox4*, *Sox11*, and *Ash1* homologue are good candidates for being intrinsic factors. *Sox4* and *11* have been shown to have a role in early neuronal differentiation in the embryo and it is possible that they are also important for the SVZ neurogenic lineage. Interestingly, other members of the *Sox* gene family are upregulated by *Noggin* (reviewed in Wegner, 1999),. *Sox 4* and *11* are strongly expressed in the embryonic developing inferior colliculus (IC) (Kuhlbrodt et al., 1998), and it is interesting to consider that this pattern of gene expression may indicate that the external signals in the IC are in some way similar to those in the SVZ; postnatal SVZ cells grafted into the embryonic brain ventricle incorporate into the IC and differentiate into neurons (Lim et al., 1997). *Dlx-1* and *2* are critical for tangential migration of embryonic neuronal precursors (Anderson et al., 1997a) and they may play similar roles in the adult SVZ.

With further confirmation, the cell-specific gene-expression identified here may provide a better means of distinguishing and separating SVZ cell types. Although there may never be markers that are expressed solely in the SVZ stem cell, a collection of markers with known differential expression among SVZ cells may be combined to provide the long sought-after ability to precisely identify the stem cell. Such a multiple-marker approach may dissect the type B cell population into subtypes (e.g., type B1, B2,

¹³ Probe set on the array cannot distinguish between these two.

B3. . .) with one subtype having more stem cell behavior than the others. Refinements in the ability to describe the SVZ cell types and the identification of regulatory genes will facilitate the formation of new hypotheses about the regulation of adult neurogenesis.

CHAPTER 6

Conclusions and Perspectives

The work presented here begins to define the SVZ cell types and molecular signals that maintain adult SVZ neurogenesis. SVZ astrocytes (type B cells) were shown to be a self-renewing cell type capable of producing new neurons; this experiment taken together with other data (Doetsch et al., 1999a) indicated that type B cells are the SVZ stem cell. To determine the cellular components of the SVZ neurogenic niche, I recreated in vitro the cellular interactions observed in vivo. Populations of type B and C cells in direct contact with other astrocytes proliferated to form large colonies of type A neuroblasts; dividing type B cells were shown to give rise to type A cells in these cultures. This recapitulation of SVZ neurogenesis in vitro was not dependent upon serum or exogenous growth factors, suggesting that astrocytes produces external factors that support SVZ neurogenesis. Using these in vitro cultures, I discovered that BMPs inhibit the birth of type A cells. Conversely, Noggin promoted SVZ cell neurogenesis. BMP signaling inhibited neurogenesis by inducing glial differentiation of SVZ precursors and not by inducing cell death of type A cells. In vivo, BMP overexpression in the ependymal layer reduced cell proliferation and abolished neuroblast regeneration in the adjacent SVZ. Furthermore, ectopic Noggin expression promoted neuronal differentiation of SVZ cells transplanted into the striatum. Ependymal cells were found to express Noggin, and SVZ cells express BMPs and their receptors. Collectively, the

experimental and expression data of Noggin and BMPs suggest a simple model in which Noggin derived from ependymal cells antagonizes BMPs signaling in the adjacent SVZ to create a neurogenic niche. To identify other molecular signals for neurogenesis, and to develop better cell-specific markers, I analyzed the transcriptional profiles of adult SVZ cells with high density oligonucleotide arrays. Initial data analysis of the expression data revealed genes that are potentially important for SVZ biology. Below, I discuss how these results and conclusions can be extended to gain a greater understanding of adult neurogenesis.

Direct observation of stem cell behavior

The strategy of self-renewal utilized by type B cells has not been directly determined. The fate of type B cells in astrocyte co-culture was followed indirectly with the RCAS virus. While some AP-positive colonies contained mixed populations, suggesting asymmetric cell divisions (Fig. 11), others contained only type A cells (not shown), suggesting stem cell populational asymmetry (schematized in Fig. 2B). However, the interpretation of retroviral clonal analysis is sometimes made difficult by cell migration. Therefore, it would be ideal to follow the fate of type B cells vitally by direct observation using time lapse video microscopy. Time-lapse records of type B cells in culture would also allow direct observation of the SVZ cell lineage, enhancing our ability to determine at which step (e.g., self-renewal v. progenitor differentiation)

external signals under study have their greatest effect. My attempts to develop time-lapse microscopy for my neurogenic cultures are described briefly in Chapter 3¹⁴.

Ependyma as niche cells

One model of stem cell biology proposes that the self-renewing behavior of stem cells and fate of their descendants is dependent upon signals in their niche (Fig. 2A and B). The signals in the stem cell niche comprise those from the stem cells themselves, progenitors, and other neighboring cells. The neighboring cells that produce factors important for stem cell biology are sometimes referred to as niche cells. In this model, removing the stem cell from signals in their niche would change the fate of the stem cell. Experiments in Chapter 4 indicate that ependymal cells are niche cells for the adult SVZ. BMPs are produced by type B cells, and BMPs inhibit SVZ neurogenesis. Noggin, a BMP antagonist, promotes neurogenesis. This data suggests that type B cells can inhibit their own neurogenesis by autocrine BMP signaling. Localizing type B cells to a region where their BMP ligands are antagonized would therefore promote their neurogenesis. Consistent with this logic, type B cells are found intimately associated with a cellular source of Noggin – the ependyma. When Noggin was overwhelmed by targeted overexpression of BMP7 in the ependyma, SVZ neurogenesis was abolished. Furthermore, antagonizing BMP signaling in a non-neurogenic brain region with ectopic Noggin expression promoted neurogenesis of transplanted SVZ cells. These data all demonstrate the importance of antagonizing BMP signaling in the SVZ, and hence

¹⁴ Dr. Hynek Wichterle, a former student, contributed a great deal of time and expertise to these experiments. Based our experience, we suggest that future attempts should incorporate faster shutter speeds and/or lower light intensities; finer control of humidity, pH, and temperature; and automated stage movements to record the behavior of multiple colonies in every culture.

indicate that the ependyma serve as niche cells for the neurogenic SVZ. Our attention should therefore be directed towards other factors that the ependyma might be providing for the SVZ. Expression profile analysis revealed high levels of the growth factor melanoma-inhibitory activity protein (MIA) in ependymal cells; the potential role of MIA in the SVZ niche will be interesting to study.

Neuronal “induction” in the adult

In the gastrula-stage frog embryo, the Spemann organizer produces Noggin, which antagonizes BMPs in the neighboring ectoderm, inducing neural tissue (Lamb et al., 1993). The proposed interaction between the ependyma and SVZ is reminiscent of this early neural induction event. One notable difference, however, is that while neural induction is a temporally restricted developmental event, SVZ neurogenesis must persist for the entire life of the animal (Kuhn et al., 1996; Goldman et al., 1997). It is intriguing to consider that the adult brain utilizes strategies similar to those in the embryo. This example of adult neurogenesis imitating a developmental plan suggests that more clues about the regulation of this adult germinal zone can be taken from lessons learned in the embryo.

The gene expression profile analysis has provided a list of genes from which to begin such an analysis. *Dlx-1* and *2* are genes required for the generation of a particular class of tangentially migrating interneurons for the developing cortex. *Sox4* and *11* are important for early neuronal differentiation (reviewed in Wegner, 1999). Neural crest cells migrate on “paths” of collagen VI (Perris et al., 1993). Wnt/Frizzled signaling is critical for the development of stem cells in the skin (Zhu and Watt, 1999) and intestine

(Wong et al., 1998). By keeping in mind the developmental roles of these and other genes, we may be able to more easily design, implement, and interpret experiments investigating their potential function in the adult SVZ. Of course, it would be perhaps even more exciting if these genes are shown to have novel functions in the adult.

A transcriptional profile for SVZ neurogenesis

Specific gene expression patterns have been recently assigned to specific cellular “behaviors” in yeast (Chu et al., 1998; Hughes and et al., 2000). In human cells, transcriptional profiles for fibroblast “wound healing” have been described (Iyer et al., 1999) and other profiles can ascribed to specific classes of tumors (Khan et al., 1998; Perou et al., 1999; Alizadeh and et al., 2000; Ross et al., 2000). It therefore follows that SVZ neurogenesis may present a specific gene expression pattern distinct from those of non-neurogenic cellular behaviors. The gene expression of neurogenesis in the adult hippocampus and SVZ may have much in common; notice that *Dlx-2* is also expressed in the SVZ as well as the neurogenic layer of the dentate gyrus (Fig. 27). Since the gene expression databases presented here are standardized, the SVZ gene expression profile will be directly comparable to the dentate gyrus (neurogenic) and CA3 region (non-neurogenic) profiles generated by F. Gage and colleagues (personal communication). The determination of gene expression similarity ('cluster analysis,' reviewed in Brazma and Vilo, 2000) can be utilized to find the patterns that may define adult neurogenesis.

Is there a transcriptional profile for neurogenesis in general? Are there patterns of gene expression utilized in the developing embryonic brain that are “replayed” in the adult SVZ? The interplay of *Noggin* and BMPs suggest that this may be so; additionally,

many “embryonic” transcription factors were here identified in the SVZ. It is unlikely that all of the SVZ-specific genes are important for neurogenesis. Furthermore, many important neurogenic genes may not be specific to neurogenic regions; their role in neurogenesis may be defined by their participation with other factors. How, then, do we identify a neurogenic profile? Perhaps it is reasonable to begin clustering the gene expression of neuronal precursors that have similar behaviors. For instance, LGE embryonic cells transplanted to the adult SVZ migrate efficiently to the OB and differentiate into interneurons (Wichterle et al., 1999). It is therefore plausible that LGE and adult SVZ cells have a common cluster of gene expression; this cluster may represent the intrinsic signals that allow the cells to respond to the SVZ microenvironment. One can think of many other comparisons that would be revealing.

A stem cell transcriptional profile?

While we may learn much from gene expression profiles of neurogenic populations, such analyses may not reveal the signals necessary for stem cell behavior. It is my final speculation that the transcriptional profiles of stem cells in adult self-renewing tissues – from blood to skin to brain – will have important and revealing similarities. The presence of Wnt signaling in stem cells of the intestine, skin, and SVZ (Table 1) for instance, supports this notion. Hence, studies of the adult SVZ stem cell and its neurogenic niche may reveal general principles of stem cell biology in the mammal.

CHAPTER 7

Methods

Ad5-GFAPP-GFP construction

As described in (Doetsch et al., 1999a).

SVZ cell dissociation and fractionation

As described in (Lim and Alvarez-Buylla, 1999).

Astrocyte medium conditioning

Cleaned 7 mm round glass coverslips coated with astrocyte monolayers, PDK, fibronectin, or laminin were placed into 35mm culture dishes containing astrocyte monolayers in 1 ml of serum-free medium. Dissociated SVZ cells were then added to the entire 35 mm dish, allowing cells to settle onto the coverslips. Medium conditioned for 2-5 days was concentrated on Centriplus 3 units (Amicon).

Cultures

SVZ co-cultures were performed as previously described (Lim and Alvarez-Buylla, 1999) with the following modifications. Neurobasal/B27 (Gibco) and DMEM/F12/N2 (Gibco) were used interchangeably. To remove dead cells and debris from dissociated adult SVZ cells, the cell suspension was layered onto 22% Percoll in 1X DPBS and centrifuged for 10 min at 500 g. The cell pellet was washed 3 times with culture medium

before plating onto astrocyte monolayers in LabTek 16-well glass culture slides (Nunc). Astrocyte monolayers were allowed to condition the medium for 1-4 days before plating SVZ cell. Type A and B/C cell populations were purified as previously described (Lim and Alvarez-Buylla, 1999). For the survival assay, pure type A cells were cultured in 96 well tissue culture plates treated with 100 $\mu\text{g/ml}$ poly-D-lysine (Sigma) at 30,000 cells/ cm^2 in Neurobasal/B27. After 10 days, dead cells were removed with a change of medium, and the remaining live cells were quantified with the CyQuant system (Molecular Probes) measured on a Dynex Fluorolite 1000. SVZ cell aggregates were formed by culturing postnatal day 3 SVZ cells in DMEM/F12/N2 at 600,000 cells/ cm^2 in untreated glass culture slides (Nunc).

Immunocytochemistry and histology

The following primary antibodies were used: rat monoclonal to human Noggin (RP57-16), 3 $\mu\text{g/ml}$, (Regeneron Pharmaceuticals); rabbit polyclonal anti-S100 β , 1:1000 (Dako); goat polyclonal anti-BMP4, 10 $\mu\text{g/ml}$, (Research Diagnostics); mouse monoclonal Tuj1, 1:1000 (Babco); mouse monoclonal anti-PSA-NCAM, 1:1000 (Rougon et al., 1986); mouse monoclonal anti-GFAP, 1:500 (Sigma), rat monoclonal anti-BrdU, 1:200 (Harlan), rabbit polyclonal anti-PLAP, 1:200 (Accurate Chemical). After blocking sections or cells with appropriate serum proteins in PBS with 0.3% Triton X100 (Sigma), incubations with primary antibodies were carried out overnight at 4°C in the blocking solution. Sections or cells were washed 3 times in PBS and incubated with appropriate secondary antibodies 1-2 hr at room temperature: biotinylated anti-rat IgG, 1:500 (Vector Laboratories); anti-rabbit IgG FITC, 1:200 (Jackson ImmunoResearch); biotinylated anti-goat IgG, 1:500

(Jackson Laboratories); anti-IgM Cy3, 1:200 (Jackson ImmunoResearch); anti-mouse IgG Cy3, 1:500 (Jackson ImmunoResearch); biotinylated anti-mouse IgG, 1:500 (Vector Laboratories). To reveal biotinylated antibodies, streptavidin-Cy3 or -Cy2 (Jackson ImmunoResearch) diluted 1:1000 in PBS, or peroxidase Vectastain ABC reagent (Vector Laboratories) were used. Peroxidase activity was revealed by diaminobenzidine staining (Doetsch and Alvarez-Buylla, 1996). Controls in which primary antibodies were omitted or replaced with irrelevant antibodies resulted in no detectable staining. The BMP4 antibody recognized a 60kD band corresponding to the size of prepro-BMP4 in SVZ Western blot analysis that was efficiently competed with the peptide to which the antibody was raised.

For Noggin protein staining, fresh frozen sections (12 μ m) were used. For BMP4 staining, both fresh frozen (12 μ m) and polyethylene glycol embedded sections (6 μ m) were used (Alvarez-Buylla et al., 1987). Cultures were fixed in 3% paraformaldehyde for 30 min at room temperature. BrdU antigen was revealed by 2N HCl, 30 min, room temperature. TUNEL staining was performed with the In Situ Cell Death Detection Kit from Boehringer Mannheim. Nuclei were counterstained with Hoechst 33258 (Molecular Probes). Processing for LacZ activity in Vibratome sections and electron microscopy was performed as previously described (Herrera et al., 1999). Whole mount PSA-NCAM staining was performed as previously described (Doetsch and Alvarez-Buylla, 1996).

Reverse-transcription polymerase chain reaction

Total RNA from SVZ dissections and purified cells was isolated with RNeasy columns (Qiagen). 1 μ g of total RNA was converted to cDNA (Superscript II, Gibco), and 1/20 of

the reaction was used in 50 µl PCR reactions (Perkin Elmer). Primers for BMP2, 4, 7, BMPR IA, BMPR IB, BMPR II were previously described (Gross et al., 1996). Primers for Noggin: TCCTCCTCAGCTTCTTGCTC, CGGCCAGCACTATCTACACA; for GAPDH: CCCTGTTGCTGTAGCCGTAT, CCCACTAACATCAAATGGGG. PCR reaction conditions: 95°C, 1 min., 60°C, 1 min., 72°C, 2 min. for 35 cycles, with a 10 min. 72°C final extension. For semi-quantitative PCR, 8µCi of ³²P-dCTP was added to the reactions. The linear range of amplification for each set of primers was determined in pilot experiments. PCR reactions at least 5 cycles before amplification plateau were run on agarose gels, transferred to Hybond-N membranes (Amersham) by Southern blot, and exposed to phosphorimager screens (Molecular Dynamics) for analysis.

Retroviruses

pBluescript plasmids containing BMPR cDNAs were obtained from Lee Niswander (Memorial Sloan-Kettering). Mutations are as follows: human BMPR IA ca, Gln-233 to Asp; mouse BMPR IB ca, Gln-203 to Asp (Zou et al., 1997). The BMPRs constructs were cloned into the retroviral vector pCLE (Gaiano et al., 1999). The retroviral plasmids were sequenced to verify the point mutations. Retroviral plasmid DNA and pCL-Eco (which provides ecotropic gag-pol-env) were cotransfected (10 µg each) by calcium phosphate precipitation into HEK293 cells at 80% confluence in 10cm plates. Virus containing supernatants were collected at 36, 48, and 60 hr after transfection, passed through a 0.45 µm filter, and frozen at -80°C. Viruses were titered on NIH 3T3 cells. B/C cell co-cultures were infected at 0.1-0.5 cfu/SVZ cell in the presence of 8µg/ml of polybrene (Sigma). 1 day after retroviral infection, the virus containing culture

medium was exchanged with fresh medium. Cultures were fixed in 3% paraformaldehyde for 30 min at room temperature, heated to 65°C for 30 min, then incubated with a BCIP/NBT solution (Boehringer Mannheim) for 3-4 hr at room temperature to reveal the alkaline phosphatase marker gene. Cultures were then immunostained as described above.

Adenovirus construction and Noggin protein purification

The mouse Noggin cDNA (pMgB950) was obtained from Richard Harland (University of California, Berkeley). Noggin was cloned into an adenoviral transfer plasmid pAd5-CMV-GFP, resulting in clone pAd5-Noggin-GFP. The adenoviral vector was generated with techniques as previously described (Doetsch et al., 1999a). The titer was 1.5×10^{12} viral particles/ml. This vector expresses Noggin and GFP from independent CMV promoters.

1 L of HELA cells grown in suspension was infected with the Ad5-Noggin-GFP virus at 600 viral particles/cell. 16 hr after infection, the HELA cell medium was changed to a serum-free MEM. 30 hr after infection, the Noggin containing medium was collected. Cells were removed by centrifugation twice, and 0.2 μ m filtration. Noggin was purified with protocols similar to those previously described (Smith et al., 1993). Briefly, Noggin containing medium was run over a SP-sepharose column (Pharmacia). Proteins were eluted with a linear NaCl gradient from 150 mM to 2 M. The major protein peak at 0.9 M-1.1M NaCl was collected, dialyzed, and then run over a Mono-S column (Pharmacia). Noggin was eluted from the Mono-S column with a NaCl gradient

(150mM to 2M). 1 L of HELA cells yielded about 1 mg of pure Noggin protein as assessed by silver stain SDS-PAGE, UV absorbance, and western blot.

Construction of Ad5-BMP7 and characterization will be published elsewhere (Hidaka, C. and R. G. Crystal).

Western blot analysis

10 ng of purified Noggin protein run on reducing and non-reducing SDS-PAGE and transferred to nitrocellulose membrane (Amersham). The membrane was blocked with 2.5% milk in PBS with 0.1% Tween-20 and then incubated with anti-Noggin antibody RP57-16 (Regeneron Pharmaceuticals) at 50 ng/ml for 4 hr at room temperature. After washes, the blot was then incubated with an anti-rat IgG peroxidase secondary antibody (Vector Laboratories) diluted 1:5000 for 1 hr at room temperature, washed, and developed with ECL (Amersham).

For Tuj1 and GFAP protein analysis of aggregate SVZ cultures: P3 CD1 mouse SVZ cells were dissociated with papain (Lim and Alvarez-Buylla, 1999), and plated in DMEM/F12/N2 at 600,000 cells/cm² into untreated glass culture wells (Nunc). Aggregates of SVZ cells form within 24 hr. After 2.5-3 DIV, cells were dissociated with 0.25% trypsin, 0.5 mM EDTA (Gibco). 100,000 cells from each well were lysed in 200 μ l of 1%NP-40, 50 mM Tris, pH 7.5, 150 mM NaCl with a protease inhibitor cocktail (Sigma). 10 μ l of the cell lysate was separated by 4-15% gradient SDS-PAGE and transferred to nitrocellulose. The blots were blocked as above and incubated with primary antibody overnight at 4°C. Tuj1 antibody (Babco) dilution, 1:1000; monoclonal anti-GFAP antibody (Sigma) dilution, 1:500. Anti-mouse IgG peroxidase secondary

antibody (Sigma) diluted 1:1000 was incubated with the blot for 2 hr at room temperature. Blots were developed with ECL and exposed to X-ray film for 1s, 3s, 9s, 30s, 90s and 5 min. Single bands of predicted size were observed for each antibody. Bands from film exposures in the linear range of the film were quantified for size and density by light transmission flatbed scanning (AGFA Duoscan) and subsequent image analysis by NIH Image 1.62b7.

BMP7 overexpression in vivo

2.6×10^9 viral particles of both Ad5-BMP7 and Ad5-GFP were co-injected in a volume of 2 μ l into the lateral ventricle as previously described (Doetsch et al., 1999a). As controls, 5.2×10^9 viral particles of Ad5-GFP in a volume of 2 μ l were injected. To measure SVZ proliferation, one hour before sacrifice, 100 μ l of 10 mg/ml BrdU was injected intraperitoneally. Animals were perfused as previously described (Doetsch and Alvarez-Buylla, 1996). Brains were serially vibratome sectioned at 40 μ m. Only animals with good GFP expression in the ependyma ipsilateral to the injection were used. BrdU positive SVZ cells were counted using a computerized mapping system (Alvarez-Buylla and Vicario, 1988) in 3 sections from each animal.

To assess BMP overexpression on SVZ regeneration, we injected viruses as above after 6 days of Ara-C (Sigma) infusion as previously described (Doetsch et al., 1999b). 5 days after viral injections, lateral ventricle whole mounts were prepared (Doetsch and Alvarez-Buylla, 1996). GFP expression in lateral ventricle wall was assessed before PSA-NCAM immunostaining. Data shown are from the ventricle wall contralateral to

the injection to avoid any potential injury caused by the osmotic pump cannula; results from the ipsilateral ventricle wall were similar.

Ectopic Noggin expression in striatum

2×10^8 Ad5-Noggin or Ad5-GFP viral particles were injected in 200 nl at 0 mm anterior, +/- 2 mm lateral to bregma, and 2.9 mm deep to the brain surface. Two days later, 10,000 hPAP SVZ cells dissociated and cleared as above were injected in a volume of 0.5 μ l using the same stereotaxic coordinates. Seven days after grafts, animals were perfused as above. 40 μ m coronal Vibratome sections containing the GFP-positive injection site were first immunostained for hPAP followed by staining with Tuj1 antibodies. 1 μ m optical sections were analyzed at the confocal microscope (Zeiss LSM 510). hPAP-positive cells were found within the GFP-positive foci, confirming the targeting of the grafts.

Production of ds T7 cDNA from adult brain regions

Adult (2-3 month) CD-1 (Charles River Laboratories) mouse brains were processed one-at-a-time. Brains from mice killed by cervical dislocation were immediately placed into ice-cold 20 mM Pipes (pH 7.4), 120 mM NaCl, 5 mM KCl, 25 mM glucose. SVZ was dissected bilaterally from a coronal slice as previously described (Lim, et al., 1997); Ctx and St were obtained from the same coronal slice. ObC was dissected from serial coronal slices of the Ob. Hp was isolated by cutting the fimbria and blunt dissection using forceps. Cb was dissections included all cerebellar layers. Dissected tissues were individually snap-frozen in 1.5 ml tubes with liquid N₂ and stored at -80°C.

Tissue fragments were rapidly thawed in RNeasy (Qiagen) lysis buffer and disrupted by 10 passes through a 21G needle, 5 passes through a 25G needle, and 1 pass through a Qias shredder column (Qiagen). Total RNA was isolated with RNeasy mini-columns with genomic DNA digestion on the column as per manufacturer protocols (Qiagen). Poly-A RNA was isolated from total RNA with magnetic oligo-dT beads (Dyna) as per manufacturer protocol with the following modifications: 1.2 ml of beads were used to isolate approximately 1 µg of poly-A RNA from each brain region. For elution, the entire magnetic block was immersed in a 65°C water bath. RNA was eluted from the beads 3 times, 15 µl each. Poly-A RNA was concentrated by vacuum centrifugation with no heat. For each brain region, 1 µg of poly-A RNA in 10 µl was combined with 1 µl of 100 µM T7LD3' primer, heated to 70°C for 5 min, then placed on ice. 40 units RNasin, 4 µl of 5x first strand buffer (Life Technologies), 2 µl 0.1M DTT, and 1 µl of 10 mM dNTPs were added, and tubes were incubated at 42°C for 5 min. 200 units of Superscript II (Life Technologies) was then added, and reactions incubated for

another 60 min at 42°C. On ice, 91 µl of H₂O, 30 µl of second strand buffer (Life Technologies), 3 µl of 10 mM dNTPs, 10 units DNA ligase (Life Technologies), 40 units DNA Pol I (New England Biolabs), and 2 units RNaseH (Life Technologies) were added, and reactions incubated at 16°C for 2 h. 10 units T4 polymerase (New England Biolabs) was added, and reactions incubated for another 15 min. ds T7 cDNAs were cleaned with QIAquick columns using buffer PB (Qiagen) and eluted in 50 µl Tris, pH 8.

FACS isolation of type B and ependymal cells and ds cDNA production

Adult SVZ cells were dissociated, cleared of dead cells and debris by 22% Percoll (Sigma) step-gradient as described above, and passed through a 40 µm nylon cell strainer (Beckdon Dickinson). All immunostaining incubations and washes were performed at 0-4°C with pre-chilled buffers. Biotinylated mCD24 antibody (Pharmingen) was used at 1:10 and rabbit GFAP antibody (DAKO) was used at 1:100. About 1 x 10⁶ SVZ cells were resuspended in 100 µl PBS containing both primary antibodies, 0.1% Tween-20 (Sigma), and 100-200 units of RNasin (Promega) and incubated for 15 minutes on ice. Cells were pelleted in 1.5 ml tubes in a Beckman table-top centrifuge with swinging buckets at 2000 rpm for 5 min at 4°C. Cells were resuspended in 100 µl of PBS and centrifuged as before; this wash step was repeated 2 more times. Cells were then resuspended in 100 µl of PBS containing streptavidin-Cy2 at 1:100 and anti-rabbit F(ab)₂ at 1:25 (Jackson ImmunoResearch), 0.1% Tween-20, and 100-200 units of RNasin and incubated for 10 minutes on ice. Cells were washed 3 times with PBS as before. Cells were resuspended in PBS at a final concentration of 500,000 cells/ml. Under

epifluorescent microscopy, CD24-positive cells were ciliated, and GFAP-positive cells were rounded and not ciliated. Omission of primary antibodies resulted in no staining.

Immunostained cells were isolated on a FACS Vantage (Beckton-Dickinson) with the laser aligned immediately prior to each run. Events were triggered off a forward scatter threshold of 52. Unstained SVZ cells and cells stained only with secondary reagents were used to determine the levels of background fluorescence. Cells were sorted at approximately 200 cells/s at 4°C yielding an abort rate of <1%, and the droplet breakoff point was monitored continuously. Gated cells were collected directly into RNeasy lysis buffer. Sorting runs that were interrupted for any reason were not used for cDNA production. Total RNA was isolated with RNeasy columns with on column genomic DNA digestion as per manufacture protocol. RNA was concentrated by vacuum centrifugation to 12 µl. 9 µl of total RNA was combined with 1 µl of 100 µM T7LD3' primer, heated to 70°C for 5 min, then placed on ice. 40 units RNasin, 4 µl of 5x first strand buffer, 2 µl of 0.1M DTT, 1 µl of 20 µM SMART III oligo, and 1 µl of 10 mM dNTPs were added, and tubes were incubated at 42°C for 5 min. 400 units of Superscript II was then added, and reactions incubated for another 60 min at 42°C. 2 units RNaseH was added and tubes incubated at 37°C for 20 min. 3 µl of total RNA was used in parallel reactions without Superscript as RT-minus controls.

For LD-PCR, 5 µl of cDNA was combined on ice with 5 µl of 10X Advantage 2 PCR buffer (Clontech), 1 µl of 10 mM dNTPs, 36 µl H₂O, 1 µl 10 µM 5'PCR primer, 1 µl 10 µM 3'PCR primer, and 1 µl 50X Advantage 2 polymerase mix (Clontech). Thermal cycling was conducted in a Perkin Elmer 480 with the following parameters: 95°C for 5 min, 68°C for 6 min, 1 cycle; then 95°C for 15 sec, 68°C for 6 min, 20 cycles. 2 µl of 20

mg/ml proteinase K was added and reactions were incubated at 45°C for 20 min. ds cDNAs were phenol/CHCl₃ extracted twice, then spun through a Chromospin400 column (Clontech). 15 µl of ds cDNA was used for a second LD-PCR reaction assembled as above. 10 µl aliquots were removed at 6, 8, 10, and 12 cycles and analyzed on agarose gels by ethidium bromide staining and Southern blotting for GAPDH to determine the linear range of amplification. Parallel secondary LD-PCR reactions were then carried out using an appropriate cycle number.

GeneChip probe production and hybridizations

Biotin-labeled cRNAs were produced from the ds cDNA libraries and hybridized to Mu11K chips according to Affymetrix (Santa Clara, CA) protocols. Chips were analyzed on a GeneArray scanner (Affymetrix). For each brain region, cRNAs were prepared from independent ds cDNA libraries generated from different dissection sessions. Likewise, for each FACS population, cRNAs were generated from independent ds cDNA libraries prepared from different dissection sessions and FACS runs.

Northern and Southern blots

Northern and Southern blots were performed according to standard protocols using ExpressHyb (Clontech) or ULTRAhyb (Ambicom). Probes for hybridizations were produced by PCR cloning. All probes were sequenced to verify their identity.

PCR primer sequences

T7LD3':

ATTCTAGAGGCCGAGGCGGCCGACATGTAATACGACTCACTATAGGGCGTTT
TTTTTTTTTTTTTTTTTTTTTTTTTTTTTVN (V=A,G,C; N=A,G,C,T)

SMART III: AAGCAGTGGTATCAACGCAGAGTGGCCATTATGGCCGGG

5'PCR: AAGCAGTGGTATCAACGCAGAGTGGCCATTATGG

3'PCR:

ATTCTAGAGGCCGAGGCGGCCGACATGTAATACGACTCACTATAGGGCG

GAPDH: CCCACTAACATCAAATGGGG, CTCACTTGTGGCCCAGGTAT

Dlx-1: TCCTGAATGGTCTTCTTCCG, CTGGGGTGGTACGAAGATGG

aa002925: AGATGATAGCTGAGCAGCGG, CTGGCAGAGAGGTTCAAAGC

Sox11: CAGGCACTTCTTCCCTTTTG, CAGCTCTGAGGTCTATGTCACC

Collagen α VI: CCCCATTTGGACCTAAAGGAT, CAGCACGAAGAGGATGTCAA

CyclinD2: CCTCACGACTTCATTGAGCA, ATGCTGCTCTTGACGGAAC

HMG2: AGCTTGGGGAAGGAAGTCTC, AGCAAAACAGGAAGAAGGCA

MIA: AGCCCAGAGACCTCGTTCTT, ATCAATTTTGCCAGGTTTCG

Dynorphin: GATCAGGTAGGGCATGAGGA, TTCTCTGGATTCTGGGATGG

References

- Akiyama, S., Katagiri, T., Namiki, M., Yamaji, N., Yamamoto, N., Miyama, K., Shibuya, H., Ueno, N., Wozney, J.M., and Suda, T. (1997). Constitutively active BMP type I receptors transduce BMP-2 signals without the ligand in C2C12 myoblasts. *Experimental Cell Research* 235, 362-369.
- Alizadeh, A.A. and et al. (2000). Distinct types of diffuse large B-cell lymphoma identified by gene expression profilin. *Nature* 403, 503-511.
- Altman, J. (1970). Postnatal neurogenesis and the problem of neural plasticity. In *Developmental neurobiology*. W.A. Himwich, ed. (Springfield: C.C.Thomas), pp. 197-237.
- Alvarez-Buylla, A., Buskirk, D.R., and Nottebohm, F. (1987). Monoclonal antibody reveals radial glia in adult avian brain. *Journal of Comparative Neurology* 264, 159-170.
- Alvarez-Buylla, A., García-Verdugo, J.M., Mateo, A., and Merchant-Larios, H. (1998). Primary neural precursors and intermitotic nuclear migration in the ventricular zone of adult canaries. *Journal of Neuroscience* 18, 1020-1037.
- Alvarez-Buylla, A. and Lois, C. (1995). Neuronal stem cells in the brain of adult vertebrates. *Stem Cells* 13, 263-272.
- Alvarez-Buylla, A. and Temple, S. (1998). Stem cells in the developing and adult nervous system. *Journal of Neurobiology* 36, 105-110.
- Alvarez-Buylla, A. and Vicario, D.S. (1988). Simple microcomputer system for mapping tissue sections with the light microscope. *Journal of Neuroscience Methods* 25, 165-173.

- Anderson, S.A., Eisenstat, D.D., Shi, L., and Rubenstein, J.L.R. (1997a). Interneuron migration from basal forebrain to neocortex: dependence on *Dlx* genes. *Science* 278, 474-476.
- Anderson, S.A., Qiu, M., Bulfone, A., Eisenstat, D.D., Meneses, J.J., Pedersen, R.A., and Rubenstein, J.L.R. (1997b). Mutations of the Homebox Genes *Dlx-1* and *Dlx-2* Disrupt the Striatal Subventricular Zone and Differentiation of Late Born Striatal Neurons. *Neuron* 19, 27-37.
- Andresen, J.L., Ledet, T., Hager, H., Josephesen, K., and Ehlers, N. (2000). The influence of corneal stromal matrix proteins on the migration of human corneal fibroblasts. *Experimental Eye Research* 71, 33-43.
- Baba, H., Nakahira, K., Morita, N., Tanaka, F., Akita, H., and Ikenaka, K. (1997). GFAP gene expression during development of astrocyte. *Developmental Neuroscience* 19, 49-57.
- Bachiller, D., Klingensmith, J., Kemp, C., Belo, J.A., Anderson, R.M., May, S.R., McMahon, J.A., McMahon, A.P., Harland, R.M., Rossant, J., and DeRobertis, E.M. (2000). The organizer factors Chordin and Noggin are required for mouse forebrain development. *Nature* 403, 658-661.
- Barde, Y.A. (1994). Neurotrophins: a family of proteins supporting the survival of neurons. *Progress in Clinical Biological Research* 390, 45-56.
- Barres, B.A. (1999). A New Role for Glia: Generation of Neurons! *Cell* 97, 667-670.
- Bignami, A., Eng, L.F., Dahl, D., and Uyeda, C.T. (1972). Localization of the glial fibrillary acidic protein in astrocytes by immunofluorescence. *Brain Research* 43, 429-435.
- Bigner, D.D., McLendon, R.E., and Bruner, J.M. (1998). Russell & Rubinstein's

- Birse, S.C., Leonard, R.B., and Coggeshall, R.E. (1980). Neuronal increase in various areas of the nervous system of the guppy, *Lebistes*. *Journal of Comparative Neurology* 194, 291-301.
- Bjornson, C.R.R., Rietze, R.L., Reynolds, B., Magli, M.C., and Vescovi, A.L. (1999). Turning Brain into Blood: A Hematopoietic Fate Adopted by Adult Neural Stem Cells in Vivo. *Science* 283, 534-537.
- Blatt, E.N., Yan, X.H., Wuerffel, M.K., Hamilos, D.L., and Brody, S.L. (1999). Forkhead transcription factor HFH-4 expression is temporally related to ciliogenesis. *American Journal of Respiratory Cell and Molecular Biology* 21, 168-76.
- Blesch, A., Bosserhoff, A.K., Apfel, R., Behl, C., Hessdoerfer, B., Schmitt, A., Jachimczak, P., Lottspeich, F., Buettner, R., and Bogdahn, U. (1994). Cloning of a novel malignant melanoma-derived growth-regulatory protein, MIA. *Cancer Research* 54, 5695-701.
- Bradford, G.B., Williams, B., Rossi, R., and Bertoncello, I. (1997). Quiescence, cycling, and turnover in the primitive hematopoietic stem cell compartment. *Experimental Hematology* 25, 445-53.
- Brazma, A. and Vilo, J. (2000). Gene expression data analysis. *FEBS* 480, 17-24.
- Brody, S.L., Yan, X.H., Wuerffel, M.K., Song, S.K., and Shapiro, S.D. (2000). Ciliogenesis and left-right axis defects in forkhead factor HFH-4-null mice. *American Journal of Respiratory Cell and Molecular Biology* 23, 45-51.
- Brunet, L.J., McMahon, J.A., McMahon, A.P., and Harland, R.M. (1998). Noggin, Cartilage Morphogenesis, and Joint Formation in the Mammalian Skeleton. *Science* 280, 1455-1457.

- Bruni, J.E. (1998). Ependymal Development, Proliferation, and Functions: A Review. *Microscopy Research Techniques* 41, 2-13.
- Bruni, J.E., Del Bigio, M.R., and Clattenburg, R.E. (1985). Ependyma: Normal and pathological. A review of the literature. *Brain Research Reviews* 9, 1-19.
- Calaora, V., Chazal, G., Nielsen, P.J., Rougon, G., and Moreau, H. (1996). mCD24 expression in the developing mouse brain and in zones of secondary neurogenesis in the adult. *Neuroscience* 73, 581-594.
- Chen, D., Ji, X., Harris, M. A., Feng, J. Q., Karsenty, G., Celeste, A. J., Rosen, V., Mundy, G. R., and Harris, S. E. Differential roles for bone morphogenetic protein (bmp) receptor type ib and ia in differentiation and specification of mesenchymal precursor cells to osteoblast and adipocyte lineages. *Journal of Cell Biology* 142(1), 295-305. 98.
- Cheng, T., Shen, H., Giokas, D., Gere, J., Tenen, D.G., and Scadden, D.T. (1996). Temporal mapping of gene expression levels during the differentiation of individual primary hematopoietic cells. *Proceedings of the National Academy of Sciences USA* 93, 13158-13163.
- Cheshier, S.H., Morrison, S.J., Liao, X., and Weissman, I.L. (1999). In vivo proliferation and cell cycle kinetics of long-term self-renewing hematopoietic stem cells. *Proceedings of the National Academy of Sciences USA* 96, 3120-3125.
- Chiasson, B.J., Tropepe, V., Morshead, C.M., and Van der Kooy, D. (1999). Adult Mammalian Forebrain Ependymal and Subependymal Cells Demonstrate Proliferative Potential, but only Subependymal Cells Have Neural Stem Cell Characteristics. *Journal of Neuroscience* 19, 4462-4471.
- Chu, S., DeRisi, J., Eisen, M., Mulholland, J., Botstein, D., Brown, P.O., and Herskowitz, I. (1998). The transcriptional program of sporulation in budding yeast. *Science*

282, 699-705.

Clarke, D.L., Johansson, C.B., Wilbertz, J., Veress, B., Nilsson, E., Karkstrom, H., Lendahl, U., and Frisén, J. (2000). Generalized Potential of Adult Neural Stem Cells. *Science* 288, 1660-1663.

Coulombe, P.A., Kopan, R., and Fuchs, E. (1989). Expression of Keratin K14 in the epidermis and Hair Follicle: Insights into Complex Programs of Differentiation. *Journal of Cell Biology* 109, 2295-2312.

Crino, P.B., Trojanowski, J.Q., Dichter, M.A., and Eberwine, J. (1996). Embryonic neuronal markers in tuberous sclerosis: Single-cell molecular pathology. *Proceedings of the National Academy of Sciences USA* 93, 14152-14157.

Davidson, B.L., Allen, E.D., Kozarsky, K.F., Wilson, J.M., and Roessler, B.J. (1993). A model system for in vivo gene transfer into the central nervous system using an adenoviral vector. *Nature Genetics* 3, 219-223.

Davis, A.A. and Temple, S. (1994). A self-renewing multipotential stem cell in embryonic rat cerebral cortex. *Nature* 372, 263-266.

Deprimo, S.E., Stambrook, P.J., and Stringer, J.R. (1996). Human placental alkaline phosphatase as a histochemical marker of gene expression in transgenic mice. *Transgenic Research* 5, 459-466.

Didier, M., Harandi, M., Aguera, M., Bancel, B., Tardy, M., Fages, C., Calas, A., Stagaard, M., Mollgard, K., and Belin, M.F. (1986). Differential immunocytochemical staining for glial fibrillary acidic (GFA) protein, S-100 protein and glutamine synthetase in the rat subcommissural organ, nonspecialized ventricular ependyma and adjacent neuropil. *Cell and Tissue Research*. 245, 343-351.

- Doetsch, F. and Alvarez-Buylla, A. (1996). Network of tangential pathways for neuronal migration in adult mammalian brain. *Proceedings of the National Academy of Sciences USA* 93, 14895-14900.
- Doetsch, F., Garcia-Verdugo, J.M., and Alvarez-Buylla, A. (1997). Cellular composition and three-dimensional organization of the subventricular germinal zone in the adult mammalian brain. *Journal of Neuroscience* 17, 5046-5061.
- Doetsch, F., Caille, I., Lim, D.A., García-Verdugo, J.M., and Alvarez-Buylla, A. (1999a). Subventricular Zone Astrocytes Are Neural Stem Cells in the Adult mammalian Brain. *Cell* 97, 1-20.
- Doetsch, F., Garcia-Verdugo, J.M., and Alvarez-Buylla, A. (1999b). Regeneration of a germinal layer in the adult mammalian brain. *Proceedings of the National Academy of Sciences USA* 96, 11619-11624.
- Doetsch, F. (1999c) Origin and migration routes of new neurons in the adult mammalian brain. New York, Rockefeller University.
- Ebendal, T., Bengtsson, H., and Soderstrom, S. Bone morphogenetic proteins and their receptors: potential functions in the brain. *Journal of Neuroscience Research* 51(2), 139-46. 98.
- Eglitis, M.A. and Mezey, E. (1997). Hematopoietic cells differentiate into both microglia and macroglia in the brains of adult mice. *Proceedings of the National Academy of Sciences USA* 4080-4085.
- Eriksson, P.S., Perfilieva, E., Bjork-Eriksson, T., Alborn, A., Nordborg, C., Peterson, D.A., and Gage, F.H. (1998). Neurogenesis in the adult human hippocampus. *Nature Medicine* 4, 1313-1317.
- Espejo, M., Cutillas, B., Ventura, F., and Ambrosio, S. (1999). Exposure of foetal

mesencephalic cells to bone morphogenetic protein-2 enhances the survival of dopaminergic neurones in rat striatal grafts. *Neuroscience Letters* 275, 13-6.

Fend, F., Emmert-Buck, M.R., Chuaqui, R., Cole, K., Lee, J., Liotta, L.A., and Raffeld, M. (1999). Immuno-LCM: Laser Capture Microdissection of Immunostained Frozen Sections for mRNA Analysis. *American Journal of Pathology* 154, 61-66.

Ferrari, G., Cusella-De Angelis, G., Coletta, M., Paolucci, E., Stornaiuolo, A., Cossu, G., and Mavilio, F. (1998). Muscle regeneration by bone marrow-derived myogenic progenitors. *Science* 1528-1530.

Flaumenhaft, R. and Rifkin, D.B. (1991). Extracellular matrix regulation of growth factor and protease activity. *Current Opinion in Cell Biology* 5, 817-823.

Fuchs, E. and Segre, J.A. (2000). Stem Cells: A New Lease on Life. *Cell* 100, 143-155.

Furuta, Y., Piston, D.W., and Hogan, B.L. (1997). Bone morphogenetic proteins (BMPs) as regulators of dorsal forebrain development. *Development* 124, 2203-2212.

Gage, F.H. (1998). Discussion point Stem cells of the central nervous system. *Current Opinion in Neurobiology* 8, 671-675.

Gage, F.H. (2000). Mammalian neural stem cells. *Science* 287. 287, 1433-8.

Gage, F.H., Kempermann, G., Palmer, T., Peterson, D.A., and Ray, J. (1998). Multipotent progenitor cells in the adult dentate gyrus. *Journal of Neurobiology* 36, 249-266.

Gage, F.H., Ray, J., and Fisher, L.J. (1995). Isolation, characterization, and use of stem cells from the CNS . *Annual Reviews in Neuroscience*. 18, 159-192.

Gaiano, N., Kohtz, J.D., Turnbull, D.H., and Fishell, G. (1999). A method for rapid gain-of-function studies in the mouse embryonic nervous system. *Nature*

Galou, M., Pournin, S., Ensergueix, D., Ribet, J.-L., Tchelingirian, J.-T., Lossouarn, L., Privat, A., Babinet, C., and Dupouey, P. (1994). Normal and pathological expression of GFAP promoter elements in transgenic mice. *Glia* 12,

Gao, W.-Q., Heintz, N., and Hatten, M.E. (1991). Cerebellar granule cell neurogenesis is regulated by cell-cell interactions in vitro. *Neuron* 6, 705-715.

García-Verdugo, J.M., Doetsch, F., Wichterle, H., Lim, D.A., and Alvarez-Buylla, A. (1998). Architecture and cell types of the adult subventricular zone: in search of the stem cells. *Journal of Neurobiology* 36, 234-248.

Globus, J.H. and Kuhlenbeck, H. (1944). The Subependymal cell plate (matrix) and its relationship to brain tumors of the ependymal type. *Journal of Neuropathology and Experimental Neurology* 3, 1-35.

Goldman, S.A. (1998). Adult neurogenesis: from canaries to the clinic. *Journal of Neurobiology* 36, 267-286.

Goldman, S.A., Kirschenbaum, B., Harrison-Restelli, C., and Thaler, H.T. (1997). Neuronal precursors of the adult rat subependymal zone persist into senescence, with no decline in spatial extent or response to BDNF. *Journal of Neurobiology* 32, 554-566.

Goldman, S.A. and Nottebohm, F. (1983). Neuronal production, migration, and differentiation in a vocal control nucleus of the adult female canary brain. *Proceedings of the National Academy of Sciences USA* 80, 2390-2394.

Goldsworthy, S.M., Stockton, P.S., Trempus, C.S., Foley, J.F., and Maronpot, R.R. (1999). Effects of Fixation on RNA Extraction and Amplification from Laser Capture Microdissected Tissue. *Molecular Carcinogenesis* 25, 86-91.

- Gould, E., Reeves, A.J., Graziano, M.S.A., and Gross, C.G. (1999). Neurogenesis in the neocortex of adult primates. *Science* 286, 548-552.
- Graham, A., Koentges, G., and Lumsden, A. (1996). Neural crest apoptosis and the establishment of craniofacial pattern: an honorable death. *Molecular and Cellular Neuroscience* 8, 76-83.
- Grill, R.J. and Pixley, S.K. (1997). In vitro generation of adult rat olfactory sensory neurons and regulation of maturation by coculture with CNS tissues. *Journal of Neuroscience* 17, 3120-37.
- Grinspan, J. B., Edell, E., Carpio, D. F., Beesley, J. S., Lavy, L., Pleasure, D., and Golden, J. A. Stage-specific effects of bone morphogenetic proteins on the oligodendrocyte lineage. *Journal of Neurobiology* 43(1), 1-17. 2000.
- Gritti, A., Parati, E.A., Cova, L., Frolichsthal, P., Galii, R., Wanke, E., Faravelli, L., Morassutti, D.J., Roisen, F., Nickel, D.D., and Vescovi, A.L. (1996). Multipotential stem cells from the adult mouse brain proliferate and self-renew in response to basic fibroblast growth factor. *Journal of Neuroscience* 16, 1091-1100.
- Grondona, J.M., Pérez-Martín, M., Cifuentes, M., Pérez, J., Jiménez, A.J., Pérez-Figares, J.M., and Fernández-LLebrez, P. (1996). Ependymal denudation, aqueductal obliteration and hydrocephalus after a single injection of neuraminidase into the lateral ventricle of adult rats. *Journal of Neuropathology and Experimental Neurology* 55, 999-1008.
- Gross, R.E., Mehler, M.F., Mabie, P.C., Zang, Z.Y., Santschi, L., and Kessler, J.A. (1996). Bone morphogenetic proteins promote astroglial lineage commitment by mammalian subventricular zone progenitor cells. *Neuron* 17, 595-606.
- Han, J., Daniel, J.C., and Pappas, G.D. (1995). Expression of type VI collagen during

- glioblastoma cell invasion in brain tissue cultures. *Cancer Letters* 88, 127-32.
- Harrison, D.E. and Lerner, C.P. (1991). Most primitive hematopoietic stem cells are stimulated to cycle rapidly after treatment with 5-fluorouracil. *Blood* 78,
- Hata, A., Seoane, J., Lagna, G., Montalvo, E., Hemmati-Brivanlou, A., and Massague, J. Oaz uses distinct dna- and protein-binding zinc fingers in separate bmp-smad and olf signaling pathways. *Cell* 100(2), 229-40. 2000.
- Hattori, A., Katayama, M., Iwasaki, S., Ishii, K., Tsujimoto, M., and Kohno, M. (1999). Bone morphogenetic protein-2 promotes survival and differentiation of striatal gabaergic neurons in the absence of glial cell proliferation. *Journal of Neurochemistry* 72, 2264-71.
- Herrera, D.G., Garcia-Verdugo, J.M., and Alvarez-Buylla, A. (1999). Adult-Derived Neural Precursors Transplanted into Multiple Regions in the Adult Brain. *Annals of Neurology* 46, 867-877.
- Ho, P.T.C. and Tucker, R.W. (1989). Centriole Ciliation and Cell Cycle Variability During G1 Phase of BALB/c 3T3 Cells. *Journal of Cellular Physiology* 139, 398-406.
- Holland, E.C. and Varmus, H.E. (1998). Basic fibroblast growth factor induces cell migration and proliferation after glia-specific gene transfer in mice. *Proceedings of the National Academy of Sciences USA* 95, 1218-1223.
- Hu, M., Krause, D., Greaves, M., Sharkis, S., Dexter, M., Heyworth, C., and Enver, T. (1997). Multilineage gene expression precedes commitment in the hemopoietic system. *Genes & Development* 11, 774-785.
- Hughes, T.R. and et al. (2000). Functional discovery via a compendium of expression profiles. *Cell* 102, 109-126.

- Iyer, V.R., Eisen, M.B., Ross, D.T., Schuler, G., Moore, T., Lee, J.C.F., Trent, J.M., Staudt, L.M., Hudson, J., Boguski, M.S., Lashkari, D., Shalon, D., Botstein, D., and Brown, P.O. (1999). The transcriptional program in the response of human fibroblasts to serum. *Science* 283,
- Jacobs, C. and Shapiro, L. (1998). Microbial asymmetric cell division: localization of cell fate determinates. *Current Opinion in Genetics & Development* 8, 386-391.
- Johansson, C.B., Momma, S., Clarke, D.L., Risling, M., Lendahl, U., and Frisén, J. (1999). Identification of a Neural Stem Cell in the Adult Mammalian Central Nervous System. *Cell* 96, 25-34.
- Johe, K.K., Hazel, T.G., Muller, T., Dugich-Djordjevic, M.M., and McKay, R.D.G. (1996). Single factors direct the differentiation of stem cells from the fetal and adult central nervous system. *Genes & Development* 10, 3129-3140.
- Jones, P.H. and Watt, F.M. (1993). Separation of Human Epidermal Stem Cells from Transit Amplifying Cells on the Basis of Differences in Integrin Function and Expression. *Cell* 73, 713-724.
- Jordan, J., Bottner, M., Schluesener, H.J., Unsicker, K., and Kriegstein, K. (1997). Bone morphogenetic proteins: neurotrophic roles for midbrain dopaminergic neurons and implications of astroglial cells. *European Journal of Neuroscience* 9, 1699-709.
- Khan, J., Simon, R., Bitner, M., Chen, Y., Leighton, S.B., Pohida, T., Smith, P.D., Jiang, Y., Gooden, G.C., Trent, J.M., and Meltzer, P.S. (1998). Gene expression profiling of alveolar rhabdomyosarcoma with cDNA microarrays. *Cancer Research* 58, 5009-5013.
- Kirschenbaum, B. and Goldman, S.A. (1995). Brain-derived neurotrophic factor promotes the survival of neurons arising from the adult rat forebrain

subependymal zone. *Proceedings of the National Academy of Sciences USA* 92, 210-214.

Kondo, T. and Raff, M. (2000). Oligodendrocyte Precursor Cells Reprogrammed to Become Multipotential CNS Stem Cells. *Science* 289, 1754-1757.

Korinek, V., Barker, N., Moerer, P., van Donselaar, E., Huls, G., Peters, P.J., and Clevers, H. (1998). Depletion of epithelial stem-cell compartments in the small intestine of mice lacking Tcf-4. *Nature Genetics* 19, 379-83.

Kretzschmar, M., Liu, F., Hata, A., Doody, J., and Massague, J. (1997). The TGF- β family mediator Smad1 is phosphorylated directly and activated functionally by the BMP receptor kinase. *Genes & Development* 11, 984-995.

Kuhlbrodt, K., Herbarth, B., Sock, E., Enderich, J., Hermans-Borgmeyer, I., and Wegner, M. (1998). Cooperative function of POU proteins and SOX proteins in glial cells. *Journal of Biological Chemistry* 273, 16050-16057.

Kuhn, H.G., Dickinson-Anson, H., and Gage, F.H. (1996). Neurogenesis in the dentate gyrus of the adult rat: age-related decrease of neuronal progenitor proliferation. *Journal of Neuroscience*. 16, 2027-2033.

Lamb, T.M., Knecht, A.K., Smith, W.C., Stachel, S.E., Economides, A.N., Stahl, N., Yancopoulos, G.D., and Harland, R.M. (1993). Neural induction by the secreted polypeptide noggin. *Science* 262, 713-718.

Lee, C.-K., Klopp, R.G., Weindruch, R., and Prolla, T.A. (1999). Gene expression profile of aging and its retardation by caloric restriction. *Science* 285, 1390-1393.

Lendahl, U., Zimmerman, L.B., and McKay, R.D.G. (1990). CNS stem cells express a new class of intermediate filament protein. *Cell* 60, 585-595.

- Lewis, J., Slack, J.M.W., and Wolpert, L. (1977). Thresholds in Development. *Journal of Theoretical Biology* 65, 579-590.
- Li, W., Cogswell, C.A., and Lo Turco, J.J. (1998). Neuronal differentiation of precursors in the neocortical ventricular zone is triggered by BMP. *Journal of Neuroscience* 18, 8853-8862.
- Li, W. and LoTurco, J.J. (2000). Noggin Is a Negative Regulator of Neuronal Differentiation in Developing Neocortex. *Developmental Neuroscience* 22, 68-73.
- Lim, D.A. and Alvarez-Buylla, A. (1999). Interaction between astrocytes and adult subventricular zone precursors stimulates neurogenesis. *Proceedings of the National Academy of Sciences USA* 96, 7526-7531.
- Lim, D.A. and Alvarez-Buylla, A. (2001). Glial Characteristics of Adult Subventricular Zone Stem Cells. In *Stem Cells in CNS Development*. New Jersey: Humana Press.
- Lim, D.A., Fishell, G.J., and Alvarez-Buylla, A. (1997). Postnatal mouse subventricular zone neuronal precursors can migrate and differentiate within multiple levels of the developing neuraxis. *Proceedings of the National Academy of Sciences USA* 94, 14832-14836.
- Liu, H.S., Jan, M.S., Chou, C.K., Chen, P.H., and Ke, N.J. (1999). Is green fluorescent protein toxic to the living cell? *Biochemistry and Biophysics Research Communications* 3, 712-717.
- Lois, C. and Alvarez-Buylla, A. (1994). Long-distance neuronal migration in the adult mammalian brain. *Science* 264, 1145-1148.
- Lois, C., Garcia-Verdugo, J.M., and Alvarez-Buylla, A. (1996). Chain migration of

- neuronal precursors. *Science* 271, 978-981.
- Lopez-Garcia, C., Molowny, A., Garcia-Verdugo, J.M., Martinez-Guijarro, F.J., and Bernabeu, A. (1990). Late generated neurons in the medial cortex of adult lizards send axons that reach the Timm-reactive zones. *Developmental Brain Research* 57, 249-254.
- Lu, B., Jan, L.Y., and Jan, Y.-N. (1998). Asymmetric cell division: lessons from flies and worms. *Current Opinion in Genetics & Development* 8, 392-399.
- Luo, L., Salunga, R.C., Guo, H., Bittner, A., Joy, K.C., Galindo, J.E., Xiao, H., Rogers, K.E., Wan, J.S., Jackson, M.R., and Erlander, M.G. (1999). Gene expression profiles of laser-captured adjacent neuronal subtypes. *Nature Medicine* 5, 117-122.
- Luskin, M.B. (1993). Restricted proliferation and migration of postnatally generated neurons derived from the forebrain subventricular zone. *Neuron* 11, 173-189.
- Luskin, M.B., Zigova, T., Soteres, B.J., and Stewart, R.R. (1997). Neuronal progenitor cells derived from the anterior subventricular zone of the neonatal rat forebrain continue to proliferate *in vitro* and express a neuronal phenotype. *Molecular and Cellular Neuroscience*. 8, 351-366.
- Mabie, P.C., Mehler, M.F., and Kessler, J.A. (1999). Multiple roles of bone morphogenetic protein signaling in the regulation of cortical cell number and phenotype. *Journal of Neuroscience* 19, 7077-7088.
- Massague, J. (1998). TGF-beta signal transduction. *Ann.Rev.Biochem.* 67, 753-791.
- McKay, R. (1997). Stem cells in the central nervous system. *Science* 276, 66-71.
- McMahon, J.A., Takada, S., Zimmerman, L.B., Fan, C.-M., Harland, R.M., and

- McMahon, A.P. (1998). Noggin-mediated antagonism of BMP signaling is required for growth and patterning of the neural tube and somite. *Genes & Development* 12, 1438-1452.
- Menezes, J.R.L., Smith, C.M., Nelson, K.C., and Luskin, M.B. (1995). The division of neuronal progenitor cells during migration in the neonatal mammalian forebrain. *Molecular and Cellular Neurosciences* 6, 496-508.
- Merino, R., Ganan, Y., Macias, D., Rodriguez-Leon, J., and Hurle, J.M. (1999). Bone morphogenetic proteins regulate interdigital cell death in the avian embryo. *Annals of the New York Academy of Sciences* 887, 120-132.
- Momma, S., Johansson, C.B., and Frisen, J. (2000). Get to know your stem cells. *Current Opinions in Neurobiology* 10, 45-9.
- Morris, R.J. and Potten, C.S. (1994). Slowly cycling (label-retaining) epidermal cells behave like clonogenic stem cells in vitro. *Cell Proliferation* 27, 279-289.
- Morrison, S.J., Hemmati, H.D., Wandycz, A.W., and Weissman, I.L. (1995). The purification and characterization of fetal liver hematopoietic stem cells. *Proceedings of the National Academy of Sciences USA* 92, 10302-10306.
- Morrison, S.J., Shah, N.M., and Anderson, D.J. (1997). Regulatory mechanisms in stem cell biology. *Cell* 88, 287-298.
- Morshead, C.M., Reynolds, B.A., Craig, C.G., McBurney, M.W., Staines, W.A., Morassutti, D., Weiss, S., and Van der Kooy, D. (1994). Neural stem cells in the adult mammalian forebrain: A relatively quiescent subpopulation of subependymal cells. *Neuron* 13, 1071-1082.
- Palmer, T.D., Markakis, E.A., Willhoite, A.R., Safar, F., and Gage, F.H. (1999). Fibroblast growth factor-2 activates a latent neurogenic program in neural stem

- cells from diverse regions of the adult CNS. *Journal of Neuroscience*. 19, 8487-8497.
- Palmer, T.D., Willhoite, A.R., and Gage, F.H. (2000). Vascular Niche for Adult Hippocampal Neurogenesis. *Journal of Comparative Neurology* 425, 479-494.
- Paulus, U., Potten, C.S., and Loeffler, M. (1992). A model of the control of cellular regeneration in the intestinal crypt after perturbation based solely on local stem cell regulation. *Cell Proliferation* 25, 559-578.
- Perou, C.M., Jeffrey, S.S., van de Rijn, M., Rees, C.A., Eisen, M.B., Ross, D.T., Pergamenschikov, A., Williams, C.F., Zhu, S.X., Lee, J.C., Lashkari, D., Shalon, D., Brown, P.O., and Botstein, D. (1999). Distinctive gene expression patterns in human mammary epithelial cells and breast cancers. *Proceedings of the National Academy of Sciences USA* 96, 9212-7.
- Perris, R., Kuo, H.J., Glanville, R.W., and Bronner-Fraser, M. (1993). Collagen type VI in neural crest development: distribution in situ and interaction with cells in vitro. *Developmental Dynamics* 135-149.
- Petersen, B.E., Bowen, W.C., Patrene, K.D., Mars, W.M., Sullivan, A.K., Murase, N., Boggs, S.S., Greenberger, J.S., and Goff, J.P. (1999). Bone marrow as a potential source of hepatic oval cells. *Science* 1168-1170.
- Pixley, S. (1992). CNS Glial Cells Support In Vitro Survival Division, and Differentiation of Dissociated Olfactory Neuronal Progenitor Cells. *Neuron* 8, 1191-1204.
- Potten, C.S. and Loeffler, M. (1990). Stem cells: attributes, cycles, spirals, pitfalls and uncertainties lessons for and from the crypt. *Development* 110, 1001-1020.
- Quesenberry, P.J. and Becker, P.S. (1998). Stem cell homing: Rolling, crawling, and

- nesting. *Proceedings of the National Academy of Sciences USA* 95, 15155-15157.
- Reynolds, B. and Weiss, S. (1992). Generation of neurons and astrocytes from isolated cells of the adult mammalian central nervous system. *Science* 255, 1707-1710.
- Ross, D. T., Scherf, U., Eisen, M. B., Perou, C. M., Rees, C., Spellman, P., Iyer, V., Jeffrey, S. S., Van de Rijn, M., Waltham, M., Pergamenschikov, A., Lee, J. C., Lashkari, D., Shalon, D., Myers, T. G., Weinstein, J. N., Botstein, D., and Brown, P. O. Systematic variation in gene expression patterns in human cancer cell lines . *Nature Genetics* 24, 227-35. 2000.
- Rougon, G., Dubois, C., Buckley, N., Magnani, J.L., and Zollinger, W. (1986). A Monoclonal Antibody against Meningococcus Group B Polysaccharides Distinguishes Embryonic from Adult N-CAM . *Journal of Cell Biology* 103, 2429-2437.
- Ruhl, M., Sahin, E., Johannsen, M., Somasundaram, R., Manski, D., Riecken, E.O., and Schuppan, D. (1999). Soluble collagen VI drives serum-starved fibroblasts through S phase and prevents apoptosis via down-regulation of Bax. *Journal of Biological Chemistry* 274, 34361-34368.
- Sanes, J.R. (1989). Extracellular matrix molecules that influence neural development. *Annual Reviews in Neurosciences*. 12, 491-516.
- Schofield, R. (1978). The relationship between the spleen colony-forming cell and the haemopoietic stem cell. *Blood Cells* 7-25.
- Shah, N. M. and Anderson, D. J. (1997) Integration of multiple instructive cues by neural crest stem cells reveals cell-intrinsic biases in relative growth factor responsiveness. *Proceedings of the National Academy of Sciences USA* 94, 11369-74.

- Shou, J., Rim, P.C., and Calof, A.L. (1999). BMPs inhibit neurogenesis by a mechanism involving degradation of a transcription factor. *Nature Neuroscience* 2, 339-345.
- Slack, J.M.W. (2000). Stem Cells in Epithelial Tissues. *Science* 287, 1431-1433.
- Smith, W.C. and Harland, R.M. (1992). Expression cloning of noggin, a new dorsalizing factor localized to the Spemann organizer in *Xenopus* embryos. *Cell* 70, 829-840.
- Smith, W.C., Knecht, A.K., Wu, M., and Harland, R.M. (1993). Secreted noggin protein mimics the Spemann organizer in dorsalizing *Xenopus* mesoderm. *Nature* 361, 547-549.
- Soderstrom, S., Bengtsson, H., and Ebendal, T. (1996). Expression of serine/threonine kinase receptors including the bone morphogenetic factor type II receptor in the developing and adult brain. *Cell and Tissue Research* 286, 267-279.
- Sotelo, J.R. and Trujillo-Cenóz, O. (1958). Electron microscope study on the development of ciliary components of the neural epithelium of the chick embryo. *Z.Zellforsch.* 49, 1-12.
- Stensaas, L.J. and Stensass, S.S. (1968). Light microscopy of glial cells in turtles and birds. *Z.Zellforsch.* 91, 315-340.
- Straznick, A. and Gaze, R.M. (1971). The growth of the retina in *Xenopus Laevis*: an autoradiographic analysis. *J.Embryol.Exp.Morph.* 26, 67-79.
- Tan, S.-S. and Breen, S. (1993). Radial mosaicism and tangential cell dispersion both contribute to mouse neocortical development. *Nature* 362, 638-639.
- Tanaka, T.S., Jaradat, S.A., Lim, M.K., Kargul, G.J., Wang, X., Grahovac, M.J., Pantano, S., Sano, Y., Paio, Y., Nagaraja, R., Doi, H., Wood, W.H., Becker, K.G., and Ko, M.S.H. (2000). Genome-wide expression profiling of mid-gestation placenta and

- embryo using a 15,000 mouse developmental cDNA microarray. *Proceedings of the National Academy of Sciences USA* 97, 9127-32.
- Temple, S. (1989). Division and differentiation of isolated CNS blast cells in microculture. *Nature* 340, 471-473.
- Valenzuela, D.M., Economides, A.N., Rojas, E., Lamb, T.M., Nuñez, L., Jones, P., Ip, N.Y., Espinosa, R.I., Brannan, C.I., Gilbert, D.J., Copeland, N.G., Jenkins, N.A., Le Beau, M.M., Harland, R.M., and Yancopoulos, G.D. (1995). Identification of mammalian noggin and its expression in the adult nervous system. *Journal of Neuroscience*. 15, 6077-6084.
- Vasioukhin, V., Degenstein, L., Wise, B., and Fuchs, E. (1999). The magical touch: Genome targeting in epidermal stem cells induced by tamoxifen application to mouse skin. *Proceedings of the National Academy of Sciences USA* 96, 8551-8556.
- Wang, S. and Barres, B.A. (2000). Up a notch: Instructing gliogenesis. *Neuron* 27, 197-200.
- Watt, F.M. and Hogan, B.L.M. (2000). Out of Eden: Stem Cells and Their Niches. *Science* 287, 1427-1430.
- Wegner, M. (1999). From head to toes: the multiple facets of Sox proteins. *Nucleic Acids Research* 27,
- Weiss, S., Dunne, C., Hewson, J., Wohl, C., Wheatley, M., Peterson, A.C., and Reynolds, B.A. (1996a). Multipotent CNS stem cells are present in the adult mammalian spinal cord and ventricular neuroaxis. *Journal of Neuroscience* 16, 7599-7609.
- Weiss, S., Reynolds, B.A., Vescovi, A.L., Morshead, C., Craig, C.G., and Van der Kooy, D. (1996b). Is there a neural stem cell in the mammalian forebrain? *Trends in*

Neuroscience 19, 387-393.

- Wichterle, H., Garcia-Verdugo, J.M., and Alvarez-Buylla, A. (1997). Direct evidence for homotypic, glia-independent neuronal migration. *Neuron* 18, 779-791.
- Wichterle, H., Garcia-Verdugo, J.M., Herrera, D.G., and Alvarez-Buylla, A. (1999). Young neurons from medial ganglionic eminence disperse in adult and embryonic brain. *Nature Neuroscience* 2, 461-466.
- Wilson, P.A. and Hemmati-Brivanlou, A. (1995). Induction of epidermis and inhibition of neural fate by Bmp-4. *Nature* 376, 331-333.
- Wilson, P.A. and Hemmati-Brivanlou, A. (1997). Vertebrate neural induction: inducers, inhibitors, and a new synthesis. *Neuron* 18, 699-710.
- Wodarz, A. and Nusse, R. (1998). Mechanisms of Wnt signaling in development. *Annual Reviews of Cell and Developmental Biology* 14, 59-88.
- Wong, M.H., Rubinfeld, B., and Gordon, J.I. (1998). Effects of forced expression of an NH2-terminal truncated beta-Catenin on mouse intestinal epithelial homeostasis. *Journal of Cell Biology* 141, 765-77.
- Yang, W.X., Model, P., and Heintz, N. (1997). Homologous recombination based modification in *Escherichia coli* and germline transmission in transgenic mice of a bacterial artificial chromosome. *Nature Biotechnology* 15, 859-65.
- Yoon, S.O., Lois, C., Alvarez, M., Alvarez-Buylla, A., Falck-Pederson, E., and Chao, M.V. (1996). Adenovirus-mediated gene delivery into neuronal precursors of the adult mouse brain. *Proceedings of the National Academy of Sciences USA* 93, 11974-11979.
- Zaheer, A., Zhong, W., Ue, E.Y., Moser, D.R., and Lim, R. (1995). Expression of

- mRNAs of multiple growth factors and receptors by astrocytes and glioma cells: detection with reverse transcription-polymerase chain reaction. *Cellular and Molecular Neurobiology* *15*, 221-237.
- Zhang, D., Mehler, M.F., Song, Q., and Kessler, J.A. (1998). Development of bone morphogenetic protein receptors in the nervous system and possible roles in regulating *trkC* expression. *Journal of Neuroscience*. *18*, 3314-3326.
- Zhu, A.J. and Watt, F.M. (1999). *b*-catenin signalling modulates proliferative potential of human epidermal keratinocytes independently of intercellular adhesion. *Development* *126*, 2285-2298.
- Zigova, T., Betarbet, R., Soteres, B.J., Brock, S., Bakay, R.A., and Luskin, M.B. (1996). A comparison of the patterns of migration and the destinations of homotopically transplanted neonatal subventricular zone cells and heterotopically transplanted telencephalic ventricular zone cells. *Developmental Biology* *173*, 1-16.
- Zigova, T., Pencea, V., Wiegand, S.J., and Luskin, M.B. (1998). Intraventricular administration of BDNF increases the number of newly generated neurons in the adult olfactory bulb. *Molecular & Cellular Neurosciences* *11*, 234-45.
- Zimmerman, L.B., De Jesus-Escobar, J.M., and Harland, R.M. (1996). The Spemann organizer signal *noggin* binds and inactivates bone morphogenetic protein 4. *Cell* *86*, 599-606.
- Zolotukhin, S., Potter, M., Hauswirth, W.W., Guy, J., and Muzyczka, N. (1996). A "humanized" green fluorescent protein cDNA adapted for high-level expression in mammalian cells. *Journal of Virology* *70*, 4646-4654.
- Zou, H., Wieser, R., Massague, J., and Niswander, L. (1997). Distinct roles of type I bone morphogenetic protein receptors in the formation and differentiation of cartilage. *Genes & Development* *11*, 2191-2203.